

**MASTER**

**Energy performance optimization of buildings using data mining techniques**

Corten, C.J.J.

*Award date:*  
2018

[Link to publication](#)

**Disclaimer**

This document contains a student thesis (bachelor's or master's), as authored by a student at Eindhoven University of Technology. Student theses are made available in the TU/e repository upon obtaining the required degree. The grade received is not published on the document as presented in the repository. The required complexity or quality of research of student theses may vary by program, and the required minimum study period may vary in duration.

**General rights**

Copyright and moral rights for the publications made accessible in the public portal are retained by the authors and/or other copyright owners and it is a condition of accessing publications that users recognise and abide by the legal requirements associated with these rights.

- Users may download and print one copy of any publication from the public portal for the purpose of private study or research.
- You may not further distribute the material or use it for any profit-making activity or commercial gain

**Department of the Built Environment**

Navigation address: De Zaale, Eindhoven  
P.O. Box 513, 5600 MB Eindhoven  
The Netherlands  
[www.tue.nl](http://www.tue.nl)

**Author:**

C.J.J. (Kai) Corten

**Student ID:**

0914198

**Graduation committee:**

Prof. Ir. W. (Wim) Zeiler  
Ir. S.S.W. (Shalika) Walker  
Ir. E.M.M. (Eric) Willems

**Date:**

October 2018

# Energy performance optimization of buildings using data mining techniques



# Energy performance optimization of buildings using data mining techniques

Master of Science thesis

October 10, 2018

## **Author**

Name: C.J.J. (Kai) Corten  
Student number: 0914198  
E-mail: kaicorten@gmail.com

## **Graduation committee**

Chair of committee:	Prof. Ir. W. (Wim) Zeiler	TU/e
Internal member:	Ir. S.S.W. (Shalika) Walker	TU/e
Company supervisor:	Ir. E.M.M. (Eric) Willems	Huygen

## **Educational institution**

Name: Eindhoven University of Technology  
Faculty: Department of the Built Environment  
Unit: Building Physics and Services (BPS)  
Address: Den Dolech 2  
5612 AZ Eindhoven  
The Netherlands

## **Company**

Name: Huygen Ingenieurs & Adviseurs BV  
Address: Parkweg 22B  
6212 XN Maastricht  
The Netherlands

## Preface

This report presents my master thesis “Energy performance optimization of buildings using data mining techniques”. This thesis is written as graduation project for the master Building Physics and Services at Eindhoven University of Technology. The reason for the study was the energy performance gap between the design and the operational phase of buildings. Therefore, the aim was to provide insights into the optimization of the building energy performance, taking into account the indoor climate. This study was conducted in collaboration with Huygen Ingenieurs & Adviseurs BV.

During my graduation project, I have gained a lot of knowledge. Despite it was sometimes a hard process, it was very interesting. Especially the combination of my background in the building field with data analysis contained major challenges. This was because I had no experience as data analyst before this study. Nevertheless, my research goal was finally achieved and the research questions could be answered, partly by the assistance of my supervisors and colleagues.

Therefore, I want to thank my graduation committee for their excellent guidance and support. My first supervisor from the university was professor Wim Zeiler. Wim, I want to thank you for our instructive conversations, where you gave me valuable feedback for obtaining a well-founded research. In addition, I want to thank my second supervisor from the university, Shalika Walker. Shalika helped me to improve the quality of the study. A special thanks goes to my third supervisor, Eric Willems from Huygen Ingenieurs & Adviseurs. Eric, thank you for offering me a great internship at your company and for always being available to give advice.

Besides my supervisors, I want to thank all my colleagues at Huygen Ingenieurs & Adviseurs for the pleasant working atmosphere. Especially, I want to thank Pegah Zolfaghari for learning me the basic skills of data analysis. Finally, I want to thank my family for their unconditional support during the study.

I hope that this report will contribute to improve the energy performance of buildings towards a low-carbon society.

Enjoy reading.

Maastricht, October 10, 2018,

Kai Corten

## Abstract

In order to achieve the European Union climate and energy targets, existing energy-intensive buildings are renovated and replaced by high-performance nearly Zero Energy Buildings (nZEB). However, the operational energy performance of these buildings often does not match with the design. The most dominant causes for these so-called performance gaps are uncertainty in modeling, occupant behavior and poor operational practices of building installations. Due to the low renovation and replacement rate of buildings, the improvement of the energy performance of operating buildings is of significant importance. Therefore, the main objective of this study is to provide recommendations in order to optimize the energy performance of operating buildings by a systematic assessment.

Nowadays, non-residential buildings are equipped with a building management system (BMS) which collects and stores large quantities of operational data. This data can be used to control and improve the operational performance. However, the BMS can only perform simple data analysis and visualizations based on a short period of historical data. This is the reason why the building sector urgently needs advanced tools. Literature presents data mining (DM) as a promising approach for extracting useful insights from the massive data sets. This technology is largely applied in various research fields, but is still in an initial phase in the building sector.

The study can be divided into three main steps, namely (i) a Pareto analysis, (ii) a performance analysis and (iii) a LEAN energy analysis. This study is conducted at two case study buildings: a care center and an office building located in the Netherlands. First, the Pareto analysis is performed to identify the performance indicators of the Heating, Ventilation and Air Conditioning (HVAC) system and the occupant behavior. Focused on these obtained performance indicators, the designed and measured performance is subsequently analyzed by means of top-down approach. This leads to identifying systems inefficiencies of which the energy saving potential is finally modeled by using regression as the DM technique.

In general, it can be concluded that the HVAC system of especially the care center is underperforming according to the design. By means of regression it is shown that the energy performance can be significantly optimized by improving the faults in the regulation of the systems. Additional measurements on component level are necessary to effectively optimize the energy performance. Moreover, this will lead to the improvement of the indoor climate and the reduction of the operating costs.

# Table of contents

	<b>Preface</b>	<b>i</b>
	<b>Abstract</b>	<b>ii</b>
	<b>Table of contents</b>	<b>iii</b>
	<b>Terminology</b>	<b>v</b>
<b>1</b>	<b>Introduction</b>	<b>1</b>
1.1	Background and motivation	1
1.2	Problem definition and scientific relevance	1
1.3	Scope	5
1.4	Hypothesis and objective	6
1.5	Research questions	6
1.6	Outline	6
<b>2</b>	<b>Literature study</b>	<b>8</b>
2.1	Building energy performance	8
2.2	Building management system	8
2.3	Data mining techniques	8
<b>3</b>	<b>Methodology</b>	<b>11</b>
3.1	Pareto analysis	11
3.2	Performance analysis	12
3.3	LEAN energy analysis	12
<b>4</b>	<b>Case study buildings</b>	<b>14</b>
4.1	Larisa	14
4.2	Kropman Breda	15
<b>5</b>	<b>Case study 1: Larisa</b>	<b>17</b>
5.1	Pareto analysis	17
5.2	Designed performance analysis	20
5.3	Measured performance analysis	23
5.4	LEAN energy analysis	37
<b>6</b>	<b>Case study 2: Kropman Breda</b>	<b>41</b>
6.1	Pareto analysis	41
6.2	Designed performance analysis	44
6.3	Measured performance analysis	45
6.4	LEAN energy analysis	53
<b>7</b>	<b>Discussion</b>	<b>56</b>
<b>8</b>	<b>Conclusion</b>	<b>57</b>
8.1	Sub-questions	57
8.2	Main research question	58

<b>9</b>	<b>Recommendations</b>	<b>59</b>
	<b>References</b>	<b>60</b>
	<b>Appendix</b>	<b>63</b>
A	Case study 1: Larisa	64
B	Case study 2: Kropman Breda	78



# Terminology

## List of abbreviations

AHU	Air Handling Unit
ATES	Aquifer Thermal Energy Storage
BES	Building Energy Simulation
BMS	Building Management System
CCA	Concrete Core Activation
CCx	Continuous Commissioning
CRISP-DM	Cross-industry Standard Process for Data Mining
Cx	Commissioning
DHW	Domestic Hot Water
DM	Data Mining
EED	Energy Efficiency Directive
EIS	Energy Information System
EPBD	Energy Performance of Buildings Directive
EU	European Union
GDPR	General Data Protection Regulation
GHG	Greenhouse Gas
HEX	Heat exchanger
HVAC	Heating, Ventilation and Air Conditioning
KDD	Knowledge Discovery in Databases
LEA	LEAN Energy Analysis
MBCx	Monitoring Based Commissioning
nZEB	Nearly Zero Energy Buildings
RCx	Retro-Commissioning
SEMMA	Sample, Explore, Modify, Model, Assess
TU/e	Eindhoven University of Technology

## List of symbols

$c_p$	Specific heat capacity	[kJ/kgK]
$CO_2$	Carbon Dioxide	[ppm]
COP	Coefficient Of Performance	[-]
EER	Energy Efficiency Ratio	[-]
EPC	Energy Performance Coefficient	[-]
GFA	Gross Floor Area	[m <sup>2</sup> ]
P	Thermal power	[kW]
Q	Thermal energy	[kWh]
R-value	Thermal resistance	[m <sup>2</sup> K/W]
RH	Relative Humidity	[%]
t	Time	[s] or [h]
$T_e$	Exterior temperature	[°C]
$T_i$	Interior temperature	[°C]
U-value	Heat transfer coefficient	[W/m <sup>2</sup> K]
V	Volume	[m <sup>3</sup> ]
$\Phi$	Flow	[m <sup>3</sup> /s]
$\lambda$ -value	Thermal conductivity	[W/mK]
$\rho$	Density	[kg/m <sup>3</sup> ]

# 1 Introduction

## 1.1 Background and motivation

The threat of climate change is one of the greatest challenges of the modern age. This is mainly caused by the drastic increase of greenhouse gas (GHG) emissions in the last half century [1]. In order to become more climate-friendly and less energy-consuming, the European Union (EU) leaders strive for a low-carbon society in 2050 and have therefore set up climate and energy targets. By 2020, the EU aims to have at least 20% reduction in GHG emissions, 20% increase in renewable energy production and 20% improvement in energy efficiency compared to 1990 levels (20-20-20 targets) [2]. By 2030, the EU aspires to have at least 40% reduction in GHG emissions, 27% increase in renewable energy production and 27% improvement in energy efficiency compared to 1990 levels [3]. This will lead to 80-95% reduction in GHG emissions by 2050 [4].

The built environment is a major contributor to the climate change. In the EU, the building sector is responsible for nearly 40% of the final energy consumption and 36% of the GHG emissions [5]. Nevertheless, the sector has huge potential for energy savings by using the currently available advanced technologies [6]. In order to promote the improvement of the energy performance of buildings within the EU, the Energy Performance of Buildings Directive (EPBD) and the Energy Efficiency Directive (EED) were launched by the European Parliament and Council. These directives are the EU's main legislative instruments and need to be converted by Member States into national legislation [7].

Despite the above-mentioned initiatives and efforts of the EU, the current rate of building energy efficiency increases at a relative slow pace. This is typically due to the low renovation rates (1.4% per year on average per country) and low replacement rates of buildings [8]. In addition, globally empirical evidence is emerging of discrepancies between the predicted (design phase) and the actual measured (operational phase) energy performance of operational buildings. This phenomenon has been termed as the “performance gap” [9] [10] [11]. Understanding this gap and at the same time reducing it, will improve the energy performance of operating buildings and therefore significantly contribute to the EU climate and energy targets.

## 1.2 Problem definition and scientific relevance

### 1.2.1 Energy performance gap

The energy consumption of buildings during the operational phase normally accounts for 80-90% of their life cycle energy demand [12]. Studies have shown that this consumption is on average 1.5 to 2.5 times higher than predicted during the design phase [13]. The underlying causes for this energy performance gap are presented in Figure 1.1. The most dominant causes are uncertainty in modeling during the design phase, occupant behavior and poor operational practice of HVAC systems [14]. This variety of reasons, caused in different phases of the building life cycle, makes it a great challenge to reduce the energy performance gap of operational and future buildings.

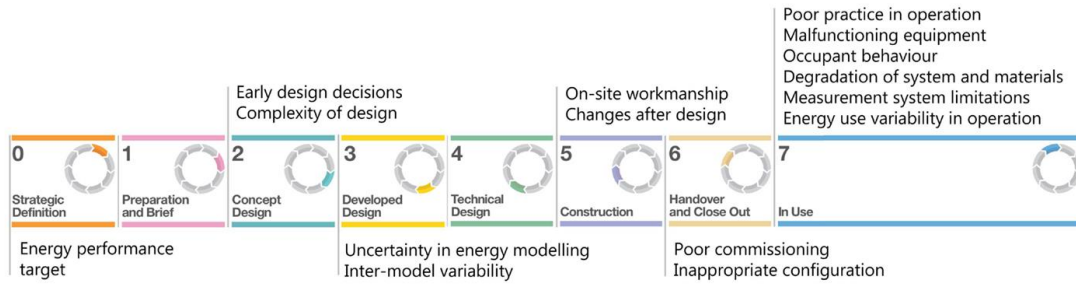


Figure 1.1: Underlying causes for performance gaps during all phases of the building life cycle [14]

This is also the case in the Netherlands, where energy can be saved at more than 70% of the existing non-residential buildings by better operation of the heating, ventilation and air conditioning (HVAC) systems. The energy consumption of these buildings is on average 25% higher than expected based on the available technology and processes [15]. This accounts for nearly 191 PJ, which is about five times larger than the total national generated solar and wind energy in 2016 [16]. Therefore, the underperforming HVAC systems offer high potential to optimize the energy performance of buildings and, consequently could improve the indoor climate and reduce the running costs. These challenges are the main reasons for this study.

### 1.2.2 Current situation

Nowadays, modern non-residential buildings are mostly equipped with an advanced building management system (BMS). Besides its control function, this system can monitor, collect and store, massive amounts of building data [6] [17]. In fact, the data represents the operational performance of the HVAC system. The process of maintaining and improving the performance during the building life cycle is grouped under the label Commissioning (Cx) [18]. This is defined as: “a quality-oriented process for achieving, verifying, and documenting that the performance of facility systems and assemblies meet defined objectives and criteria” [19].

Literature provides three steps of energy saving by Monitoring Based Commissioning (MBCx), shown in Figure 1.2 [20]. The first step involves the implementation of energy information systems (EIS) and diagnostic tools. The next step includes savings based on the obtained information from these tools. The final step is continually identifying new measures which is called Continuous Commissioning (CCx). There is growing attention for this ongoing process due to the reduction in yearly energy costs combined with low investment costs of most CCx measures. As a result, a short pay-back period of the investment costs is 1 to 5 years [18].

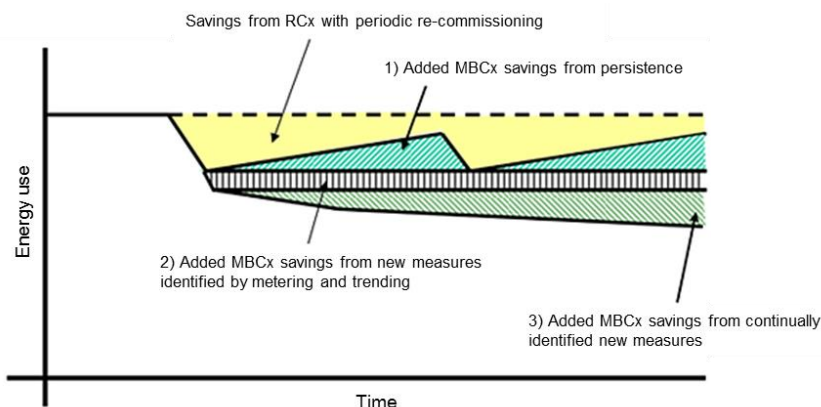


Figure 1.2: The three steps of additional energy savings by Monitoring Based Commissioning (MBCx) [20]

If the operational performance of HVAC systems is periodically controlled, e.g. once a year, it is called periodic re-commissioning (RC<sub>x</sub>). But the reality of today is that in most of the buildings the settings of the system are in general only checked or adjusted to solve complaints of occupants, sometimes in combination with a limited number of measurements. Other indicators such as energy efficiency and operational excellence are not taken into account. Therefore, system inefficiencies are principally caused by controllable parameters [15]. In order to solve these problems, a CCx process should be implemented that will result in a significant optimization of the energy performance.

### 1.2.3 Performance indicators

The key to develop efficient strategies to reduce the energy performance gap of operational buildings is the identification of the root causes of the underperformance of HVAC systems and the influences of the occupant behavior. These root causes, called performance indicators, have to be assessed by comparing the predicted performance with the actual measured performance. The performance indicators can be used to provide aggregated information about the performance in a clear and efficient way.

The purpose of a performance indicator is: “to provide a measure of current performance, a clear statement of what might be achieved in terms of future performance targets and a yardstick for measurement of progress along the way” [21]. The use of performance indicators and benchmarking is fundamental to any improvement strategy as indicators reflect the goals of a project and provide means for the measurement and management of the progress towards those goals for further learning and improvement [22]. This is necessary to obtain financially attractive business cases.

### 1.2.4 Data mining

When the performance indicators are identified, building operational data regarding these indicators can be analyzed. Nevertheless, building data are far from being fully used, mainly due to the lack of methods and tools for handling those big data [6]. The BMS can only perform simple data analysis and visualizations based on a short period of historical data [12]. In addition, the quality of the data analysis is dependent on the knowledge and experience of the particular investigator. Therefore, there is an urgent need for systematically analyzing the operational data in order to understand, control and improve the building energy performance. In fact, a good energy and environmental design, by itself, cannot guarantee predicted performance levels during the whole building life cycle without proper commissioning and technical management [17].

Data mining (DM) technology is a promising approach for extracting useful insights from large data sets [6]. It is the process of turning data into information and gaining knowledge from information [23]. DM techniques are already successfully applied in various research fields. However, the application of a DM framework for building energy consumption and operational data is still in an elementary phase [24].

In order to guide the implementation of DM on big data, Fayyad et al. considered DM as one of the steps of the knowledge discovery in databases (KDD) process [25]. This traditional process is the basis for other developed process models, such as Cross-industry Standard Process for Data Mining (CRISP-DM) and Sample, Explore, Modify, Model, Assess (SEMMA) [26]. The KDD process contains five main steps, presented in Figure 1.3.

First, a target data set has to be selected on which knowledge discovery is performed. Second, the cleaning and preprocessing of the target data in order to get complete and consistent data. This step resolves data conflicts, removes outliers and checks for and solves problems, like noise and missing values [27]. Third, the transformation of the data into such forms so that DM techniques, such as classification, regression and clustering, can be implemented. This means, for example, the transformation of the measured data to the same timescale. Fourth, the appropriate DM technique is chosen and implemented for searching different patterns from data. Fifth, the mining patterns are interpreted and evaluated by means of visualization. This leads to the use of the discovered knowledge for different purposes [26].

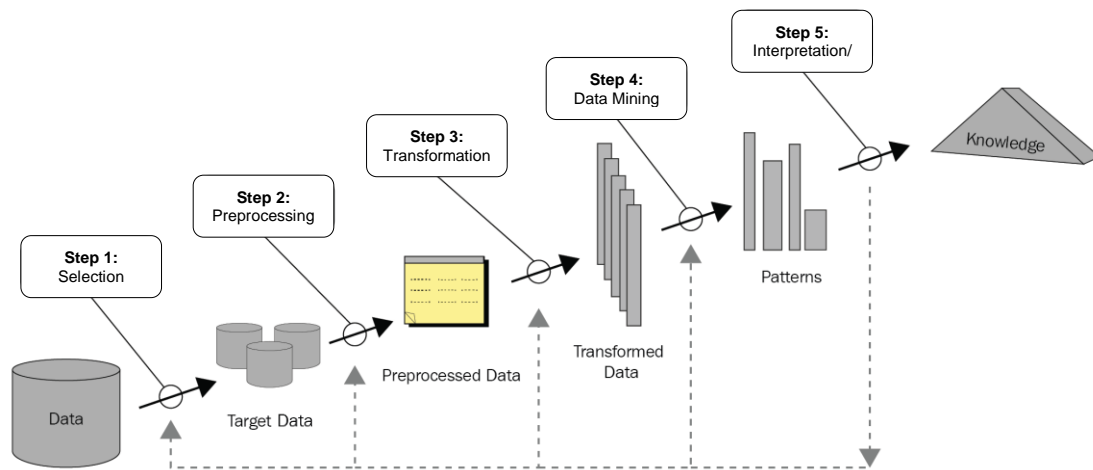


Figure 1.3: The traditional KDD process for obtaining knowledge from data using DM techniques (modified from [28])

## 1.2.5 Pareto analysis and LEAN energy analysis

In order to control and improve the building energy performance, the combination of the Pareto analysis and LEAN energy analysis seems to be an effective way [29]. The Pareto analysis is a systematic approach to identify the major causes of problems [30]. In addition, the LEAN energy analysis is a useful method to assess the building energy performance [31] [32].

### Pareto analysis

The Pareto analysis enables to solve the majority of problems by assessing only a few causes, called performance indicators. The analysis assumes that roughly 80% of the problems can be identified by 20% of the major causes, or roughly 80% of the problems can be solved by 20% of the effort, visualized in Figure 1.4 [30]. This principle is often used in decision-making issues or in solving complex problems [33].

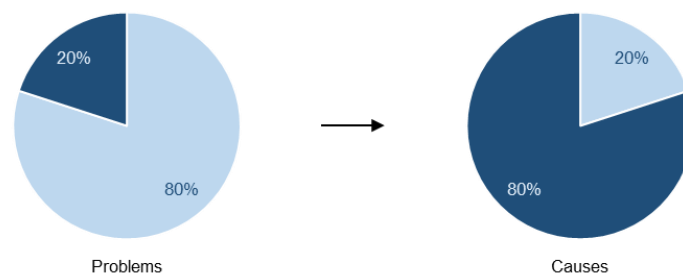


Figure 1.4: Principle of the Pareto analysis

The Pareto analysis can be divided into the following four main steps [29] [34]:

**1. Identification of the problems**

The building is modeled and the simulated energy consumption is compared with the measured energy consumption, to identify the energy performance gap.

**2. Identify root causes of each problem**

Since the behavior of the energy consumption depends on a large amount of parameters, only the main parameters are selected.

**3. Rank, score and group problems & causes**

The impact of the main parameters on the annual energy consumption is assessed by a sensitivity analysis to identify the performance indicators of the energy performance gap.

**4. Assessment energy gap by selected critical parameters**

The investigation whether the energy performance gap can be explained by the selected performance indicators.

**LEAN energy analysis**

The LEAN energy analysis is used to predict energy use, to estimate savings and to assess building energy performance trends. The analysis is derived from the general LEAN management philosophy. This means that the analysis aims to avoid a complex and time-consuming process by developing regression models of annual energy consumption from readily available utility and weather data [31] [32].

The LEAN energy analysis can be divided into the following four main steps [29] [34]:

**1. Collect weather & utility data**

The collection of the measured data for a comparison with the simulation energy consumption.

**2. Create baseline/benchmark models**

The identification of characteristic correlations in energy performance of the building and the creation of benchmark models, which can be used to assess the measured energy efficiency.

**3. Identify energy gaps with regression coefficients of benchmark regression models**

The identification of the energy performance gap by the assessment with the coefficients of multi-parameterized regression models.

**4. Assessment of remaining energy gaps**

The results are used to assess the energy performance gap, additionally to the earlier results of the Pareto analysis.

## 1.3 Scope

The study is conducted to support decision-making regarding the improvement of underperforming HVAC systems of operational non-residential buildings by focusing on the controllable parameters. This provides insights how to reduce the energy performance gap, taking into account the indoor climate. The building-related parameters have been left out of consideration in this study due to the low renovation and replacement rates of buildings in the EU.

The research is based on two case study buildings, namely the modern care center Larisa located in Maastricht (NL) and the traditional office building Kropman located in Breda (NL). The operational performance of these buildings is analyzed using data measured by the BMS. By comparing the actual measured performance with the predicted performance based on the design and settings, the system inefficiencies are discovered. This leads to energy saving potential which is investigated by using regression.

## 1.4 Hypothesis and objective

The hypothesis for this study is: "The improvement of an underperforming HVAC system leads to significant optimization of the building energy performance". This is investigated by means of both case study buildings.

The main objective of this study is to provide recommendations in order to optimize the energy performance of operational buildings by a systematic assessment. Achieving this objective will contribute to:

- focus on the most important performance indicators of the HVAC system and the occupant behavior;
- efficiently control and improvement of the energy performance of operational buildings which is necessary to achieve the EU climate and energy targets.

## 1.5 Research questions

This report answers the following main research question:

*"Which effective strategies can be used to improve underperforming HVAC systems of operational buildings using data mining techniques?"*

In order to answer the main research question, the following three sub-questions are formulated:

- I. What are the performance indicators of the case study buildings regarding the HVAC system and the occupant behavior?
- II. Which parts of the HVAC system of the case study buildings are underperforming based on the performance indicators?
- III. To which extent can data mining contribute to improving the overall energy performance of the case study buildings?

## 1.6 Outline

This research is executed according to the phases presented in Figure 1.5.

Chapter 2 elaborates on the literature which is relevant for the study. Chapter 3 describes the methodology of the study. Chapter 4 introduces the two case study buildings.

Chapters 5 (Larisa) and 6 (Kropman Breda) discuss the conducted research at both case study buildings. This research consists of the following three main steps, which are described in detail in chapter 3:

- First, the performance indicators of the buildings are identified according to the Pareto analysis by performing a sensitivity analysis using the building energy simulation (BES) program EnergyPlus.
- Second, the designed and measured performance are analyzed regarding the performance indicators by means of top-down approach. This leads to the system inefficiencies.
- Third, the potential energy performance of both buildings is investigated based on the LEAN energy analysis. For the visualization of the building performance, the program RStudio is used.

Chapters 7, 8 and 9 provide the discussion, conclusion and recommendations of the performed research.

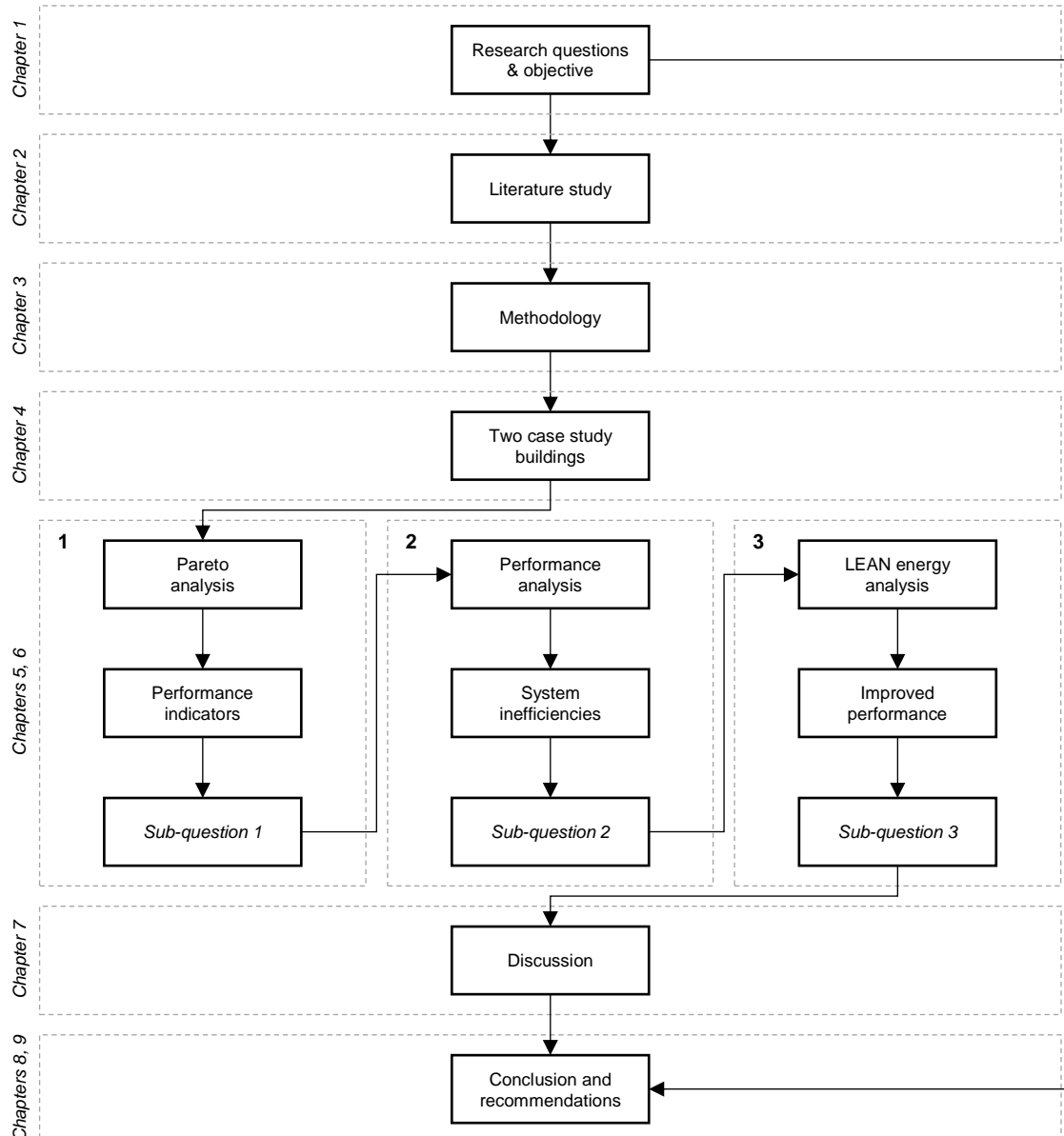


Figure 1.5: Schematic overview of the research method



## 2 Literature study

This chapter discusses the most relevant literature with regards to the building energy performance, the potential of the BMS and the need to use DM techniques in order to control and improve the building energy performance. Hereafter, the different DM techniques are described.

### 2.1 Building energy performance

The building energy performance is not only related to the amount of energy consumption during the building operation. There is a clear difference between a building which uses low energy inefficiently and a building which uses much energy efficiently to provide a higher level of service [35]. Therefore, a good building energy performance includes three elements according to a study by Borgstein et al. (2016). The building must:

1. be energy efficient, through its design, systems and technologies;
2. supply amenities and features typical for its typology;
3. be low in energy consumption, in other words, it must be operated in such a manner as to be efficient.

### 2.2 Building management system

Nowadays, modern non-residential buildings are equipped with a BMS which collects and stores operating data, such as temperature, flow rate, pressure, control signals and states of equipment in the HVAC system. This data can be used to control and improve the building performance. However, the BMS can only perform simple data analysis and visualizations based on a short period of historical data, such as historical data tracking, moving averages and alarming of simple abnormalities. The system is not capable to systematically analyze the large data sets in their database. Therefore, the operational data are rarely completely interpreted and used [12] [36].

The building sector urgently needs advanced methods and tools to analyze the massive data to obtain knowledge for controlling and improving the operational building performance. DM is an emerging powerful technology with great potential for discovering hidden knowledge in massive data sets. Last years, various research fields have gained increasing interest in DM, such as healthcare, marketing and social science. The use of DM techniques in the building field also yields encouraging results in energy saving and improvement of the indoor climate [12] [36].

### 2.3 Data mining techniques

In 2001, DM was defined as: “The analysis of large observation data sets to find unsuspected relationships and to summarize the data in novel ways so that owners can fully understand and make use of the data” [37]. In general, it can be divided into two main categories, namely supervised and unsupervised learning [38]. Additionally, these two categories can also be combined which is called semi-supervised learning.

### 2.3.1 Supervised learning

Supervised learning is powerful in predictive modeling. In the building field, supervised DM is generally applied for predictive modeling of the energy consumption, system performance and indoor climate [36]. In supervised learning, an algorithm is used to learn the quantitative and qualitative relationship between input variables and output variables. Supervised learning algorithms can be further grouped into regression and classification. The acceptable level of performance of this systematic computational analysis is dependent on two factors, namely domain expertise and training data.

For the development of functional models where the model architecture, model inputs and model parameters are specified and tuned, domain expertise is vital. Nevertheless, involvement of domain expertise decreases the number of variables used to develop the model. Therefore, the added value of big data can be get diminished. Training data is a set of already available input and output data used to fit the model parameters. The model iteratively makes predictions and finds the best fit for the model parameters using the training data set. Training data set has a direct and major impact on the quality and reliability of the model [38].

#### **Classification**

In classification, the output variable represents a data class or category. The model learns from the input and training data sets and classifies the new observations. Decision trees, support vector machines and linear classifiers are some of the classification algorithms used in supervised learning [39].

#### **Regression**

Regression analysis is often used for numeric prediction and/or for predicting outputs that are continuous. In regression, the output can be determined by the inputs of the model without being confined to a set of labels/categories as is the case in classification. Regression problems with time-ordered inputs such as seasonal energy demand patterns of buildings are called time-series forecasting problems. Linear regression is the most used example of regression algorithms which involves finding the best line to fit two attributes (or variables) so that one attribute can be used to predict the other [39].

### 2.3.2 Unsupervised learning

Unsupervised learning is more practical in discovering new knowledge given limited prior knowledge from test data that has not been already classified/labeled. The knowledge obtained by unsupervised learning is usually identified commonalities in the data set represented as data clusters, association rules, and anomalies.

In contrast with supervised learning, instead of responding to labeled training data and focuses on discovering the intrinsic correlations, unsupervised learning reacts based on the presence and absence of identified commonalities/features in the data sets. Besides, the non-necessity to explicitly pre-define a problem or target makes unsupervised learning less dependent on expertise knowledge. Other than that, the realization of unsupervised analytics is not subjected to obtainability of high-quality training data [38]. These facts make unsupervised learning favorable in discovering new knowledge in real applications [40]. In data mining, the most commonly used unsupervised learning algorithms, clustering and association are discussed below.

**Clustering**

Clustering is the process of generating class labels for a group of data. The objects in the same cluster or group inhabit maximized similarities while the similarities in-between clusters are minimized. The cluster can be analyzed by viewing it as a class of objects, from which rules can be derived [39].

**Association**

Association has the ability to discover relations among variables and express this knowledge in a rule format. Typically, association rules require to satisfy a user-specified minimum support and a user-specified minimum confidence threshold [39]. The associations are discarded as uninteresting if they do not satisfy both these requirements at the same time.

**2.3.3 Conclusion**

DM makes it possible to successfully use BMS data. However, it is complex to apply DM techniques in the building field. DM delivers enormous amounts of varied knowledge and therefore requires sufficient domain knowledge to use this in practice. Furthermore, the DM technology is constantly being improved. This makes it a difficult task for building professionals to follow these developments. Therefore, it is necessary to know how to choose the most suitable DM technique and how to select valuable knowledge. It would be a major breakthrough if the entire building sector could benefit from the advantages of applying DM techniques. For this purpose, a generic method is needed for knowledge discovery in massive BMS data using DM techniques [41].

## 3 Methodology

This chapter describes the methodology of the study which is conducted at two case study buildings.

Underperforming HVAC systems are a major problem in the built environment. The most inefficiencies are related to controllable parameters. This study provides an efficient method to control and optimize the energy performance of operational buildings by a better operation of the HVAC system. The two case study buildings are analyzed by the next three main steps:

1. Pareto analysis
2. Performance analysis
3. LEAN energy analysis

### 3.1 Pareto analysis

Since modern non-residential buildings have large data sets, it is important to find out which data is the most important to analyze. Therefore, the first step of the study is the identification of the performance indicators by means of the Pareto analysis with the BES program EnergyPlus. This worldwide recognized program can be used to model both energy consumption (heating, cooling, ventilation, lighting and plug and process loads) and water use in buildings. It is funded by the U.S. Department of Energy's Building Technologies Office [42]. For the simulations with EnergyPlus, a 3D model of both case study buildings is created by means of the OpenStudio SketchUp Plug-in.

When both case study buildings are modeled according to the design, the sensitivity analysis is started following the schematic overview presented in Figure 3.1. First, the main parameters regarding the HVAC system and occupant behavior are selected. In this analysis, the building-related parameters are not taken into account because the most buildings in Europe will not be renovated or replaced in the coming years. The impact of each selected parameter on the heating, cooling and electricity consumption is determined by simulating 10% higher and lower values than designed. This 10% deviation is determined in order to compare realistic possible values.

After the simulations, the parameters are ranked, scored and grouped based on the size of the impact. According to the Pareto analysis, roughly 20% of the selected parameters with the largest impact causes 80% of the energy performance gap. The challenge is to identify the 20% of parameters which are responsible for the underperformance of the building system. These major parameters are presented as performance indicators. Finally, it can be concluded whether the "80/20 rule" also applies to this study.

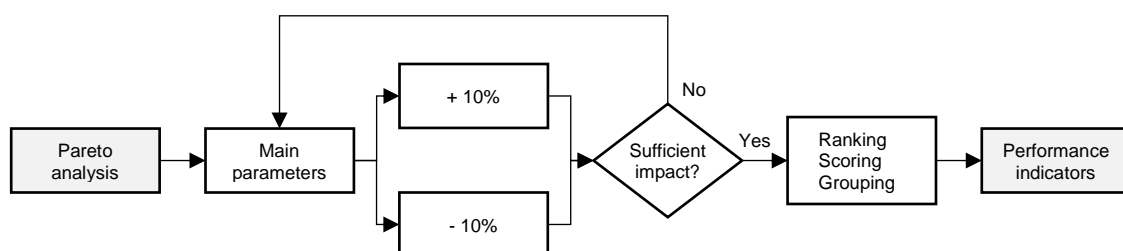


Figure 3.1: Schematic overview of the Pareto analysis

## 3.2 Performance analysis

The second step consists of the performance analysis following the schematic overview shown in Figure 3.2. The performance analysis is divided into the designed and measured performance analysis.

The designed performance of the HVAC system is analyzed using the technical documents of the case study buildings. This includes the specifications and operation of the installations which is necessary to understand the controllable parameters. Based on this analysis, the measured performance of the installations can be properly assessed.

From both buildings operational data regarding the installations was logged, measured by sensors of the BMS. When the obtained data is sufficient, the measured performance regarding the performance indicators is analyzed by means of a top-down approach and assessed based on the design and settings. This implies that the performance is analyzed first on building level, then on system level and finally on component level. For the visualization of the building performance, the program RStudio is used which is developed for statistical computing and graphics [43].

For the performance on building level the electricity and gas consumption including the indoor climate are analyzed. Since the indoor climate related parameters are often not measured by the BMS, a questionnaire has been drawn up to determine possible problems. In the case that occupants have explicit complaints, additional measurements are necessary. Subsequently, the performance of the installations of the HVAC system is analyzed. Research has shown that this can be done quickly by means of energy profiles which provides insight into energy waste. These energy profiles primarily show the dependency of the outdoor temperature on the energy consumption [15]. When the general system performance is clear, the components of the underperforming installations are analyzed in detail. This will provide insights into the system inefficiencies.

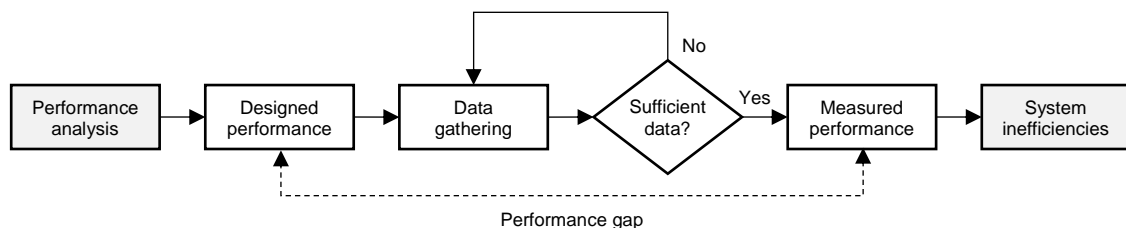


Figure 3.2: Schematic overview of the performance analysis

## 3.3 LEAN energy analysis

At the third step, the potential energy performance of both case study buildings is modeled based on the LEAN energy analysis. The schematic overview of this performance modeling is shown in Figure 3.3. First, a framework is determined with the needed variables. Then, the modeling consist of a benchmark model and empirical data. The benchmark model that uses regression can be obtained in various ways. In this study, historical data from both buildings is used to create the benchmark model. When the model is validated, the performance is predicted and compared with empirical data. The difference between the predicted energy consumption by the benchmark model and the actual measured energy consumption represents an indication of the energy saving potential. This will lead to a conclusion about the potential energy performance.

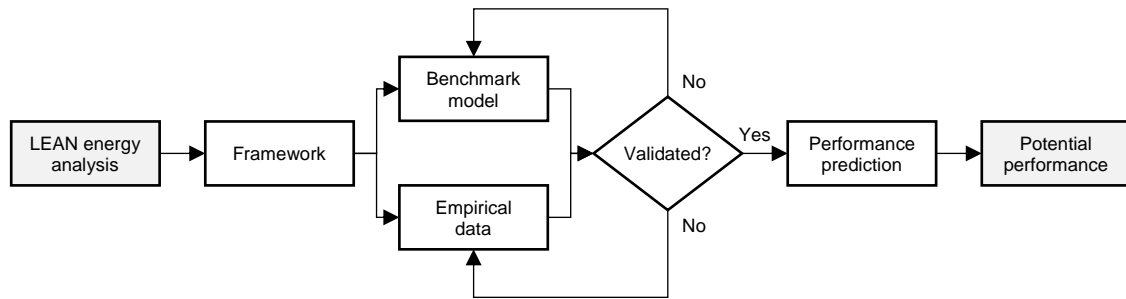


Figure 3.3: Schematic overview of the LEAN energy analysis

## 4 Case study buildings

This chapter introduces the two case study buildings: Larisa and Kropman Breda.

### 4.1 Larisa

#### Building description

The care center Larisa is located in the southwest of the city center of Maastricht, see Figure 4.1. The five-story building is constructed in 2016 and has a gross floor area (GFA) of 7,070 m<sup>2</sup>. In contrast to the developments in the last decade in which small-scale group homes have been designed, larger living groups are accommodated in this building. The care center has 90 housing units of about 28 m<sup>2</sup>, mainly for people who suffer from dementia. In addition to the private rooms there is a restaurant on the ground floor, a small cinema, a beauty salon, a library and a music room [44]. The general building properties are presented in Table 4.1. Appendix A.1 provides the floor plans (Figures A.1 to A.5).

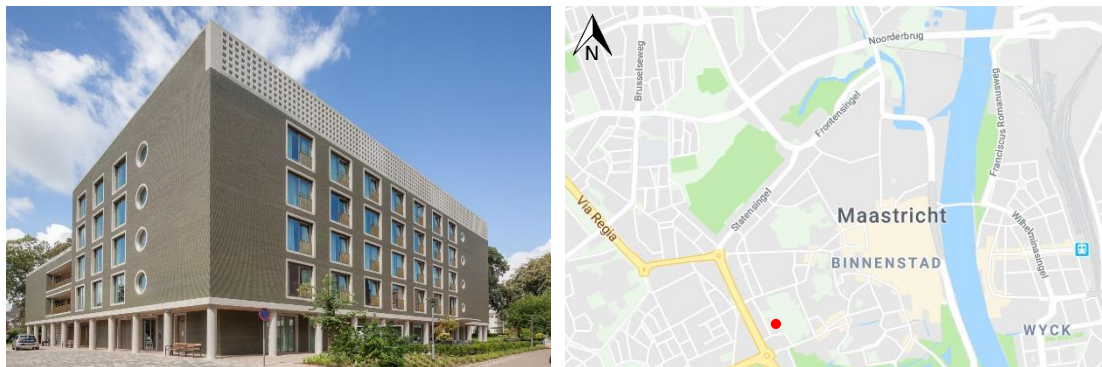


Figure 4.1: Impression (left) and location (right) of Larisa

Table 4.1: Building properties of Larisa

General information	
Name	Larisa
Location	Maastricht, the Netherlands
Year of construction	2016
Year of renovation	-
Building function	Healthcare
Gross floor area	7,070 m <sup>2</sup>
Number of floors	5
EPC	0.933
Building envelope	Floor: R = 4.5 m <sup>2</sup> -K/W, wall: R = 3.5 m <sup>2</sup> -K/W, roof: R = 3.5 m <sup>2</sup> -K/W
External windows	U = 1.7 W/m <sup>2</sup> -K

#### System description

The building contains modern installations, shown in Figure 4.2. The heating and cooling demand of the building is generated by an ATES system with a heat pump. For heating peaks, the building is equipped with two gas boilers. The cold is generally provided directly by the ATES system without heat pump. The heat and cold is subsequently supplied by three air handling units (AHUs) and by three concrete core activation (CCA) systems which use the thermal mass. On floor level, the supplied air is reheated by electrical duct heaters.

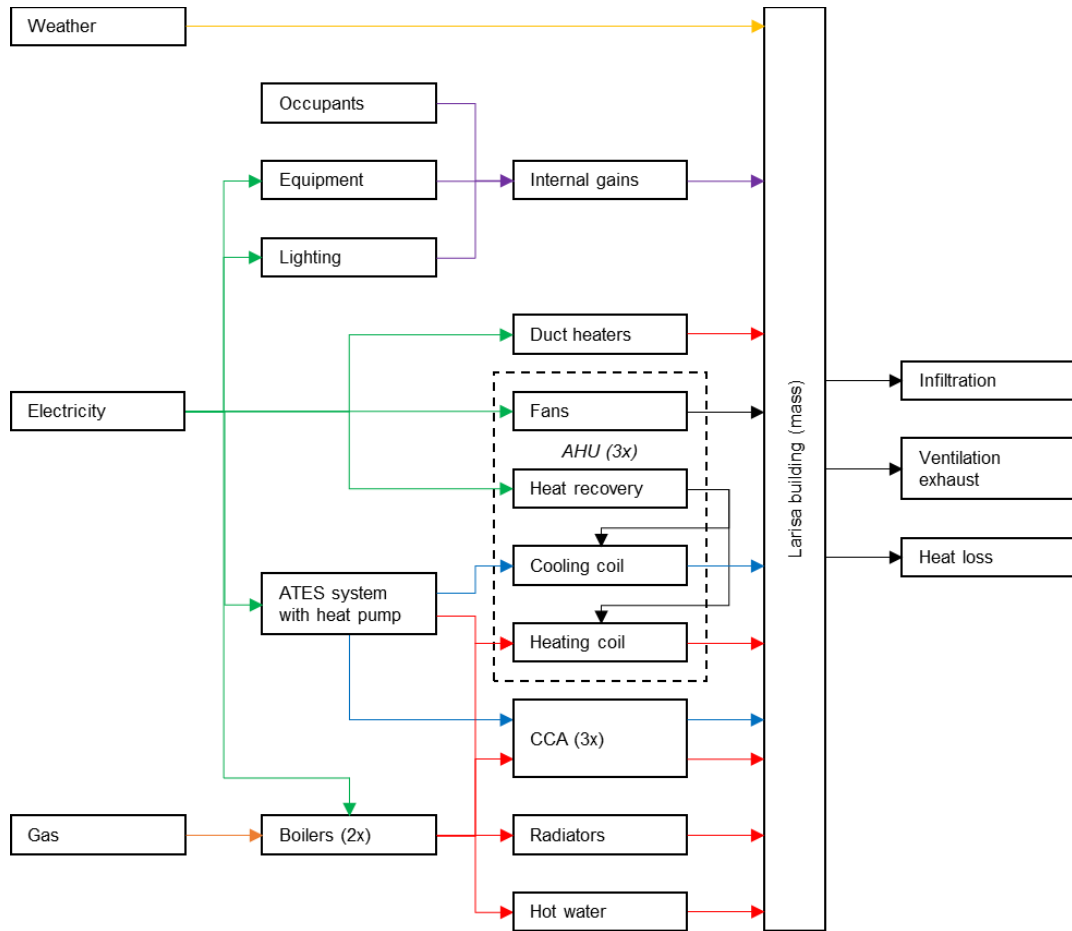


Figure 4.2: Flowchart principle of Larisa

## 4.2 Kropman Breda

### Building description

The office building Kropman is located in the west of the city Breda, see Figure 4.3. Kropman is a large building services company in the Netherlands with experience in the field of design, realization, management and operation of HVAC systems. The building is built in 1993 and renovated in 2009. The three-story high building has a GFA of 1,650 m<sup>2</sup>. This makes it a representative office building for the Dutch building stock. The building contains 59 workplaces, a storage and a restaurant. The general building properties are presented in Table 4.2. The floor plans of the building can be found in appendix B.1 (Figures B.1 to B.3).



Figure 4.3: Impression (left) and location (right) of Kropman Breda



Table 4.2: Building properties of Kropman Breda

General information	
Name	Kropman Breda
Location	Breda, the Netherlands
Year of construction	1993
Year of renovation	2009
Building function	Office
Gross floor area	1,650 m <sup>2</sup>
Number of floors	3
EPC	Unknown
Building envelope	Floor: R = 2.5 m <sup>2</sup> -K/W, wall: R = 2.5 m <sup>2</sup> -K/W, roof :R = 2.5 m <sup>2</sup> -K/W
External windows	U = 3.2 W/m <sup>2</sup> -K

**System description**

Currently, the office building is equipped with quite traditional installations, shown in Figure 4.4. The heating demand is generated by a gas boiler which provides heat to the AHU and the radiators. The cooling demand is produced by a cooling machine. The building is ventilated by the AHU which contains a heat recovery wheel and an electric steam humidifier. On room level, the air is supplied by ventilation vents. In addition, the building is equipped with PV-panels on the roof in order to provide a part of the electricity demand.

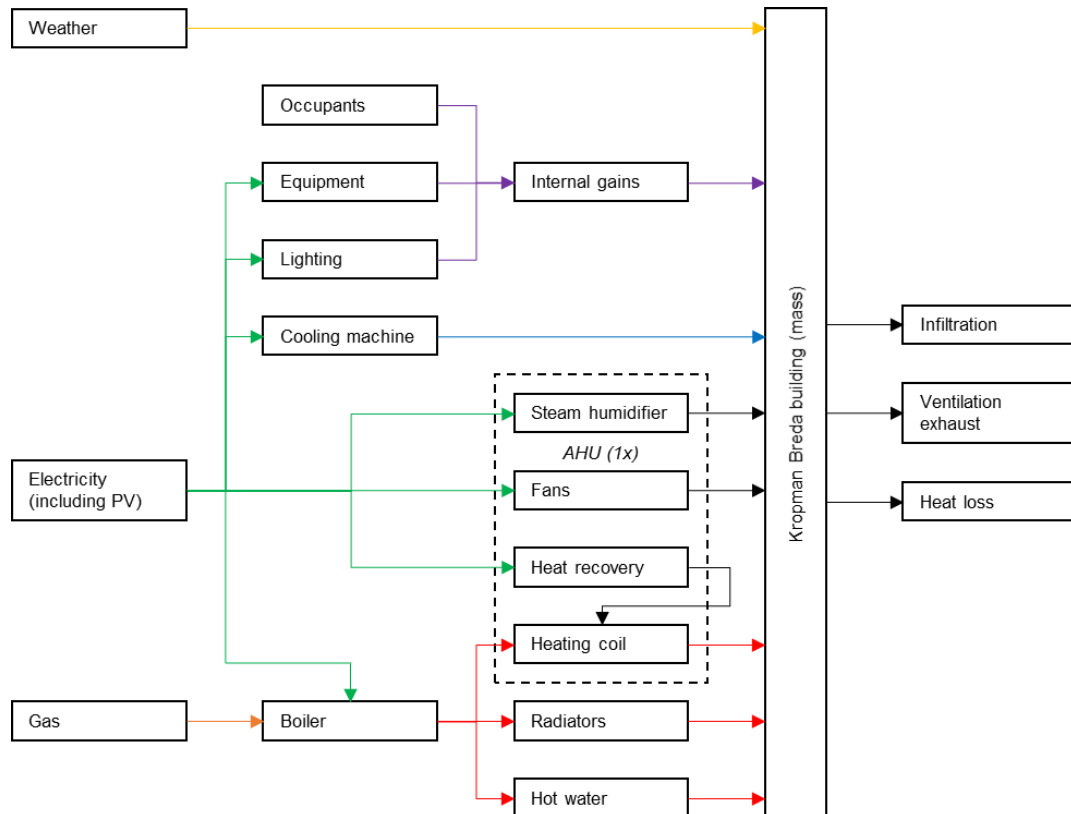


Figure 4.4: Flowchart principle of Kropman

## 5 Case study 1: Larisa

This chapter presents the first case study of the research, care center Larisa. First, the performance indicators are identified by means of the Pareto analysis. Subsequently, the designed performance is analyzed. Then, the measured performance is analyzed which leads to the system inefficiencies. Finally, the energy saving potential is investigated based on the LEAN energy analysis.

### 5.1 Pareto analysis

For the sensitivity analysis, the impact of various main parameters on the electricity, heating and cooling consumption of Larisa is simulated by using EnergyPlus. The created 3D model in SketchUp can be seen in Appendix A.2 (Figure A.6).

#### 5.1.1 Parameters

Ten main parameters are selected related to the HVAC system and the occupant behavior (see Table 5.1). The number of occupants is based on 90 patients and 81 employees. The impact of each parameter is determined by simulating the 10% higher and lower values compared to the design. According to the Pareto analysis, roughly 80% of the performance gap can be identified by 20% of the major selected parameters. This means that the two parameters with the highest impact will be presented as the performance indicators of the case study building.

Table 5.1: Selected main parameters

Parameters	Unit	Design	+10%	-10%	
<i>HVAC system</i>					
1	Set-point heating temp.	°C	21.0	23.1	18.9
2	Set-point cooling temp.	°C	23.5	25.8	21.2
3	Max. heating supply temp.	°C	22.0	24.2	19.8
4	Min. cooling supply temp.	°C	17.0	18.7	15.3
5	Ventilation flow rate:				
	- AHU intake	m <sup>3</sup> /s	3.34 / 4.12 / 3.30	3.67 / 4.53 / 3.63	3.01 / 3.71 / 2.97
	- AHU exhaust	m <sup>3</sup> /s	3.16 / 4.13 / 2.36	3.48 / 4.54 / 2.60	2.84 / 3.72 / 2.12
6	Heat recovery	%	80	88	72
<i>Occupant behavior</i>					
7	Occupant presence	n	171	188	154
8	Internal heat occupants	W/pers.	85.0	76.5	93.5
9	Internal heat lighting	W/m <sup>2</sup>	8.0	8.8	7.2
10	Internal heat equipment	W/m <sup>2</sup>	5.4	5.9	4.9

#### 5.1.2 Performance Indicators

The impact of the selected parameters on the annual electricity, heating and cooling consumption is presented in Figure 5.1. By stimulating 10% higher and lower values than designed, the energy consumption can increase or decrease.

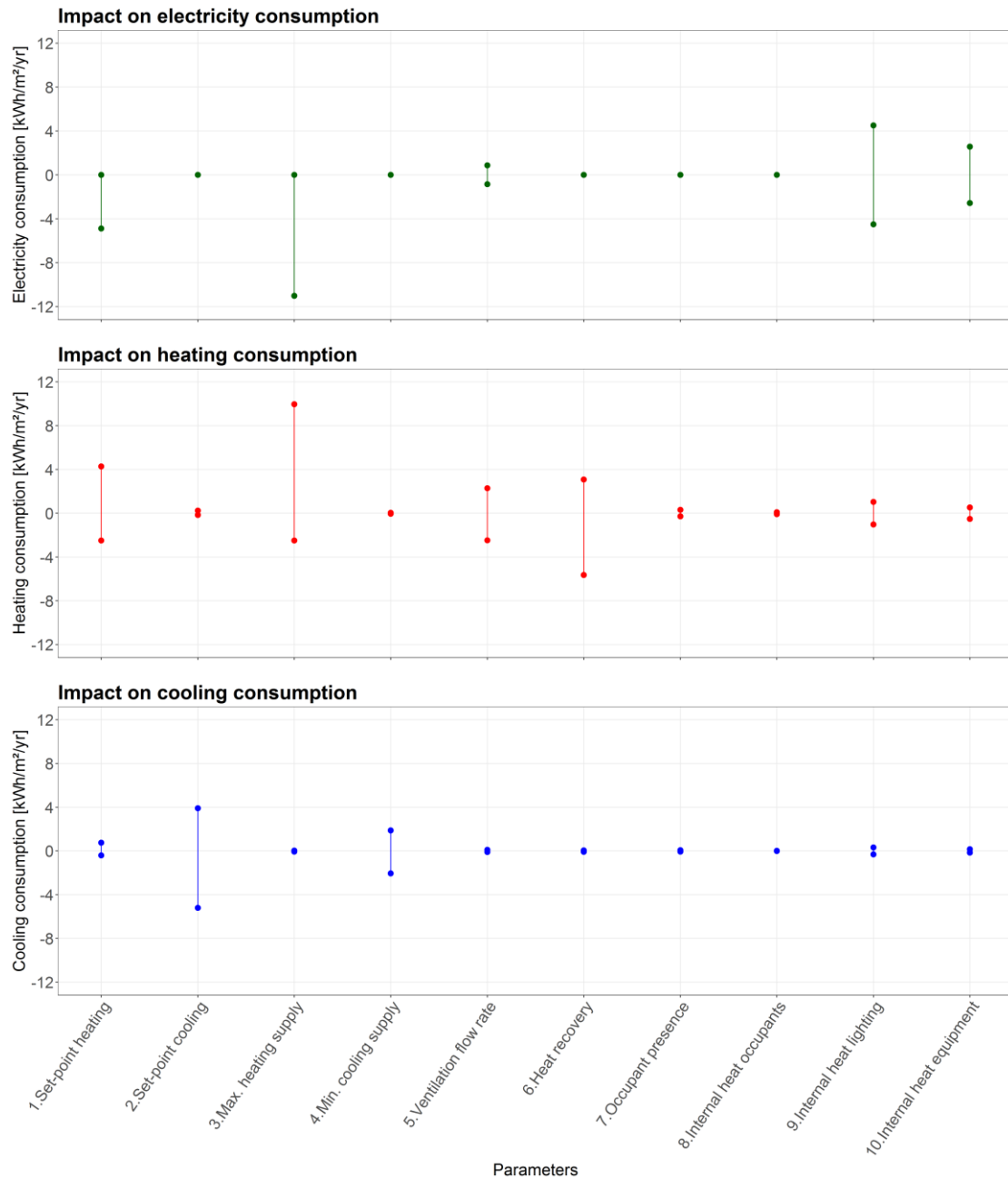


Figure 5.1: Impact on the electricity (green), heating (red) and cooling (blue) consumption when the parameters are 10% higher or lower than designed

In order to determine the performance indicators, the maximum impact (positive or negative) of each parameter on the total impact of all parameters is ranked, scored and grouped. The impact on the annual electricity, heating and cooling consumption is shown in Figures 5.2 to 5.4. As mentioned before, the two parameters with the highest impact are the performance indicators of the case study building.

On the electricity consumption, the maximum heating supply temperature (46%) and the set-point heating temperature (20%) have the highest impact. For the heating consumption, the most important parameters are the maximum heating supply temperature (41%) and efficiency of heat recovery (23%). On the cooling consumption, the set-point cooling temperature (59%) and the minimum cooling supply temperature (23%) have the largest impact. This means that the performance indicators are only related to the parameters of the HVAC system.

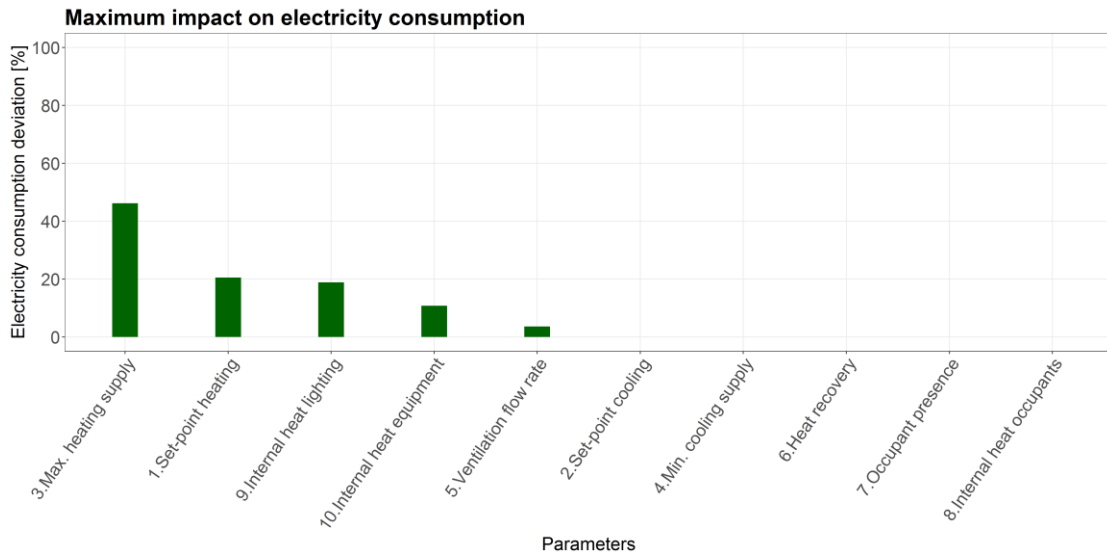


Figure 5.2: Ranking of the maximum impact on the electricity consumption

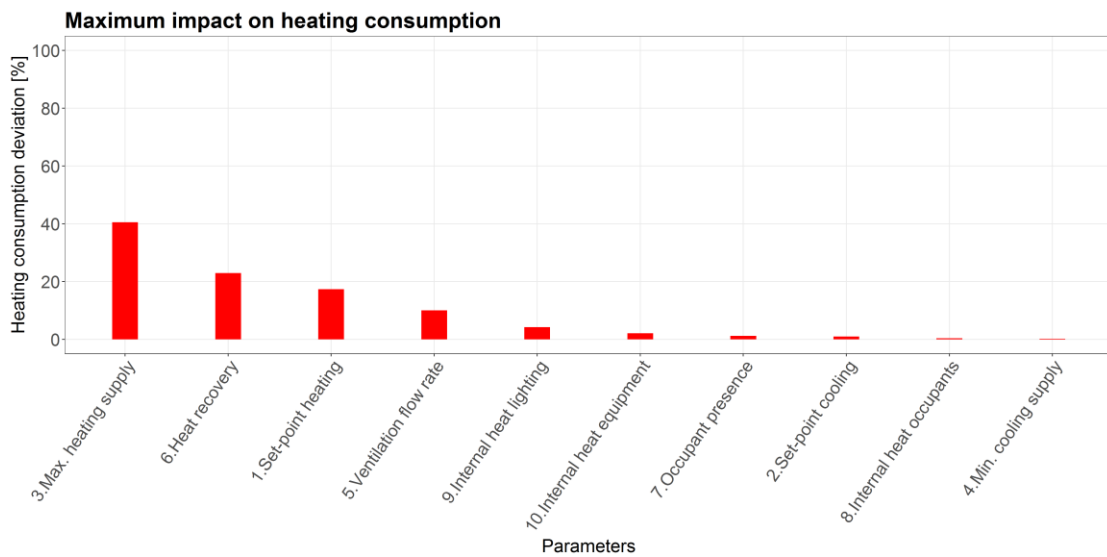


Figure 5.3: Ranking of the maximum impact on the heating consumption

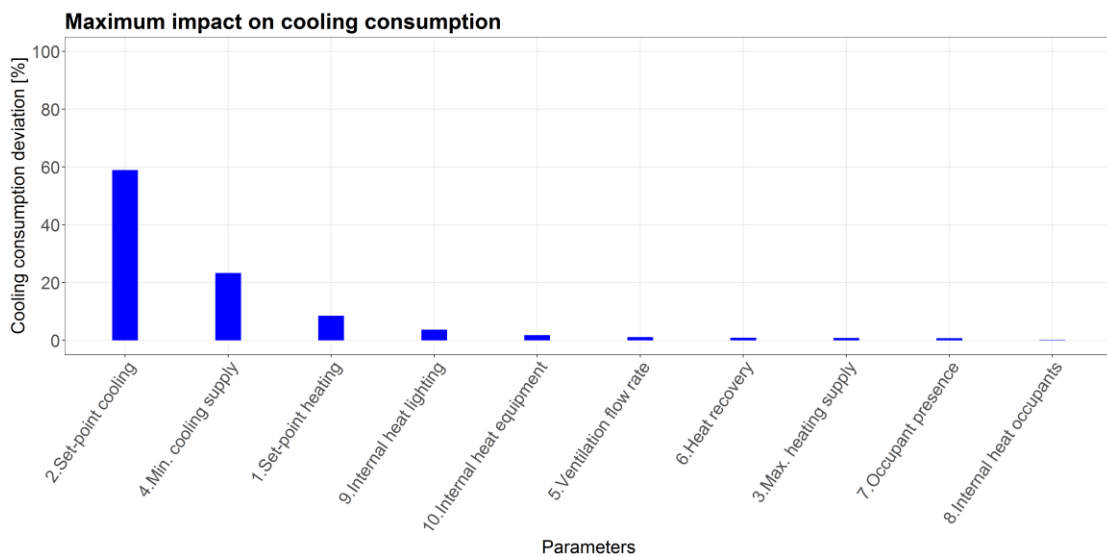


Figure 5.4: Ranking of the maximum impact on the cooling consumption

### 5.1.3 Discussion

Since energy performance gaps are caused by many reasons, it is hard to identify the 20% most important parameters which are accounted for 80% of these gaps. Based on the sensitivity analysis, the two parameters with the highest impact on the electricity consumption are responsible for 66% of the total impact. On the heating consumption of the building, the two major parameters are accounted for 64%. On the cooling consumption, the two parameters are responsible for 82%. This means that only the parameters of the cooling consumption comply with the principle of Pareto analysis.

Nevertheless, the Pareto analysis is a systematic way to identify performance indicators. At the first case study building, the set-points for heating and cooling and the related supply temperatures are the most important parameters. Although the selected parameters not always identify the 80% of the performance gap, it contributes to focus on the major parameters of the HVAC system during the designed and measured performance analysis.

## 5.2 Designed performance analysis

To provide a pleasant indoor climate the building contains a state of art HVAC system summarized in Table 5.2.

Table 5.2: HVAC system of Larisa

HVAC system	Energy conversion	Distribution	Supply	Recovery
Heating	- ATES + heat pump (base load) - Gas-fired boiler (peak load + DHW)	- Air - Water	- Balanced ventilation - Concrete Core Activation - Radiators - Local duct heaters	- Heat recovery wheel
Cooling	- ATES + heat pump in cooling mode	- Air - Water	- Balanced ventilation - Concrete Core Activation - Night ventilation	- Heat recovery wheel
Ventilation	- Air handling unit	- Air	- Balanced ventilation	- Heat recovery wheel
Humidification	- Not applied	-	-	-

### 5.2.1 Energy conversion

#### ATES with heat pump

The ATES system consists of a warm and a cold well on a depth of 60 m (Figure 5.5). The system has two operation modes: a heating mode and a cooling mode. The pumps of the wells are limited at a maximum flow rate of 30 m<sup>3</sup>/h. Appendix A.3 provides the installation principle of the ATES system including heat pump and two stratified thermal buffers (Figure A.7).

During the heating mode, groundwater is extracted from the warm well and transferred to the condenser of the heat pump. The heat pump increases the extracted temperature in order to make it useful to warm up the building. The cold of the building is subsequently injected into the cold well with a temperature of about 7°C. The heat pump has a theoretical coefficient of performance (COP) of 5.25 at full load condition according to the technical specifications of the manufacturer. This document can be found in Appendix A.3 (Figure A.8).

When the system switches to cooling mode, the direction of the groundwater flow is reversed. Groundwater is extracted from the cold well which has been cooled down during the heating mode. In general, the extracted temperature corresponds to the desired supply temperature of the building. This means that the building is directly cooled by groundwater, without assistance of the heat pump (passive cooling). When the cooling power is not sufficient or the extracted temperature is too high, the heat pump will be used as cooling machine to assist (active cooling). The heat of the building during this mode is injected with a temperature about 18°C into the warm well. The energy efficiency ratio (EER) of the heat pump during cooling mode is shown in the technical specifications (Figure A.8 of Appendix A.3).

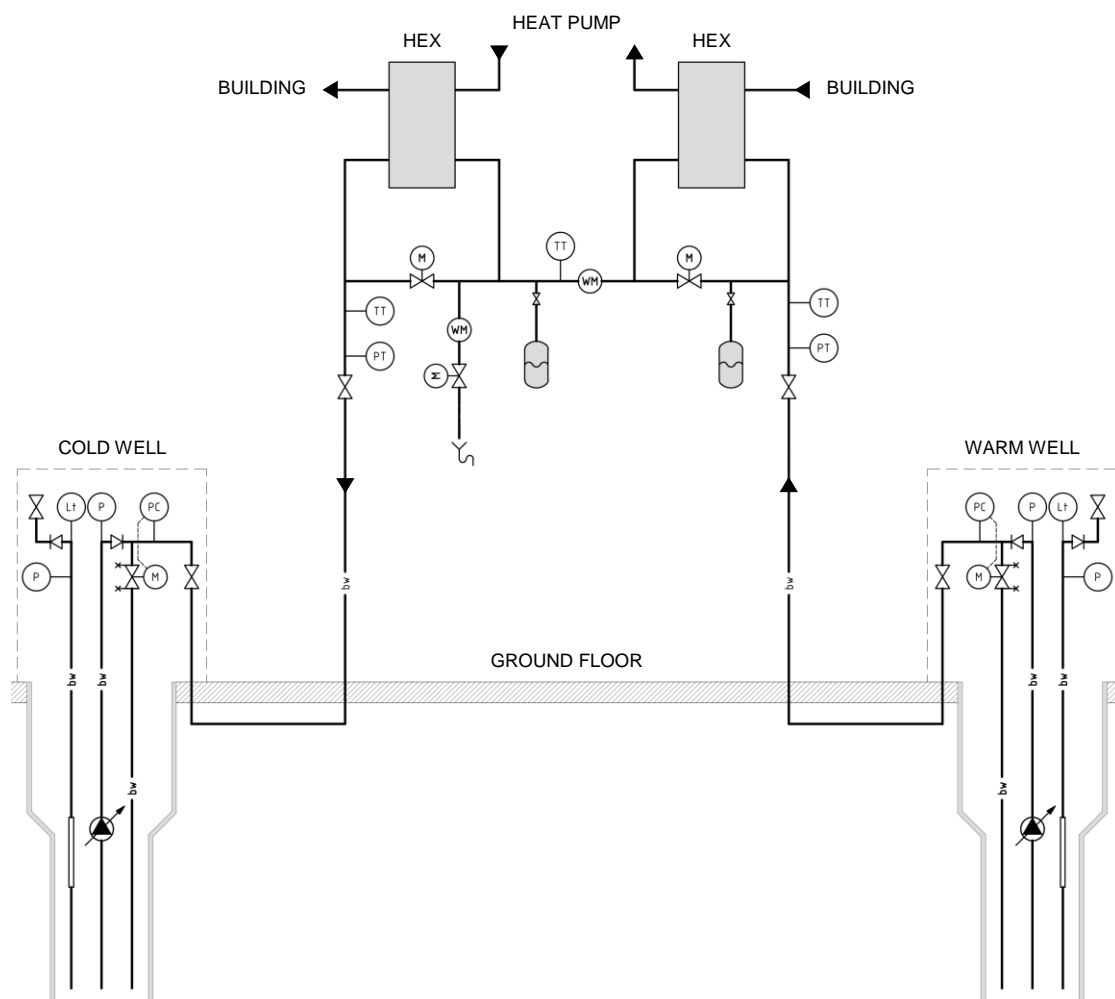


Figure 5.5: ATEs system during heating mode

## 5.2.2 Supply

### Air handling units

The building is equipped with three AHUs: one for the low-rise part (AHU-1), one for the high-rise part (AHU-2) and one for the restaurant (AHU-3). Because the building is 24/7 in operation, AHU-1 and AHU-2 continuously ventilate the rooms. AHU-3 is not operating during the night, since then the restaurant is not used then. The AHUs contain a heat recovery wheel and a central heating and cooling coil.

The supply temperature of the ventilation air is centrally controlled by means of heating curves which are based on the outdoor temperature ( $T_e$ ) (Figure 5.6). The heating curve of AHU-1 deviates from AHU-2 and AHU-3. On room level, the air is supplied to the room by ventilation vents and if necessary reheated by electrical duct heaters. The air is extracted by the AHUs again and leaves the building by passing the heat recovery wheel. During summer nights, night ventilation is used to passively cool down the building with outside air. The building does not provide humidification of the supplied air.

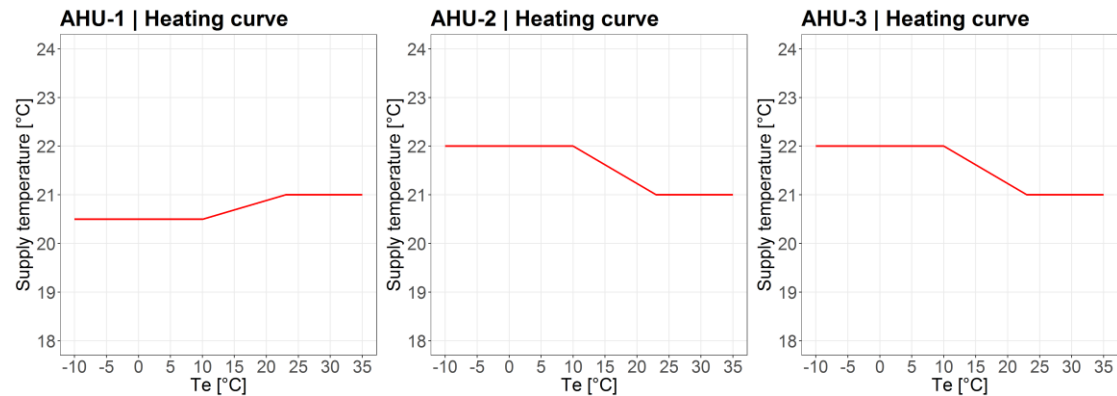


Figure 5.6: Heating curve of the three AHUs (AHU-1 for low-rise, AHU-2 for high-rise and AHU-3 for restaurant)

### Concrete core activation

The three CCA systems use the thermal mass of the building in order to contribute to the desired indoor temperature. Due to the high insulated outer walls combined with concrete floors, a thermal buffer between the indoor and outdoor climate is created. The systems slowly increase or decrease the indoor temperature by 1°C in about five hours. The heating and cooling mode is determined by a heating curve depending on the outdoor temperature of the last three days (Figure 5.7). Between these modes, a neutral zone is set between an outdoor temperature of 18°C and 22°C. The minimum supply temperature of 18°C is determined in order to prevent condensation on the floors. All three systems have similar heating curves.

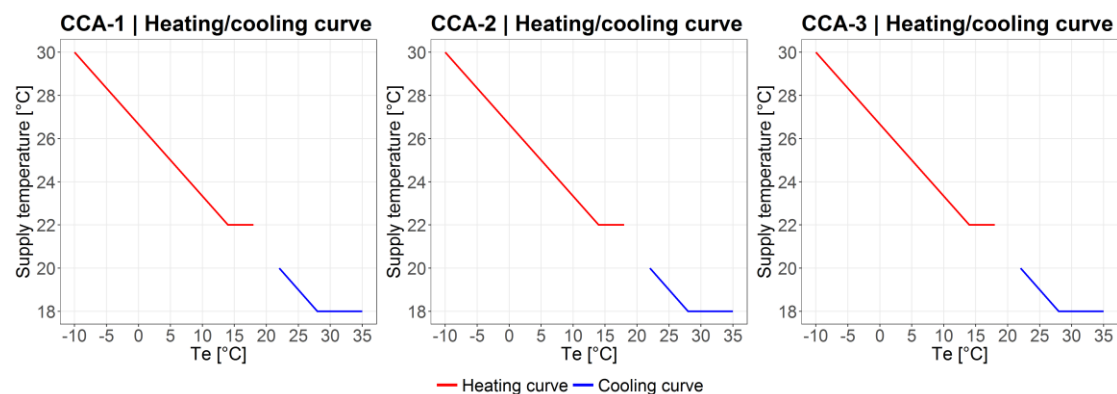


Figure 5.7: Heating and cooling curve of the three CCA systems (CCA-1 for low-rise, CCA-2 and CCA-3 for high-rise and restaurant)

## 5.2.3 Discussion

The best way to analyze and assess the operational performance of the ATES system is by means of the measured amount of thermal energy extraction in combination with the extraction and injection temperatures. The performance of the heat pump can be determined by the COP.

The operational performance of the supply installations can be analyzed and assessed by means of the designed and set heating and cooling curves. When measurements deviate strongly from these curves, this indicates inefficiencies of the system. Therefore, these underperforming parts of the system must subsequently be analyzed on component level.

## 5.3 Measured performance analysis

The performance analysis is conducted following a top-down approach. First, the total measured energy consumption is compared with the designed energy consumption. Subsequently, the analysis of the electricity and gas consumption on building level including the indoor climate is discussed. Then, the HVAC system is analyzed, divided into energy conversion and supply installations. Finally, the underperforming installations are analyzed on component level.

The analysis is based on data derived in different reading levels and time steps (see Table 5.3). The data is measured in the period August 2017 up to and including July 2018. However, data related to the HVAC system has not been logged in April 2018 due to a technical failure. A detailed overview of specific sensors of the BMS can be found in Appendix A.4 (Table A.1). Moreover, Appendix A.4. given the heat maps of the energy consumption including the outdoor temperature (Figures A.9 to A.11)

Table 5.3: Available data of the building

Data	Source	Reading level	Interval	Period
Electricity	Smart meter	Building level	15-minute	August 2017 - July 2018
Gas	Smart meter	Building level	Hourly	August 2017 - July 2018
HVAC system	BMS	System level	32-minute	August 2017 - July 2018 <sup>[1]</sup>

[1]: Data not logged in April 2018

### 5.3.1 Energy consumption

#### Energy performance gap

During the design of the building, an Energy Performance Coefficient (EPC) of 0.933 and a total primary energy consumption of 756 MJ/m<sup>2</sup>/year was calculated. This is only based on the building-related energy consumption. To compare the measured with the designed energy consumption, the expected user-related energy consumption is added to the designed energy consumption. In addition, the measured energy consumption has to be converted to the primary energy, by multiplying the measured electricity consumption with 2.5 and the measured gas consumption with 1.0 [45].

The results of the comparison are presented in Figure 5.8. In the period August 2017 up to and including July 2018, the measured primary energy consumption is 1.26 times higher than designed. This leads to a theoretically energy saving potential of about 21% when the EPC calculation is correctly performed. Nevertheless, the measured energy consumption is lower than the average energy consumption of care centers in the Netherlands [46].



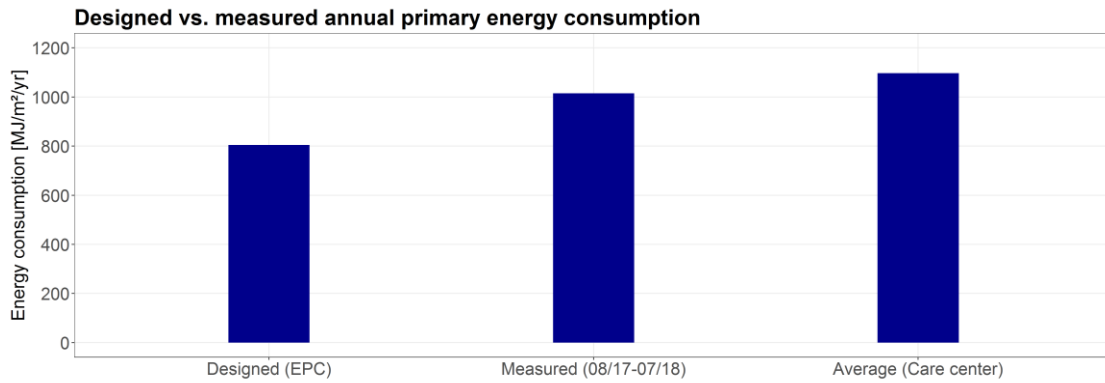


Figure 5.8: Comparison between the designed and measured annual primary energy consumption of care center Larisa including the average in the Netherlands

### Electricity consumption

The electricity consumption is only obtained on building level by means of a smart meter. Figure 5.9 shows the hourly electricity consumption during the year and related to the outdoor temperature ( $T_e$ ), where the density of the measured points is indicated. The base load of the electricity consumption is nearly  $7 \text{ Wh/m}^2/\text{h}$ . Based on a calculation it can be concluded that the fans are accounted for about 70% ( $5 \text{ Wh/m}^2$ ) of this base load. This is because the building is 24/7 in operation.

The increase in electricity consumption is very dependent on the outdoor temperature. The outliers only occur relatively few hours per year. At outdoor temperatures lower than about  $15^\circ\text{C}$  the consumption rises significantly, while the consumption is relatively low at higher outdoor temperatures. This is due to the increasing demand of the AHUs and to a lesser extent due to the heat pump. The maximum electricity consumption is approximately  $20 \text{ Wh/m}^2/\text{h}$ .

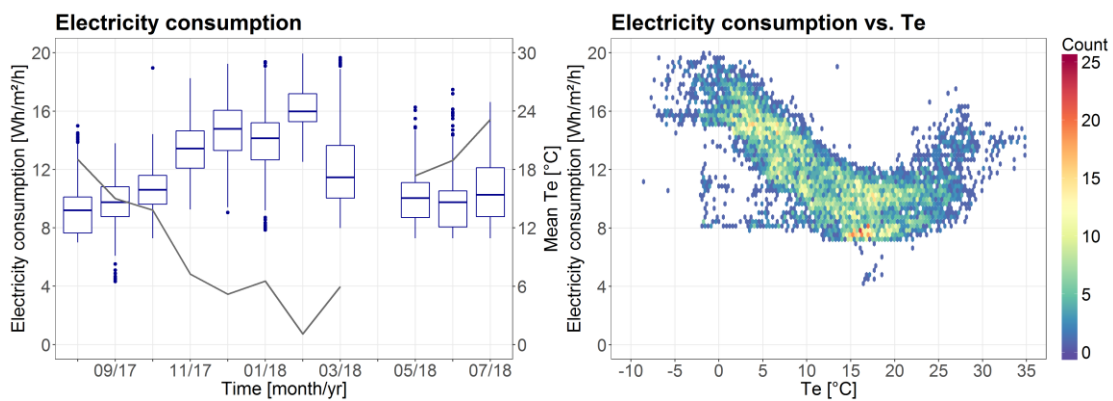


Figure 5.9: Hourly electricity consumption during the year (left) and in relation to the outdoor temperature including the density of the measured points (right)

The mean hourly electricity consumption during the seasons is presented in Figure 5.10. As expected, the patterns during the weekdays and the weekend are very similar to each other. Most days start with a peak during the morning, in order to obtain a pleasant indoor climate. This is followed by a decrease in the afternoon and a small peak in the late afternoon. Only the base load of the electricity consumption varies between the seasons, with the lowest load during the summer and the highest load during the winter.

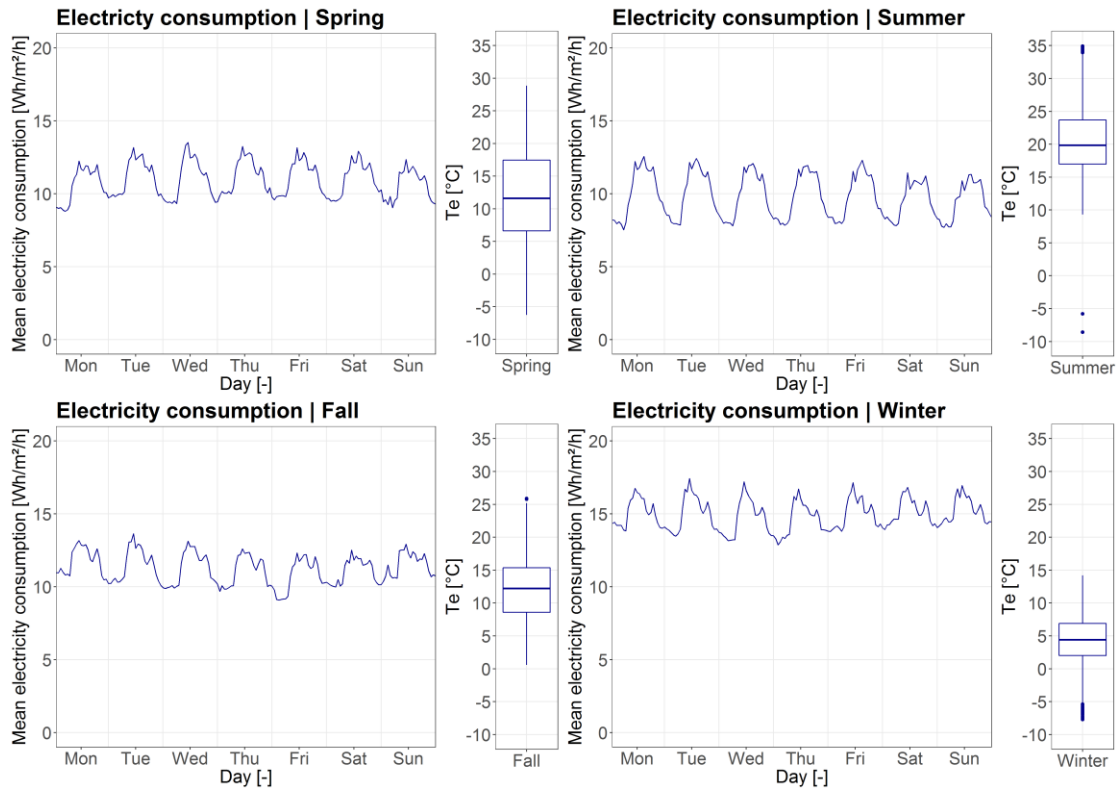


Figure 5.10: Mean hourly electricity consumption and outdoor temperature during the seasons

### Gas consumption

Gas is used by the two boilers and in the kitchen of the restaurant. Figure 5.11 shows the gas consumption during the year and related to the outdoor temperature. During the measured period, the bandwidth fairly remains relatively low and constant, also at a low outdoor temperature. Only when the outdoor temperature is below 2°C, the consumption increases during some hours.

In the Netherlands, a heat pump normally provides about 70% of the total heating demand and a secondary installation (gas boiler) is used for peak heating loads. Based on the measurements, it can be concluded that the gas is generally used for domestic hot water (DHW). This means that the heat pump of this building is larger dimensioned than normally financially attractive. However, this system could be appealing in the long run due to the gas free transition.

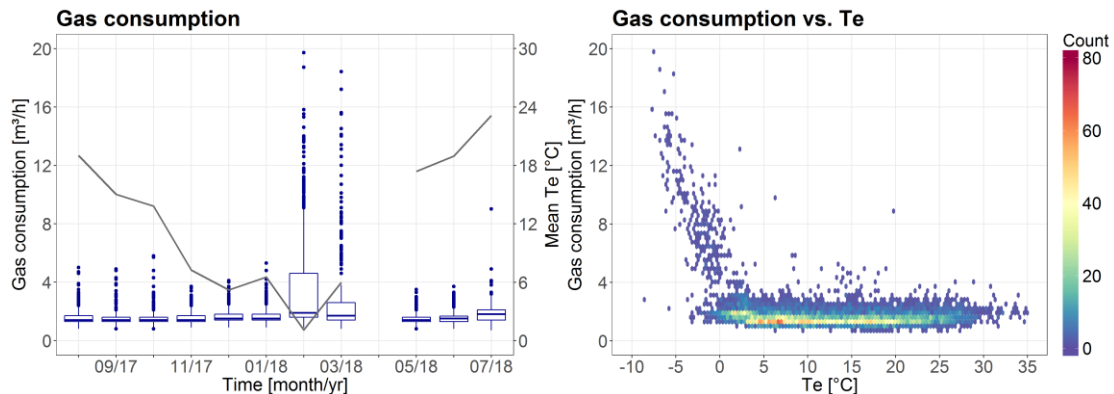


Figure 5.11: Hourly gas consumption during the year (left) and in relation to the outdoor temperature including the density of the measured points (right)

The mean hourly gas consumption during the seasons is presented in Figure 5.12. As usual, the gas consumption is the highest in the winter. On every day of the week there are peaks to generate heat for the building. During the other seasons, the consumption is quite constant. The small peaks are particularly caused by occupant behavior. The base load between all seasons is about the same.

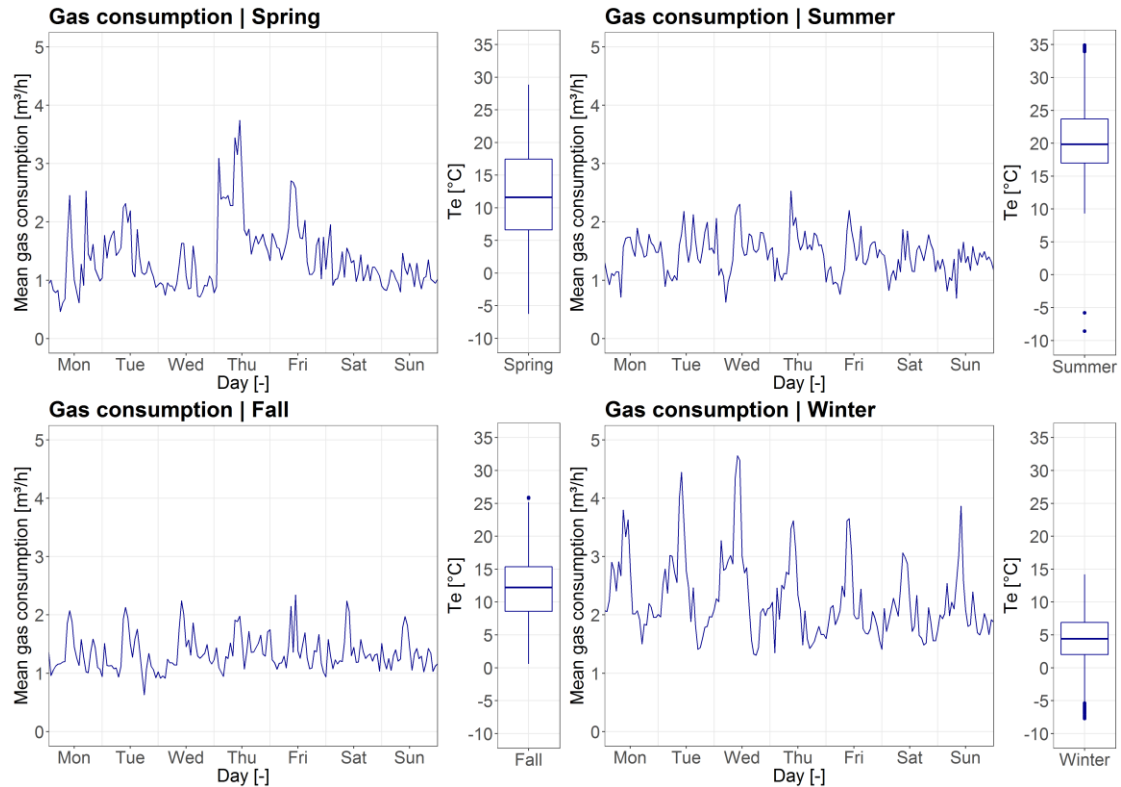


Figure 5.12: Mean hourly gas consumption and outdoor temperature during the seasons

### 5.3.2 Indoor climate

In order to properly assess the performance of the HVAC system, the indoor climate has to be taken into account. These results are very important, since they determine the well-being and productivity of the patients and employees. However, the BMS of Larisa does not measure any of the parameters related to the indoor climate. Therefore, the exhaust temperature by the three AHUs is used as indication for the indoor temperature.

During day and night, the minimum required indoor temperature is 21°C and the maximum required indoor temperature is 24°C. These requirements are compared with the measured exhaust temperature, see Table 5.4. It shows that the exhaust temperature is sometimes higher than the required indoor temperature. Nevertheless, in Figure 5.13 can be seen that the mean air temperature in the low-rise, the high-rise and the restaurant meets the requirements.

Table 5.4: Required and measured indoor temperature

Air temperature	Unit	Required		Measured		
		Min.	Max.	Min.	Max.	Avg.
AHU-1 (low-rise)	°C	21.0	24.0	21.6	24.3	22.5
AHU-2 (high-rise)	°C	21.0	24.0	22.3	25.2	23.6
AHU-3 (restaurant)	°C	21.0	24.0	21.5	24.9	23.1

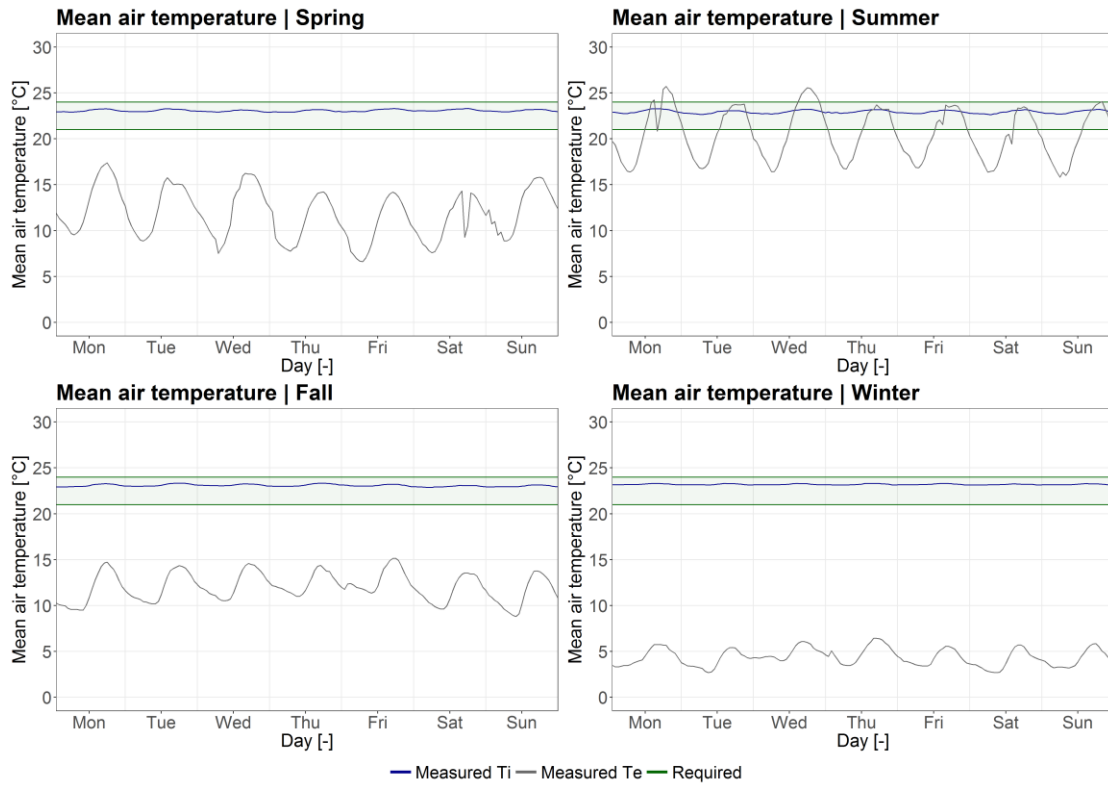


Figure 5.13: Mean hourly indoor and outdoor temperature during the seasons

To obtain a good impression about the other aspects of the indoor climate, five employees have filled out a questionnaire (see Figures 5.14 to 5.16). In general, the employees of the building are satisfied about the performance, except for a few complaints. In the winter, they sometimes find the indoor temperature too high and the air too dry. In the summer, the employees sometimes suffer from drafts and dry air in the building. Since these complaints do not occur very often, no additional measurements regarding the indoor climate are needed.

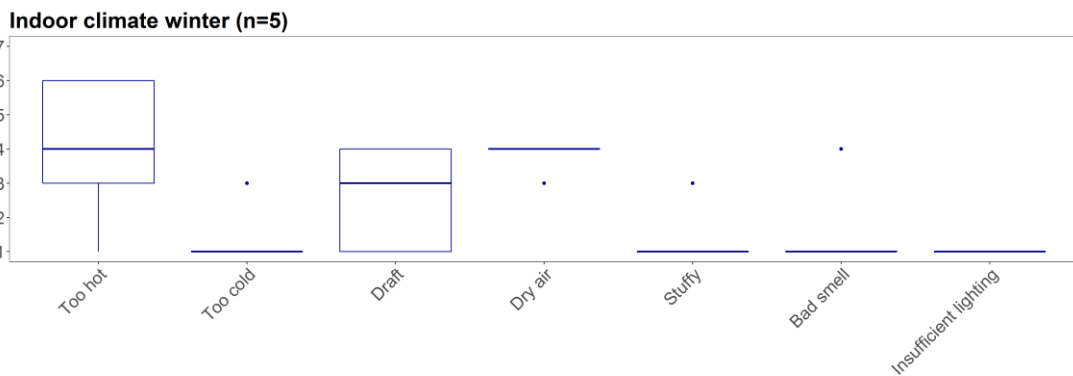


Figure 5.14: Experience of the employees during the winter, where 1=never (positive), 2=very rarely, 3=rarely, 4=sometimes, 5=often, 6=very often, 7=always (negative)

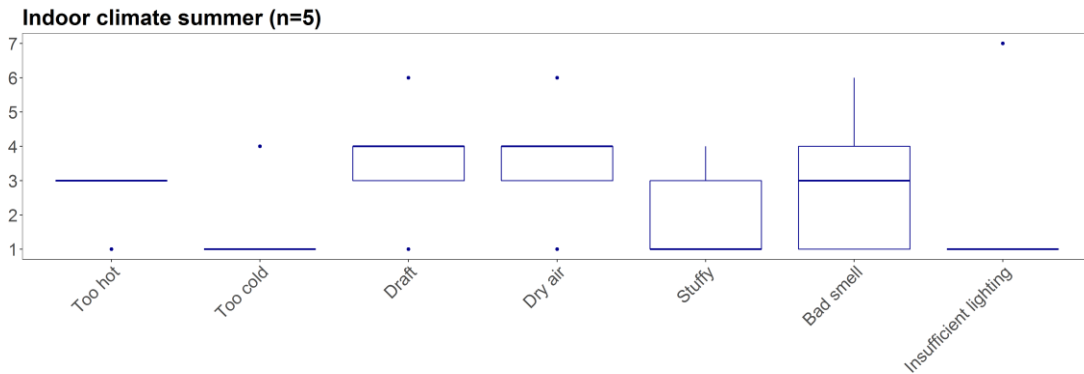


Figure 5.15: Experience of the employees during the summer, where 1=never (positive), 2=very rarely, 3=rarely, 4=sometimes, 5=often, 6=very often, 7=always (negative)

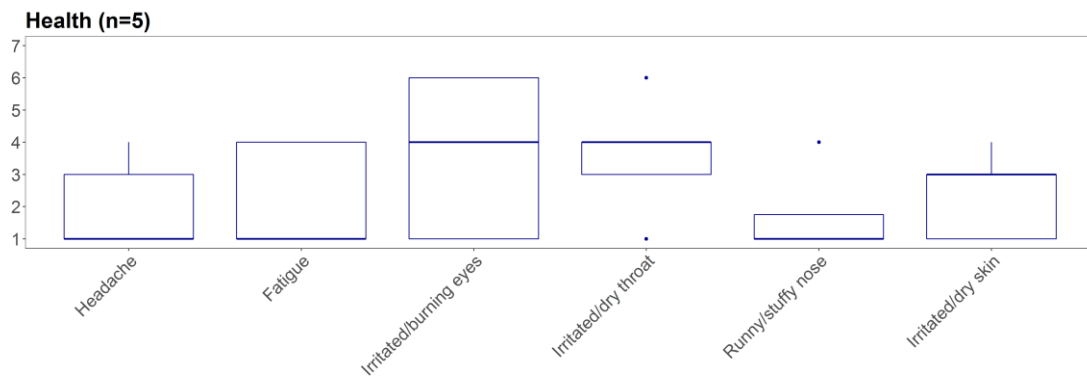


Figure 5.16: Experience of the employees regarding health, where 1=never (positive), 2=very rarely, 3=rarely, 4=sometimes, 5=often, 6=very often, 7=always (negative)

### 5.3.3 Energy conversion

#### ATES system with heat pump

The thermal energy extraction ( $Q$ ) is calculated by multiplying the power of the ATES system (equation 5.1) with time. However, whether the power is related to heat or cold is unknown because the direction of the flow is not measured. Therefore, this is determined based on several criteria, explained in Appendix A.4. This appendix also provides the heat maps (Figures A.16 to A.18) and the related R-script.

$$P = \rho \cdot c_p \cdot \Phi \cdot \Delta T \quad (5.1)$$

With:

$P$	: Thermal power	[kW]
$\rho$	: Density of water (constant)	[kg/m <sup>3</sup> ]
$c_p$	: Specific heat capacity of water (constant)	[kJ/kgK]
$\Phi$	: Water flow in the circuit	[m <sup>3</sup> /s]
$\Delta T$	: Temperature difference between warm and cold water	[°C]

The results of the calculation during the year and related to the outdoor temperature are presented in Figure 5.17. It clearly shows that the extracted amount of energy is very dependent on the outdoor temperature. Only at some high outdoor temperatures, the extracted cooling is significantly high. Since the pattern is very linear, the density of the measured points is not analyzed. The heating process starts at outdoor temperatures lower than 19°C and the cooling process starts at outdoor temperatures higher than 10°C. The slope of the points is a function of the building envelope, ventilation and infiltration air, and the efficiency of the heating or cooling system [32]. The less the slope, the more energy-efficient the building.

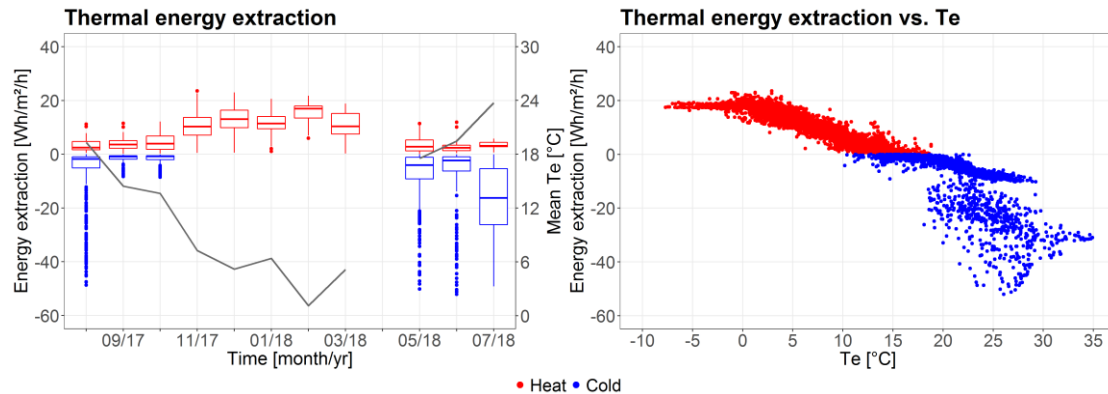


Figure 5.17: Hourly thermal energy extraction during the year (left) and in relation to the outdoor temperature (right)

In order not to disturb nature, it has been laid down by Dutch law that the ATES systems must not disturb the thermal balance in the subsoil. Since the heat and cold demand is dependent on weather conditions and building use, which both change every year, the government requires an equilibrium energy supply over a period of five years [47]. For this reason it is important to determine the thermal balance. This can be calculated by using equation 5.2 [48].

$$Balance_{ATES} = \frac{Q_{cold} - Q_{heat}}{Q_{cold} + Q_{heat}} \tag{5.2}$$

With:

- $Balance_{ATES}$  : Balance of the ATES [%]
- $Q$  : Thermal energy extraction [kWh]

The monthly thermal energy extraction including the thermal balance is shown in Figure 5.18. During the whole measured period, the thermal balance is negative. This means that more heat than cold is extracted, which leads to a total cold surplus of 38%. This is partly inherent to the Dutch climate. Research has shown that the average thermal unbalance of ATES systems in the Netherlands is 22% (positive or negative) [49].

To solve the unbalanced situation, the amount of extracted heat by the system must be reduced. This can be achieved by producing more heat with a secondary installation. However, the generation of more heat by the gas-fired boilers is not sustainable. A more suitable solution is to provide more heat to the warm well during the summer by means of a dry cooler [50]. This principle is called regeneration.

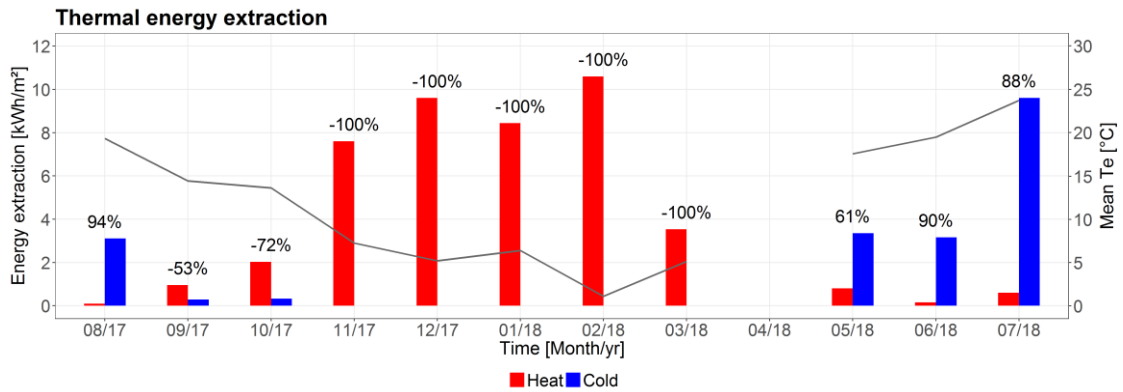


Figure 5.18: Monthly thermal energy extraction by means of the ATES system which results to a total cold surplus of 38%

The mean hourly heat and cold extraction during the seasons is presented in Figure 5.19. Since the building is 24/7 in operation, the daily patterns are similar during each season. As mentioned earlier, the thermal energy extraction is dependent on the outdoor temperature. That is why the extraction varies greatly per season.

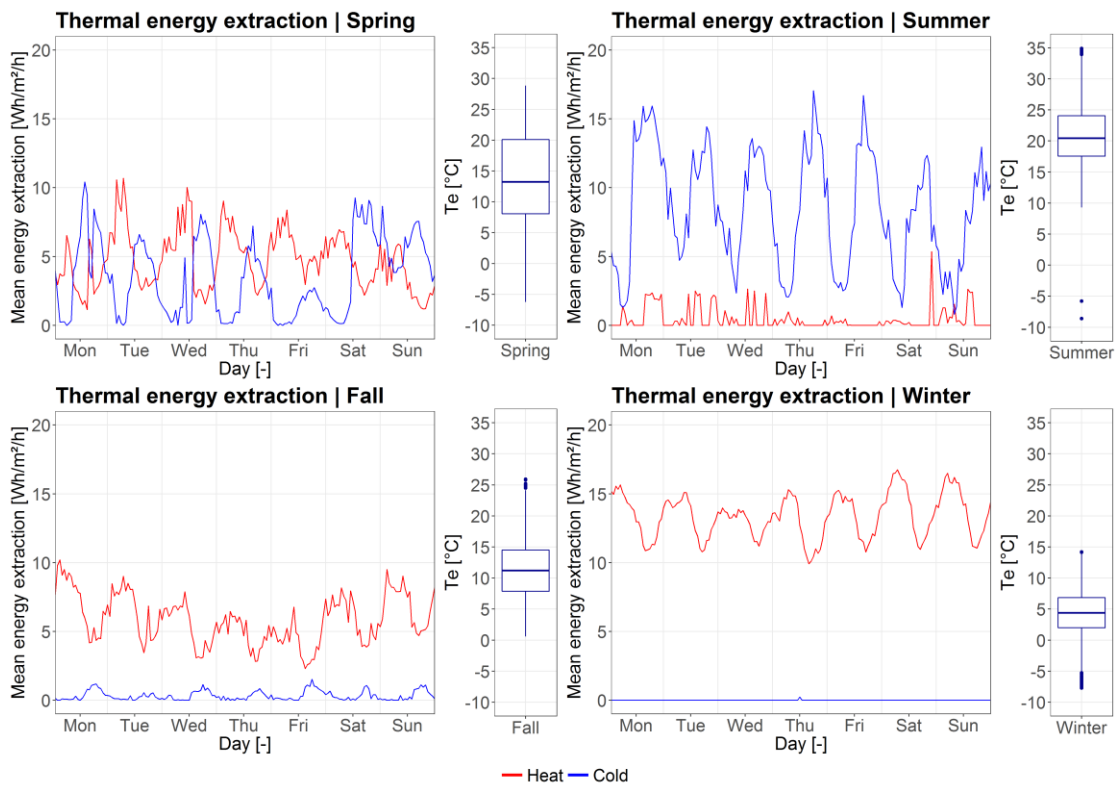


Figure 5.19: Mean hourly thermal energy extraction and outdoor temperature during the seasons

The warm and cold well extraction and injection temperatures are shown in Figure 5.20. The temperature of the ATES varies throughout the year due to the influence of heat losses to the surroundings and the amount of injection and extraction of heat and cold to and from the ground [51].

During heating mode, heat between 13°C and 18°C is extracted from the warm well and injected into the cold well with a temperature between 9°C and 15°C. In the winter, a clear trend of a decreasing extraction temperature from the warm well is shown. This is because the available heat in the warm well decreases during this season.

During cooling mode, cold between 9°C and 15°C is extracted from the cold well and injected with a temperature between 13°C and 18°C into the warm well. According to the design, the injection temperature into the cold well is too high and the injection temperature into the warm well is too low. This is caused by the unbalanced situation.

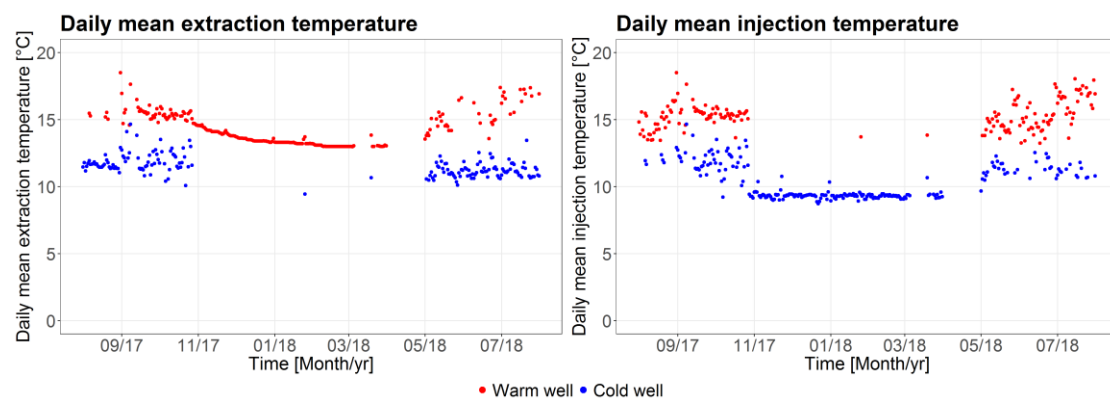


Figure 5.20: Daily mean extraction (left) and injection (right) temperature of groundwater in the warm and cold well during the year

Figures 5.21 and 5.22 presents the hourly extraction and injection temperature during May 2018 up to including August 2018. It clearly shows the deviation in groundwater temperature when the system does not operate continuously in heating mode. This deviating groundwater temperature in both wells leads to a higher energy consumption. This is due to the fact that more groundwater needs to be extracted by the pumps. In addition, it is necessary to increase the capacity of the extracted thermal energy by the heat pump which uses electricity. In order to prevent the depletion of the wells in the future and to comply with the Dutch law, the unbalanced situation has to be solved.

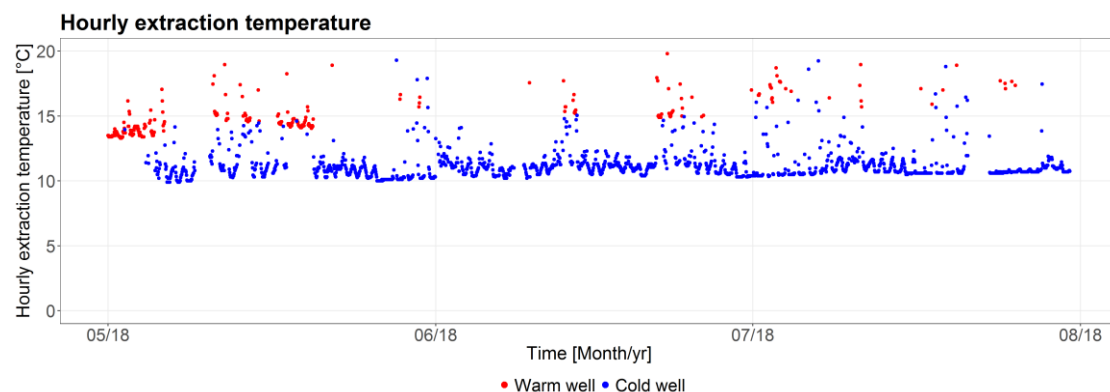


Figure 5.21: Hourly extraction temperature of groundwater in the warm and cold well from May 2018 up to and including July 2018



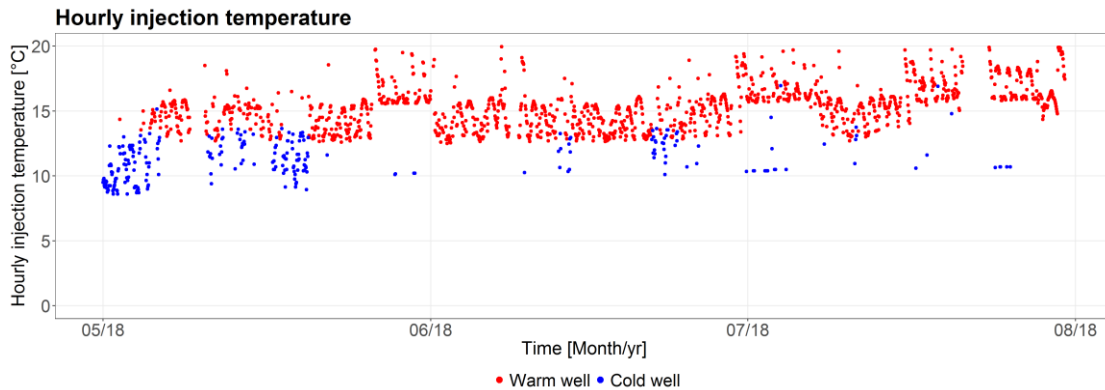


Figure 5.22: Hourly injection temperature of groundwater in the warm and cold well from May 2018 up to and including July 2018

The efficiency of the heat pump is determined by the Coefficient of Performance (COP) during heating and cooling mode. This is the ratio between the transported heat or cold and the difference between the net transported heat and cold (equation 5.3).

$$COP_{heating} = \frac{Q_{heat}}{Q_{heat} - Q_{cold}}, COP_{cooling} = \frac{Q_{cold}}{Q_{heat} - Q_{cold}} \quad (5.3)$$

With:

$COP$  : Coefficient of Performance [-]  
 $Q$  : Transported thermal energy at the heat pump [kWh]

The COP during heating and cooling mode are presented in Figure 5.23. When the heat pump operates as a cooling machine, the daily mean  $COP_{cooling}$  is 2.4. However, most of the time (75%), the building is directly cooled by groundwater, without assistance of the heat pump (passive cooling). The remaining part (25%) is provided using the condenser of the heat pump (active cooling). During heating mode, the daily mean  $COP_{heating}$  is 2.3. Therefore, the measured COP is considerably lower than the designed COP of 5.25.

When the thermal unbalance continues, the  $COP_{heating}$  will decrease and the  $COP_{cooling}$  will increase. This is due to the decreasing groundwater temperature which is caused by the higher heating than cooling load [52]. This leads to more thermal energy extraction in combination with a higher electricity and gas consumption.

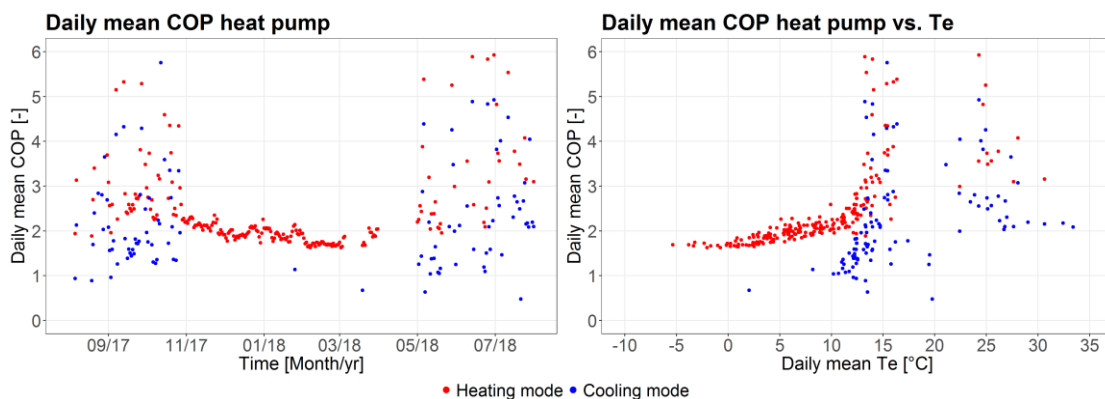


Figure 5.23: Daily mean COP of the heat pump, divided into heating and cooling mode, during the year (left) and in relation to the outdoor temperature (right)

The measured COP is more fluctuating when the outdoor temperature increases. This can be explained by the capacity of the heat pump, shown in Figure 5.24. The heat pump generally operates in part load. From November until April the heat pump runs almost all the time with a capacity larger than 25%. This leads to a COP which slowly decreases due to depletion of the warm well. During the other months, the heat pump runs particularly with a capacity below 25%, resulting in a fluctuating COP. More data is needed to obtain more information regarding the regulation of the operating modes of the system.

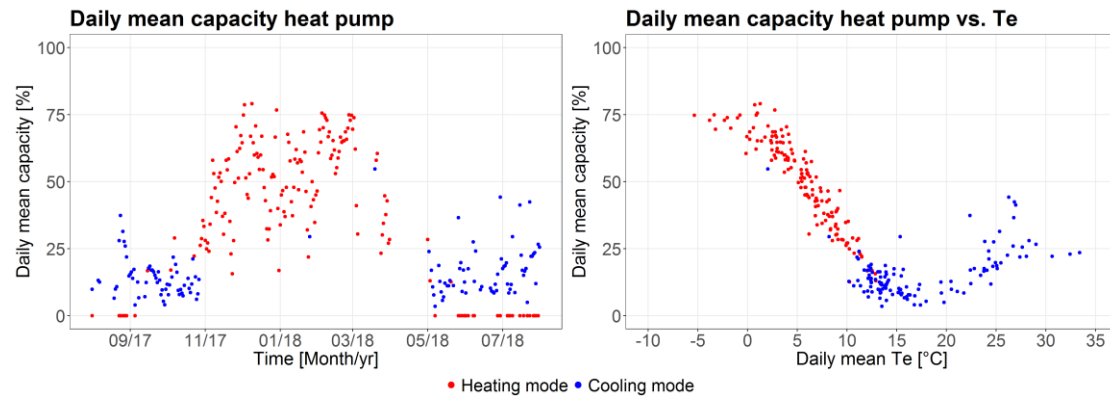


Figure 5.24: Daily mean capacity of the heat pump, divided into heating and cooling mode, during the year (left) and in relation to the outdoor temperature (right)

### 5.3.4 Supply

#### Air handling units

The performance of the three AHUs can be assessed by comparing the measured supply temperature with the designed and set heating curve. Figures 5.25 to 5.27 show the supply temperature of the AHUs during the year and related to the outdoor temperature, where the density of the measured points is indicated.

The supply temperature of AHU-1 fluctuated during the whole measured period. Besides, a clear pattern can be seen that the supply temperature is not according to the heating curve. Therefore, the performance of AHU-1 has to be analyzed more in detail. In comparison with AHU-1, the supply temperature of AHU-2 and AHU-3 is much more in line with the heating curve. This is especially the case when the outdoor temperature is lower than about 8°C and higher than about 30°C. For the temperatures in between, the outliers only occur relatively few hours per year. Since this is quite acceptable, AHU-2 and AHU-3 are not analyzed on component level.

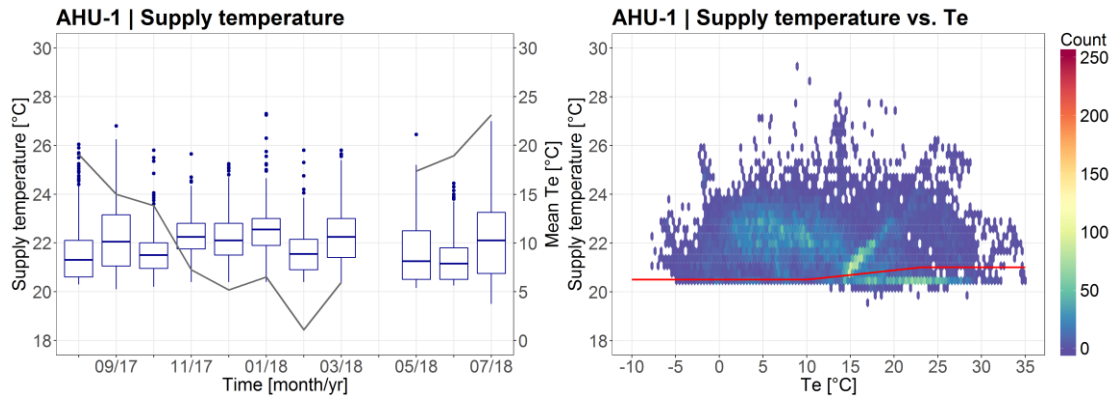


Figure 5.25: Supply temperature in the low-rise (AHU-1) during the year (left) and in relation to the outdoor temperature including the density of the measured points (right)

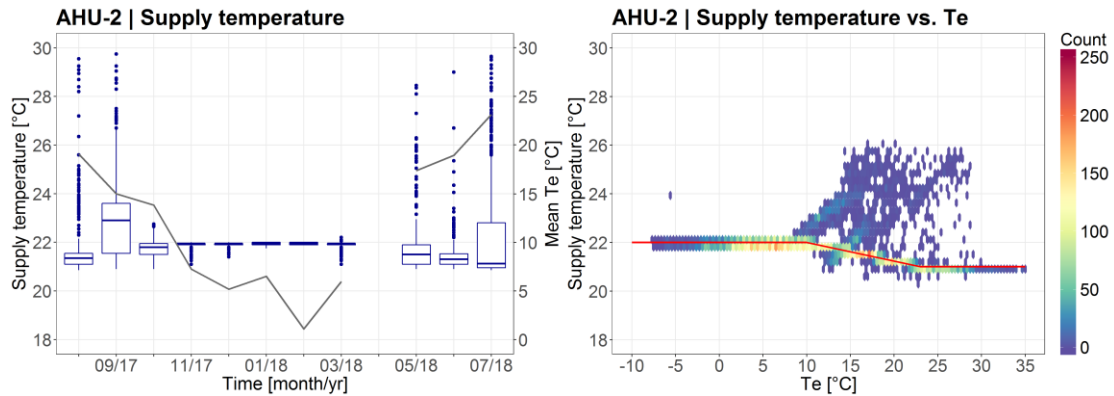


Figure 5.26: Supply temperature in the high-rise (AHU-2) during the year (left) and in relation to the outdoor temperature including the density of the measured points (right)

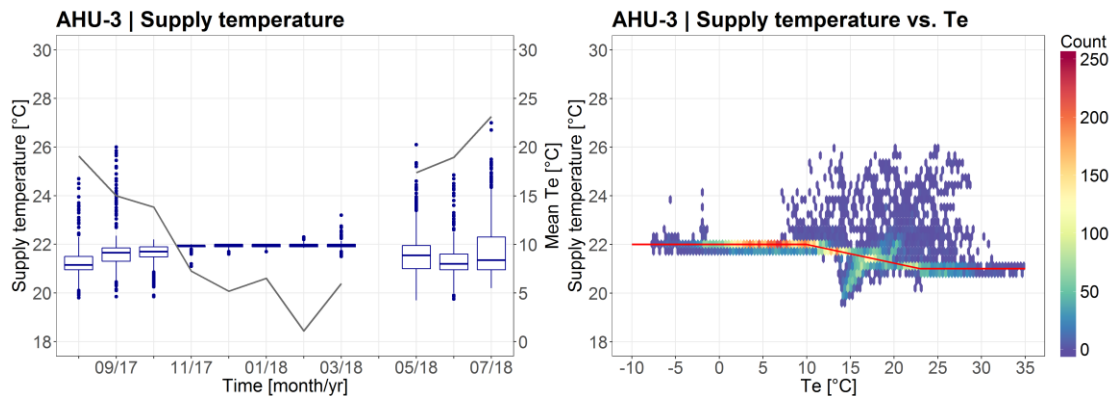


Figure 5.27: Supply temperature in the restaurant (AHU-3) during the year (left) and in relation to the outdoor temperature including the density of the measured points (right)

The supply and exhaust temperature during one typical week is presented in Figure 5.28. The supply temperature increases sometimes due to unknown reasons. This is also necessary to obtain a constant exhaust temperature. Nevertheless, the regulation of AHU-1 can be improved to reduce the peak demands. To determine the exact reason for these peaks, this part of the HVAC system has to be analyzed on component level. However, due to the lack of sensors, only the pressure drop across the filters can be analyzed in more detail. This has no influence on the supply temperature.

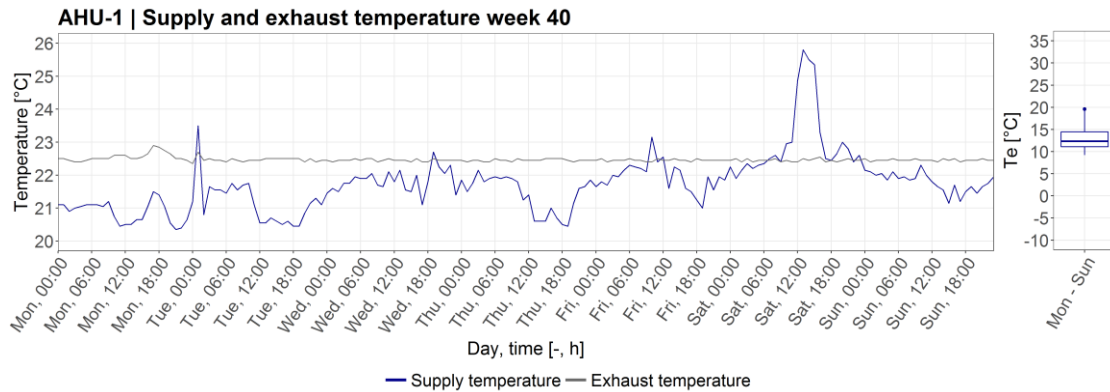


Figure 5.28: Supply and exhaust temperature of AHU-1 (left) and the outdoor temperature (right) from 2<sup>nd</sup> October of 2017 up to and including 8<sup>th</sup> of October 2017 (week 40)

Figure 5.29 presents the supply pressure drop across the filters of the AHUs. However, the sensor of AHU-2 is defect and the sensor of AHU-3 is not working properly due to the unlikely low measured pressure. Therefore, only AHU-1 can be analyzed. According to the design, the maximum pressure drop across the filter may be 200 Pa. Nevertheless, the data shows higher values until the filter was replaced in October 2017. After the replacement of the filter, the pressure increases over time. This will continue until the filter will be replaced again.

When the filters become dirty, the pressure drop increases and the airflow rate drops. This leads to a higher electricity consumption [53]. Therefore, a more frequent replacement of the filter could be an opportunity for energy saving. However, sometimes it is financially more attractive to combine the replacement with yearly maintenance.

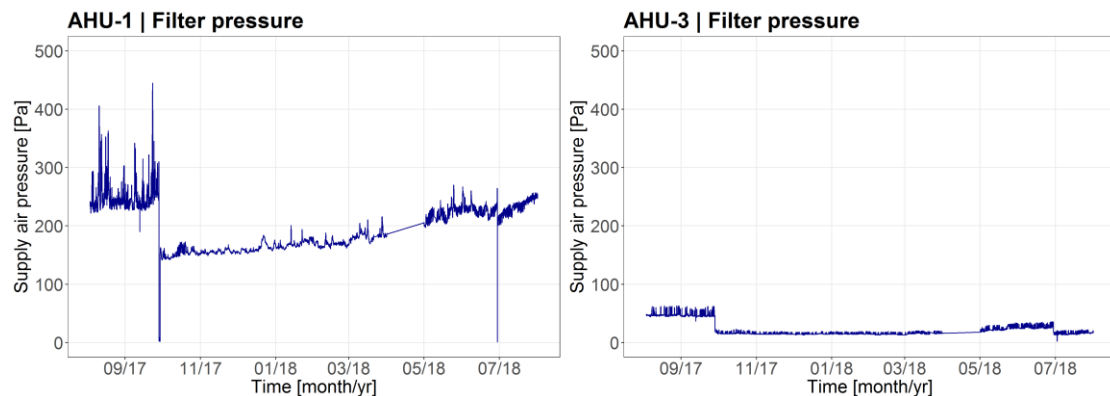


Figure 5.29: Supply pressure drop during the year across the filter of AHU-1 (left) and AHU-3 (right)

**Concrete core activation**

Figures 5.30 to 5.32 show the supply temperature of the three CCA systems during the year and in relation to the outdoor temperature, where the density of the measured points is indicated. During heating mode, CCA-1 provides a lower supply temperature compared to the heating curve. This could be related to the higher supply temperature of AHU-1, which supplies air in the same part of the building. Besides, the supply temperature of CCA-2 is predominantly higher than set and CCA-3 performs the best according to the heating curve.

During cooling mode, all three systems supply most of the time higher temperatures than expected. However, this is also not needed based on the results of the questionnaires. In addition, when the Relative Humidity (RH) in the building is between 75% and 100%, a floor temperature of 18°C can cause condensation on the floors according to the Mollier diagram.

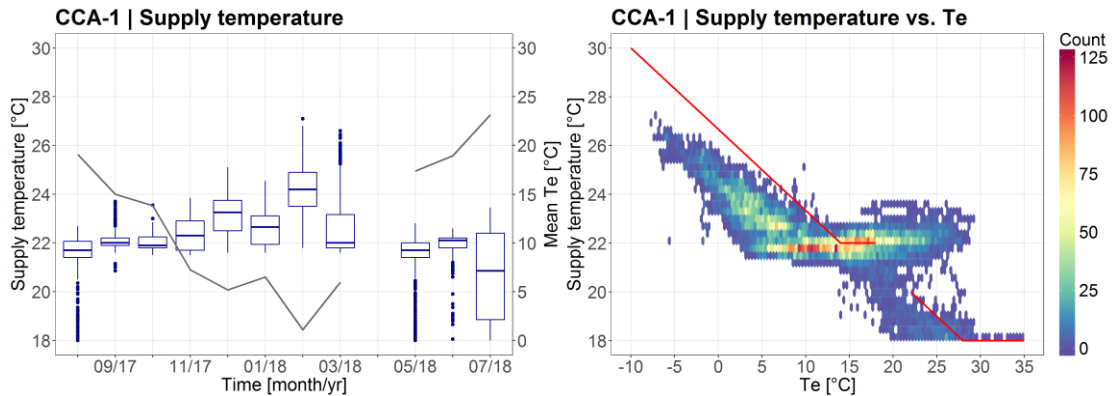


Figure 5.30: Supply temperature in the low-rise (CCA-1) during the year (left) and in relation to the outdoor temperature including the density of the measured points (right)

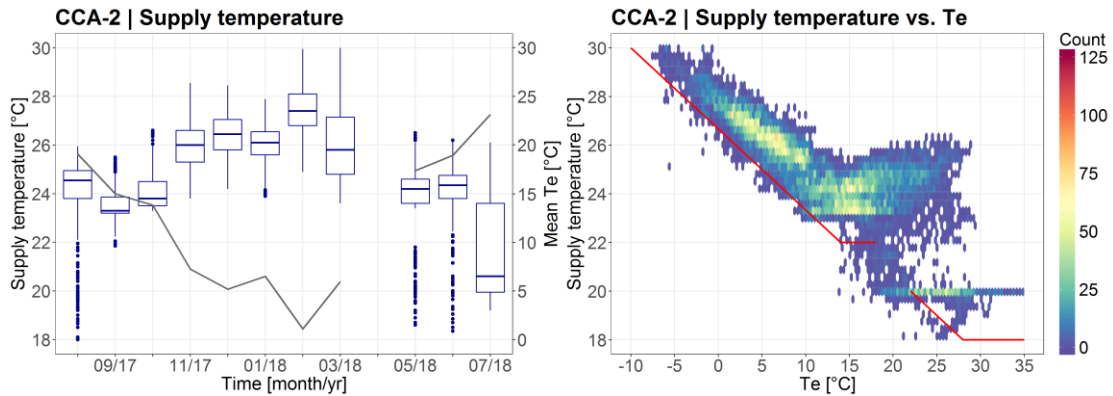


Figure 5.31: Supply temperature in the high-rise (CCA-2) during the year (left) and in relation to the outdoor temperature including the density of the measured points (right)

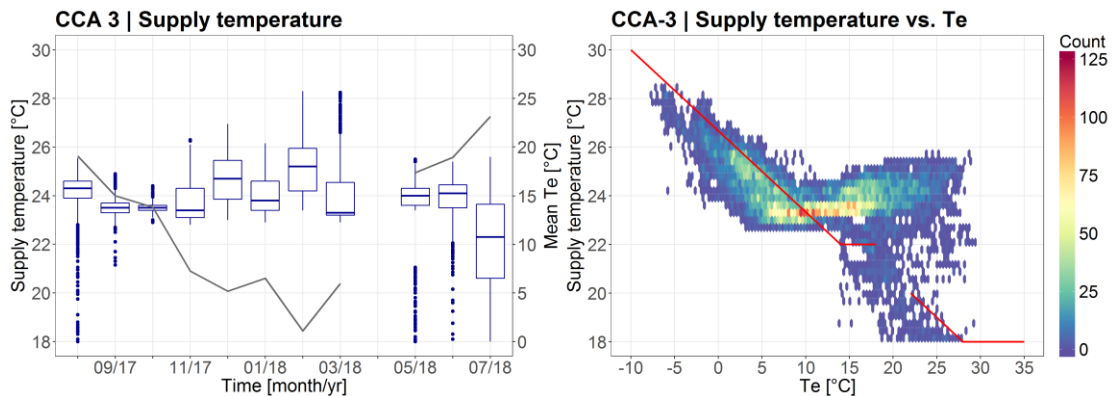


Figure 5.32: Supply temperature in the high-rise (CCA-3) during the year (left) and in relation to the outdoor temperature including the density of the measured points (right)

### 5.3.5 Discussion

In general, the performance analysis has shown that the HVAC system of the case study building is underperforming according to the design. Especially the thermal unbalance of the ATES system and the relatively high supply temperature of AHU-1 are major problems. To save more energy, both problems need to be solved.

When the supply temperature of AHU-1 is lowered, the heating and electricity consumption of the AHU will decrease. This improvement will also have a positive impact on the thermal unbalance of the ATES system. In addition, the energy consumption of the ATES system, heat pump, boilers and AHUs will be reduced due to the lower heating demand. However, the measured exhaust temperature of AHU-1 and the results of the questionnaire show that the indoor temperature in fact meets the requirements. Therefore, a reduced supply temperature can cause a too low indoor temperature. In order to keep the required pleasant indoor climate, the best solution is to reduce the supply temperature of AHU-1 in combination with increasing the supply temperature of CCA-1.

However, the small difference between the measured supply temperature of the three CCA systems can be caused by the associated temperature sensors. Therefore, the accuracy and reliability of the BMS sensors must be questioned. Accuracy describes the relationship between the measured value by the sensor related to the actual value. The smaller this difference, the higher the accuracy. Reliability is the reproducibility of the measurement. When the values during the same conditions are grouped together, the reliability is high. In order to improve the accuracy and reliability of measurements, calibration and maintenance are necessary [54]. In addition, the measurements can deviate when the position of the sensor in each system is not the same. That is why a correct placement of the sensors is needed.

## 5.4 LEAN energy analysis

The energy saving potential of the HVAC system is investigated based on the LEAN energy analysis. The performance modeling is conducted by comparing thermal energy benchmark models with historical data. These models can also be used to control the operational energy performance.

### 5.4.1 Benchmark model

The main function of the thermal energy extraction is to bridge the difference between the outdoor temperature and the required indoor temperature and to provide hot water for hygiene purposes. Therefore, as a first attempt the relation between the thermal energy extraction and the outdoor temperature is determined using regression. The results are evaluated by means of the coefficient of determination ( $R^2$ ) which indicates to which extent the dependent variable (thermal energy extraction) is predictable. The closer the value is to 1, the better the correlation of the parameters.

In order to reduce the impact of time-dependent parameters (such as internal heat, solar irradiance and stored energy in the thermal mass), the daily mean thermal energy extraction is used. Moreover, it is investigated whether multi-parameter regression improves the correlation of the models.

The results are shown in Figure 5.33. The extracted heat correlates linear with the outdoor temperature. This relationship is strong since the  $R^2$  is 0.930. The cold extraction correlates non-linear with the outdoor temperature. This leads to a still acceptable relationship with a  $R^2$  of 0.758. Therefore, these models can be used as benchmark models.

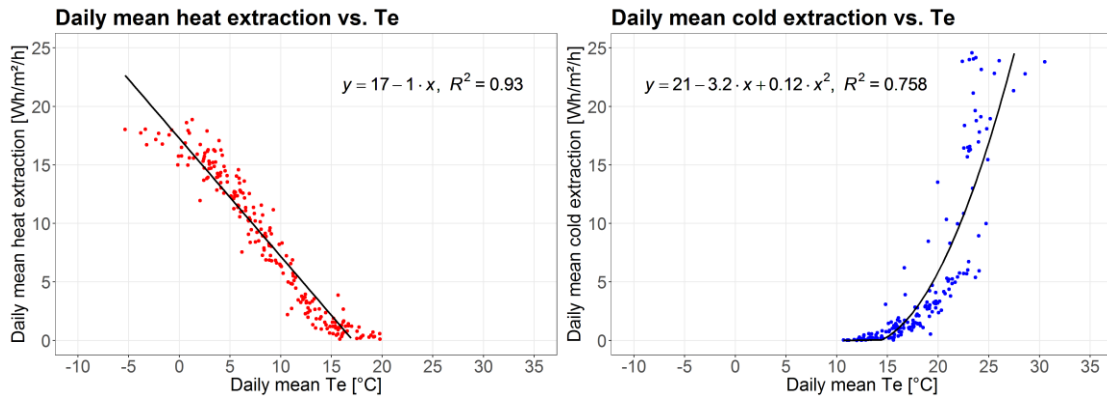


Figure 5.33: Regression for the daily mean heat (left) and cold (right) extraction as function of the outdoor temperature

The benchmark models are tested to determine the deviation of the residuals (predicted minus measured heat extraction). This is done by using 75% of the data set for training the model. To validate the model, the other 25% of the data set is used for testing. The R-script for training and testing of the models can be found in Appendix A.5.

The results related to the heat extraction are presented in Figure 5.34. The deviation of the residuals is almost normally distributed (positive and negative). Figure 5.35 shows the results of the cold extraction. In this case, the deviation of the residuals is negatively distributed to a larger extent.

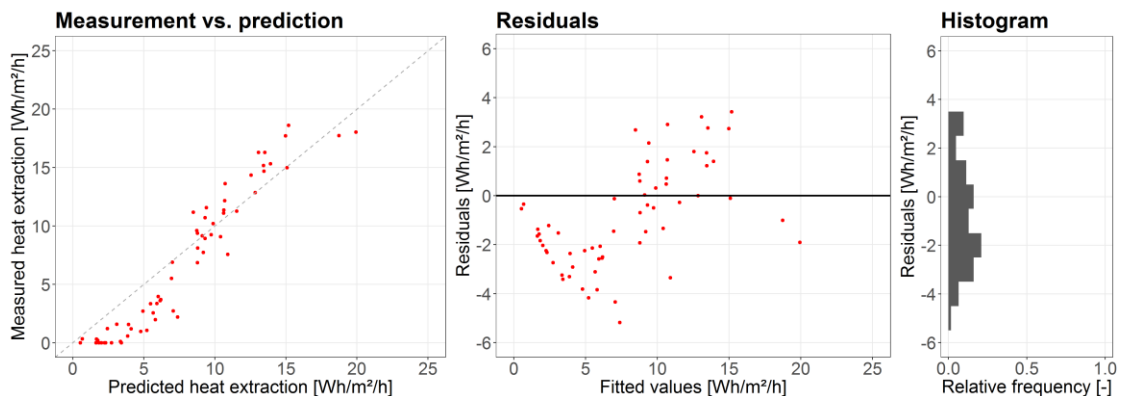


Figure 5.34: Deviation between the predicted and measured heat extraction (left), the deviation of the residuals (middle) and distribution of the residuals (right)

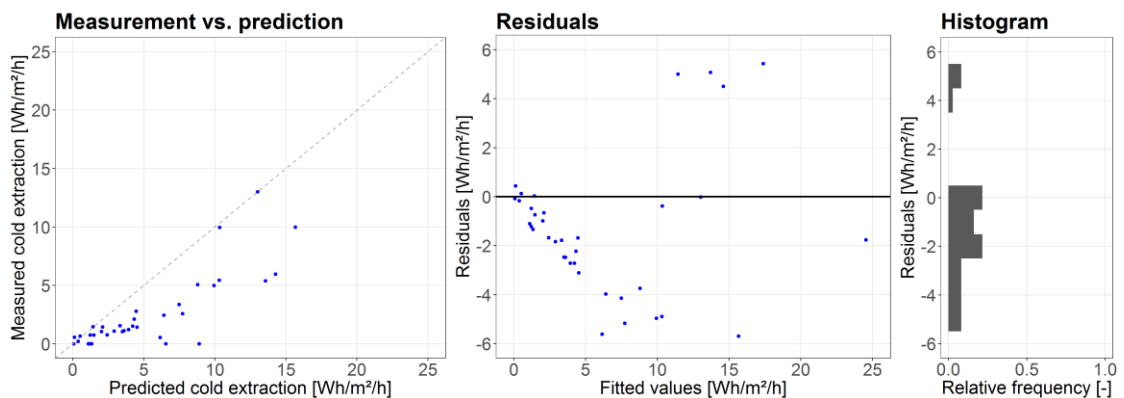


Figure 5.35: Deviation between the predicted and measured cold extraction (left), the deviation of the residuals (middle) and distribution of the residuals (right)

## 5.4.2 Energy saving potential

The predicted energy extraction by benchmark models based on historical data and actual measured energy extraction are compared in order to provide an indication of energy saving potential. These models can also be used to assess the energy performance trends. The difference between the predicted and measured heat extraction from October 2017 up to and including December 2017 is shown in Figure 5.36. Figure 5.37 presents the difference between the predicted and measured cold extraction from May 2018 up to and including July 2018. Based on the figures, the most energy can be saved at the cold extraction.

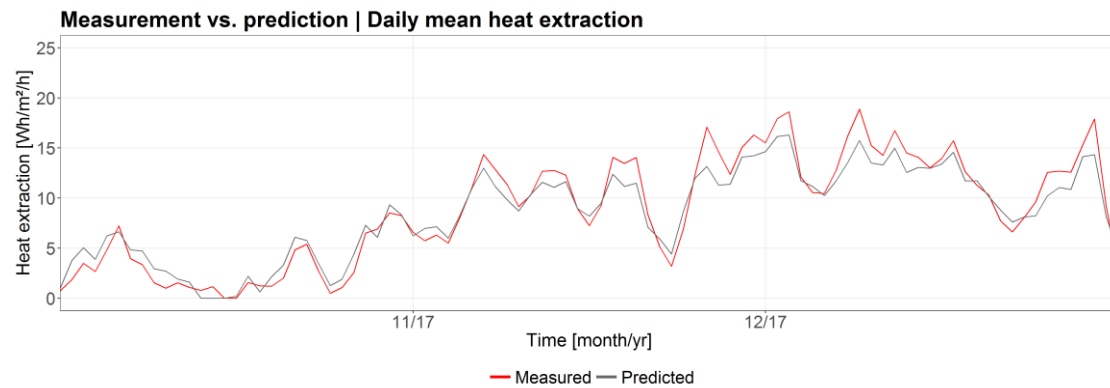


Figure 5.36: Difference between the predicted and measured heat extraction from October 2017 up to and including December 2017

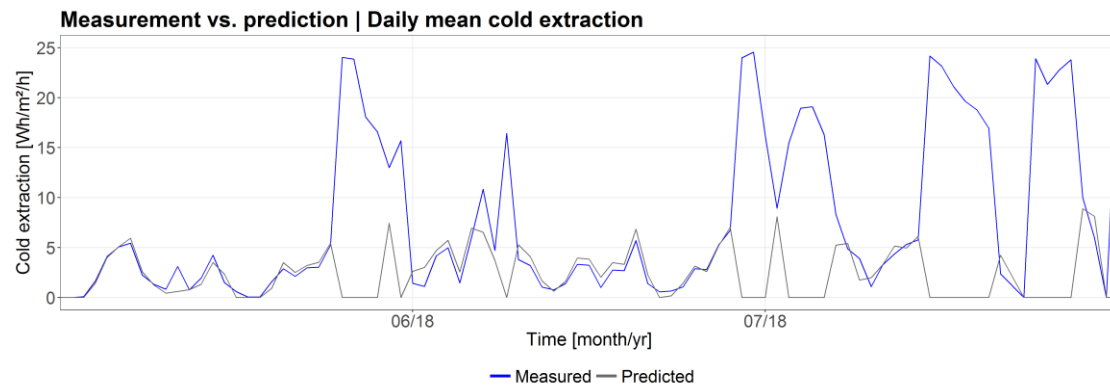


Figure 5.37: Difference between the predicted and measured cold extraction from May 2018 up to and including July 2018

The indication of the energy saving potential is calculated by using equation 5.4.

$$Q_{\text{saving}} = \sum_{j=1}^m (Q_{\text{Predicted},j} - Q_{\text{measured},j}) \quad (5.4)$$

With:

$Q_{\text{saving}}$	: Energy saving potential	[kWh]
$Q_{\text{Predicted}}$	: Predicted thermal energy extraction	[kWh]
$Q_{\text{measured}}$	: Measured thermal energy extraction	[kWh]



The results of this calculation are shown in Table 5.5. The yearly energy saving potential of the heat extraction is 7%, while the energy saving potential of the cold extraction is 70%. However, the uncertainty of the models has to be taken into account, especially with regard to cooling because it has a lower  $R^2$  than heating. The high amount of saving on the cold extraction can be explained by the CCA systems which are rarely in cooling mode during high outdoor temperatures. Therefore, the model is mainly based on data when the systems are not cooling mode. As a result, the effect on the predicted cold extraction is large when the system is operating in cooling mode.

*Table 5.5: Indication of the yearly energy saving potential*

	<b>Measured</b> [kWh/m <sup>2</sup> ]	<b>Energy saving potential</b> [kWh/m <sup>2</sup> ]	<b>Energy saving</b> [%]
Heat extraction	44.9	3.0	7
Cold extraction	22.9	16.0	70

### 5.4.3 Discussion

Benchmark models using regression are useful to give an indication of the energy saving potential. However, the results are dependent on the accuracy of the models. In addition, the models can be valuable to control the energy performance. Regular check-up of data can ensure that the energy consumption does not increase unexpectedly. The LEAN energy analysis normally uses data of buildings with similar type, use, age, and other characteristics as benchmark model. However, this data is not available in this study. Therefore, the benchmark models are created by the historical building operational data.

## 6 Case study 2: Kropman Breda

This chapter presents the second case study of the research, office building Kropman Breda. First, the performance indicators are identified by means of the Pareto analysis. Subsequently, the designed performance is analyzed. Then, the measured performance is analyzed which leads to the system inefficiencies. Finally, the energy saving potential is investigated based on the LEAN energy analysis.

### 6.1 Pareto analysis

For the sensitivity analysis, the impact of different parameters on the electricity, heating and cooling consumption of Kropman Breda is simulated by using EnergyPlus. The created 3D model in SketchUp can be seen in Appendix B.2 (Figure B.4).

#### 6.1.1 Parameters

Ten main parameters are selected related to the HVAC system and the occupant behavior (see Table 6.1). The impact of each parameter is determined by simulating the 10% higher and lower values compared to the design. According to the Pareto analysis, roughly 80% of the performance gap can be identified by 20% of the major selected parameters. This means that the two parameters with the highest impact will be presented as the performance indicators of the case study building.

Table 6.1: Selected main parameters

Parameters	Unit	Design	+10%	-10%	
<i>HVAC system</i>					
1	Set-point heating temp.	°C	21.5	23.7	19.4
2	Set-point cooling temp.	°C	24.0	26.4	21.6
3	Max. heating supply temp.	°C	25.0	27.5	22.5
4	Min. cooling supply temp.	°C	16.5	18.2	14.9
5	Ventilation flow rate	m <sup>3</sup> /s	4.35	4.79	3.92
6	Heat recovery	%	70	77	63
<i>Occupant behavior</i>					
7	Occupant presence	n	45	50	40
8	Internal heat occupants	W/pers.	110	121	99
9	Internal heat lighting	W/m <sup>2</sup>	9.0	9.9	8.1
10	Internal heat equipment	W/m <sup>2</sup>	10.0	11.0	9.0

#### 6.1.2 Performance Indicators

The impact of the selected parameters on the annual electricity, heating and cooling consumption is presented in Figure 6.1. By stimulating 10% higher and lower values than designed, the energy consumption can increase or decrease.

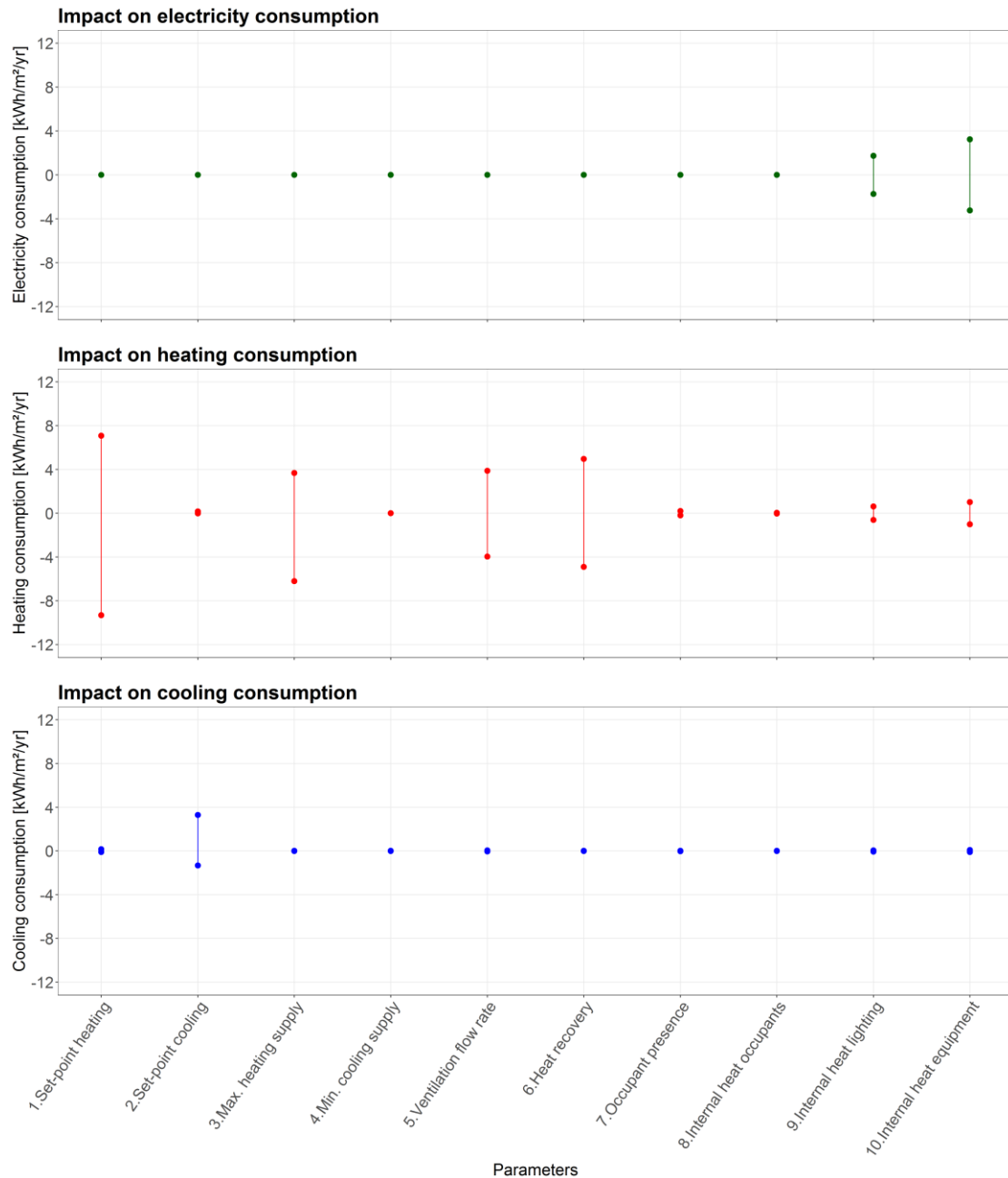


Figure 6.1: Impact on the electricity (green), heating (red) and cooling (blue) consumption when the parameters are 10% higher or lower than designed

In order to determine the performance indicators, the maximum impact (positive or negative) of each parameter on the total impact of all parameters is ranked, scored and grouped. The impact on the annual electricity, heating and cooling consumption is shown in Figures 6.2 to 6.4. As mentioned before, the two parameters with the highest impact are the performance indicators of the case study building.

On the electricity consumption, the internal heat of equipment (65%) and the internal heat of lighting (35%) have the highest impact. For heating, the most important parameters are the set-point heating temperature (35%) and the maximum heating supply temperature (23%). On the cooling consumption, the set-point cooling temperature (89%) and the set-point heating temperature (4%) have the largest impact.

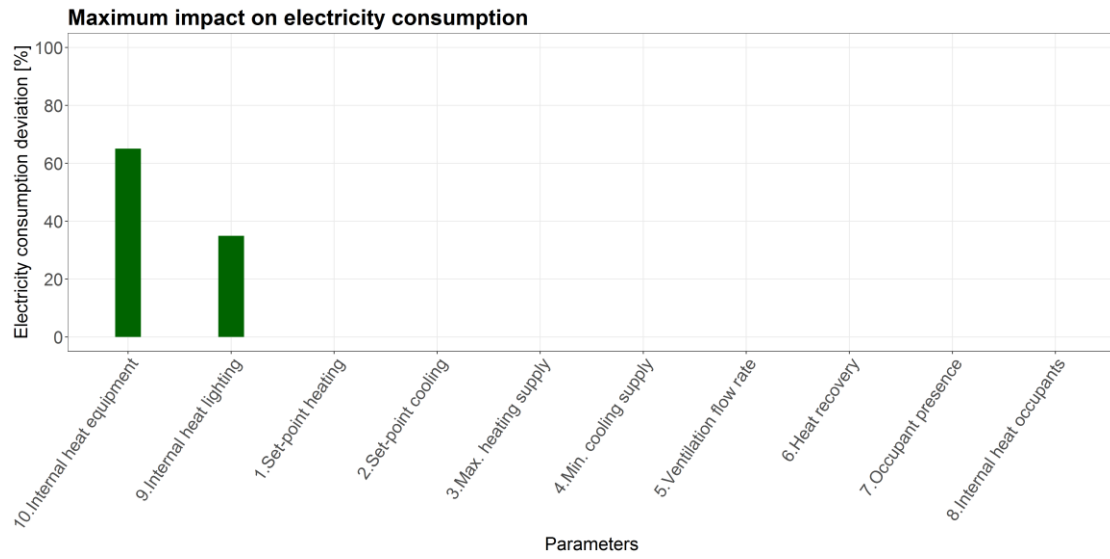


Figure 6.2: Ranking of the maximum impact on the electricity consumption

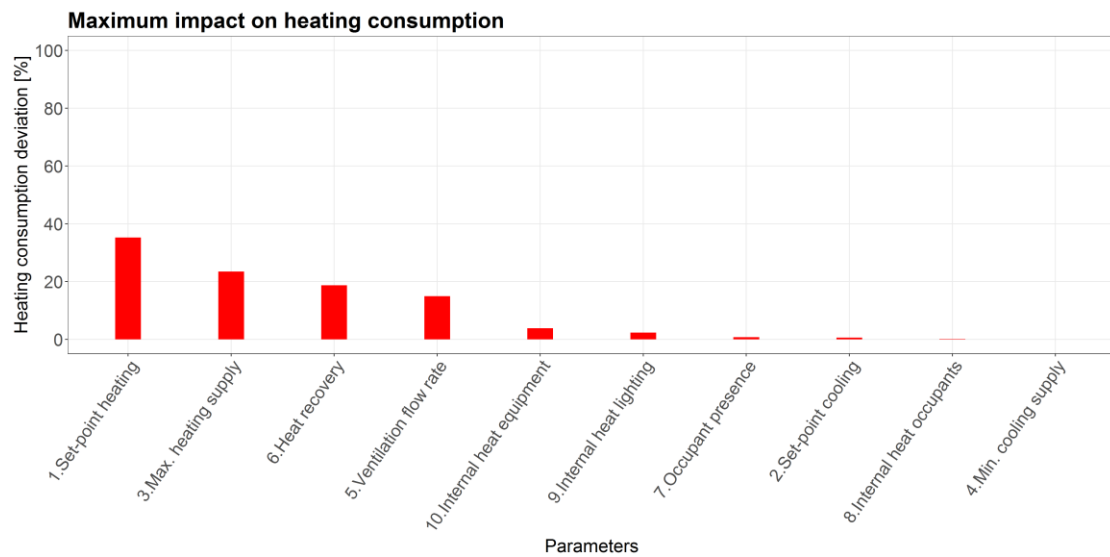


Figure 6.3: Ranking of the maximum impact on the heating consumption

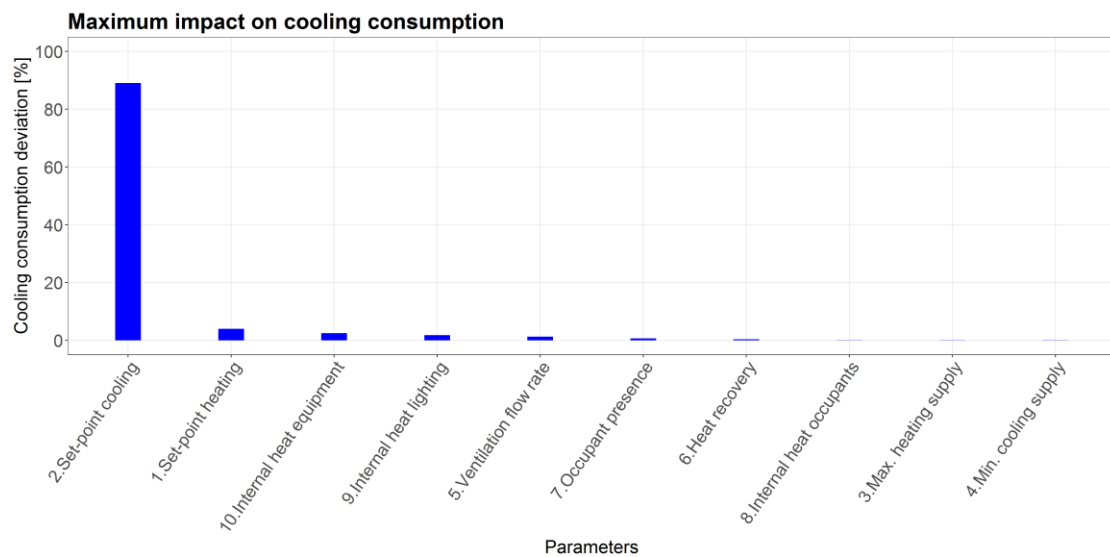


Figure 6.4: Ranking of the maximum impact on the cooling consumption

### 6.1.3 Discussion

The sensitivity analysis of this building also shows that the 20% most important parameters not exactly account for 80% of the gap. The two parameters with the highest impact on the electricity are responsible for 100% of the total impact. On the heating consumption of the building, the two major parameters are accounted for 58%. On the cooling consumption, the two parameters are responsible for 93%. This means that the performance indicators of the electricity and cooling consumption meet the principle of the Pareto analysis.

At the second case study building, also the set-points for heating and cooling and the related supply temperatures are the most important parameters. Despite the selected parameters not always identify the 80% of the performance gap, it contributes to focus on the major parameters of the HVAC system during the designed and measured performance analysis.

## 6.2 Designed performance analysis

To provide a pleasant indoor climate the building contains a quite common used HVAC system summarized in Table 6.2.

Table 6.2: HVAC system of Kropman Breda

HVAC system	Energy conversion	Distribution	Release	Recovery
Heating	- Gas-fired boiler	- Air - Water	- Balanced ventilation - Radiators	- Heat recovery wheel
Cooling	- Cooling machine	- Air	- Balanced ventilation - Night ventilation	- Heat recovery wheel
Ventilation	- Air handling unit	- Air	- Balanced ventilation	- Heat recovery wheel
Humidification	- Electric steam humidifier	- Air	- Balanced ventilation	-

### 6.2.1 Energy conversion

#### Boiler and Cooling machine

The building is equipped with a central boiler which generates the heating demand of the building. The cooling demand is provided to the distribution system by a central cooling machine. Appendix B.3 presents the installation principle of the heating (Figure B.5) and cooling (Figure B.6) systems.

### 6.2.2 Supply

#### Air handling unit

The AHU supplies and exhausts air in three different parts of the building. It contains a heat recovery wheel and a central heating coil. The supply temperature of the ventilation air is centrally controlled by means of heating curves which are based on the outdoor temperature. (Figure 6.5). On room level, the air is supplied to the room by ventilation vents. The air is extracted by the AHU again and leaves the building by passing the heat recovery wheel. During summer nights, night ventilation is used to passively cool down the building with outside air. When the relative humidity of the supplied air becomes too low, the air is humidified.

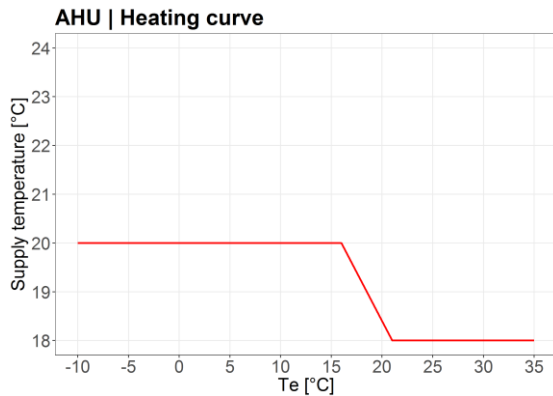


Figure 6.5. Heating curve of the AHU

### 6.2.3 Discussion

The operational performance of the AHU can be analyzed and assessed by means of the designed and set heating curve. When measurements deviate strongly from this curve, this indicates inefficiencies of the system. Therefore, these underperforming parts of the system must subsequently be analyzed on component level.

## 6.3 Measured performance analysis

The performance analysis is conducted following a top-down approach. First, the analysis of the electricity and gas consumption on building level including the indoor climate is discussed. Subsequently, the HVAC system is analyzed, divided into energy conversion and supply installations. Finally, the underperforming installations are analyzed on component level.

The analysis is based on data derived in different reading levels and time steps (see Table 6.3). The data is measured in the period January 2017 up to and including December 2018. A detailed overview of specific sensors of the BMS is provided in Appendix B.4 (Table B.1). This Appendix gives also the heat maps of the energy consumption including the outdoor temperature (Figures B.7 to B.11).

Table 6.3: Available data of the building

Data	Source	Reading level	Interval	Period
Electricity	Smart meter	Building + system level	1-minute	January 2017 - December 2017
Gas	Smart meter	Building level	Hourly	January 2017 - December 2017
HVAC system	BMS	System level	8-minute, hourly	January 2017 - December 2017

### 6.3.1 Energy consumption

#### Electricity consumption

Figure 6.6 shows the hourly electricity consumption during the year and related to the outdoor temperature, where the density of the measured points is indicated. The clear constant pattern in density represents the base load of the building during unoccupied hours. The minimum electricity consumption is about 2 Wh/m<sup>2</sup>/h, while the maximum consumption is approximately 28 Wh/m<sup>2</sup>/h. At low outdoor temperatures the consumption rises significantly due to the increasing demand of the fans.

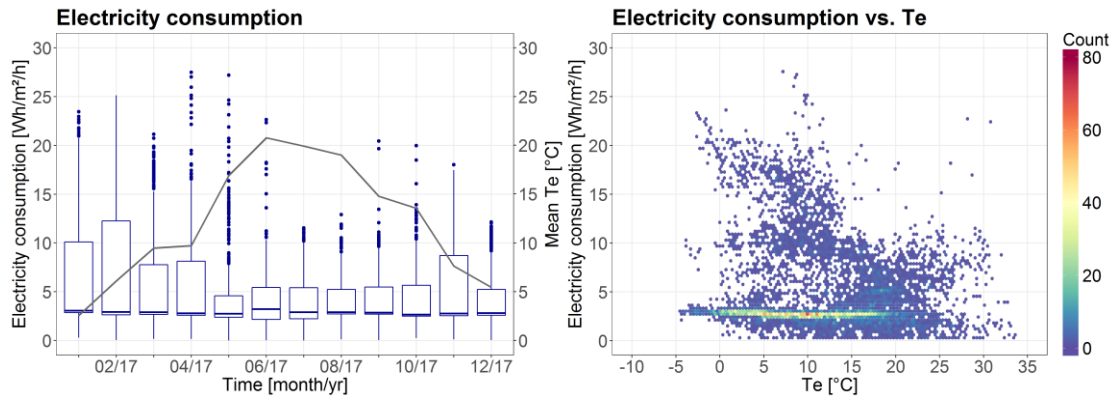


Figure 6.6: Hourly electricity consumption during the year (left) and in relation to the outdoor temperature including the density of the measured points (right)

The mean hourly electricity consumption per week is presented in Figure 6.7. The patterns of each workday generally start with the highest peak caused by the HVAC system that begins to heat or cool the building. This is followed by a decrease in the afternoon and a small peak in the late afternoon. As expected, during the night and in the weekend the electricity consumption is quite low.

The electricity consumption measured by the smart meter represents not the actual total electricity consumption. When electricity is generated by the PV-panels and directly used, this is not measured by the smart meter. At these moments, the actual total electricity consumption is higher. In addition, the measured electricity consumption is sometimes negative, especially during the weekend. This is when the generated electricity is supplied to the grid.

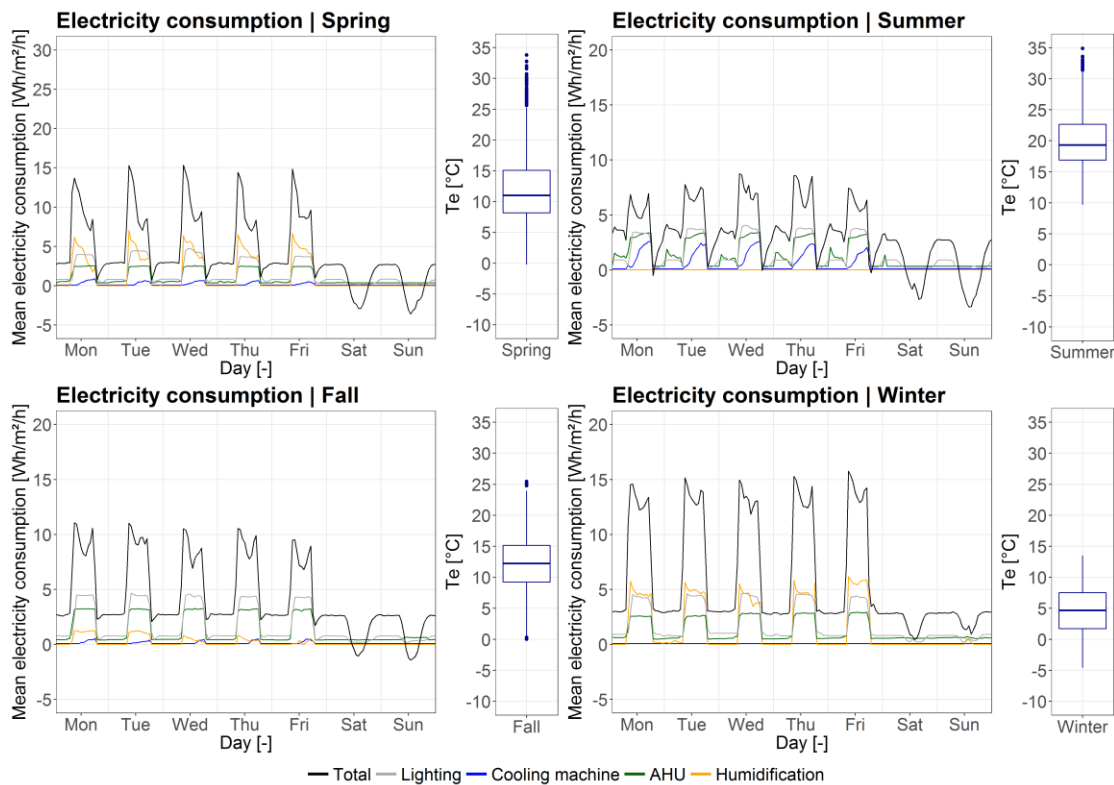


Figure 6.7: Mean hourly electricity consumption and outdoor temperature during the seasons

**Gas consumption**

Gas is used by one boiler to generate heat and in the kitchen of the restaurant. Figure 6.8 shows the hourly gas consumption during the year and related to the outdoor temperature, where the density of the measured points is indicated. The smart meter that measures the gas consumption only gives whole numbers which results in less accurate values. As usual, the gas consumption of the boiler increases as the outdoor temperature decreases. The large bandwidth is in principle caused by peaks at the beginning of each workday in order to heat the building.

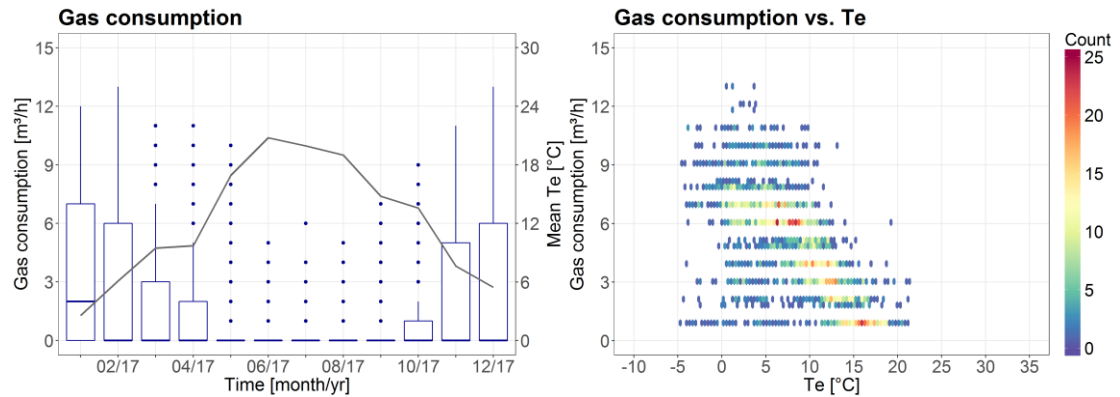


Figure 6.8: Hourly gas consumption during the year (left) and in relation to the outdoor temperature including the density of the measured points (right)

The average hourly gas consumption per week is presented in Figure 6.9. Most weekday starts with a peak in order to heat the building. When the indoor temperature reaches the desired temperature, the consumption slowly decreases. As expected, during the night and in the weekend the gas consumption is low.

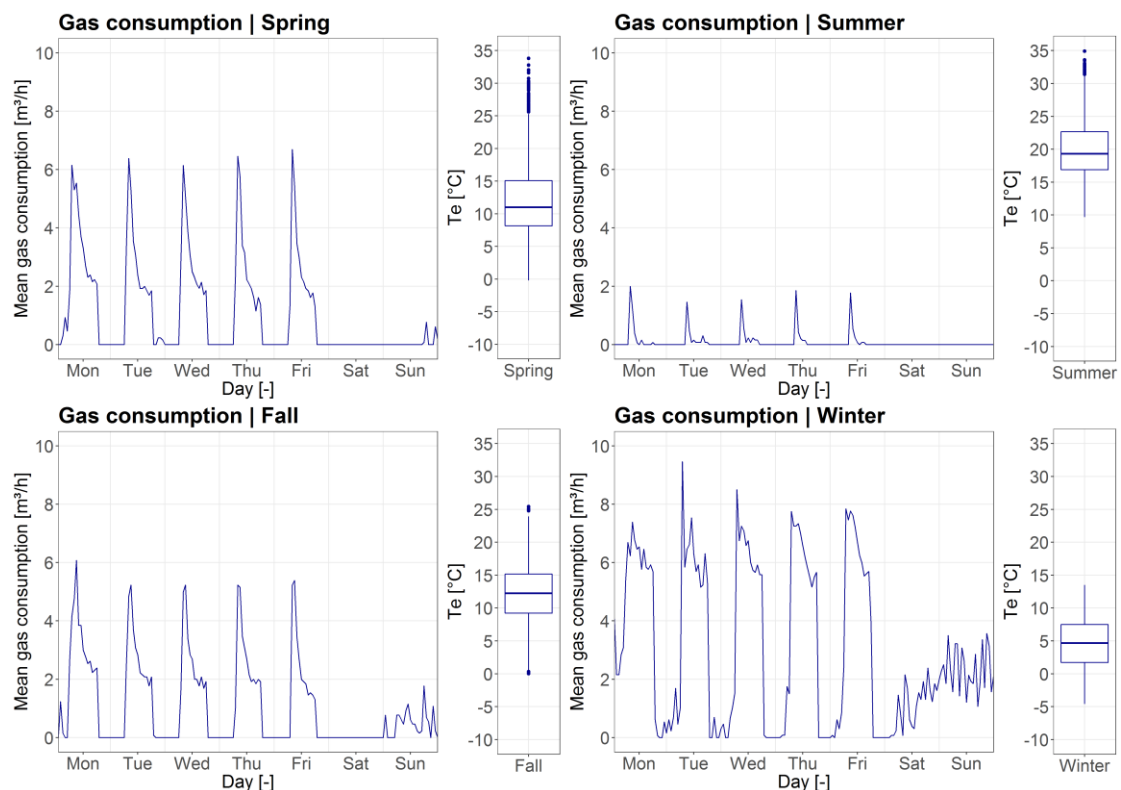


Figure 6.9: Mean hourly gas consumption and outdoor temperature during the seasons



### 6.3.2 Indoor climate

Based on one office room (room 1.05), the indoor climate of the building is analyzed. This room is occupied by twelve employees. The measured indoor climate is compared with the required indoor climate, see Table 6.4.

Table 6.4: Required and measured indoor climate in room 1.05 during occupation (weekdays between 09.00-17.00h)

Indoor climate	Unit	Required		Measured		
		Min.	Max.	Min.	Max.	Avg.
Air temperature	°C	21.0	24.0	19.9	24.4	22.5
CO <sub>2</sub> -concentration	ppm	400	700	355	629	499
RH	%	30	70	28	70	49

The mean hourly indoor air temperature in relation to the mean outdoor air temperature per season is shown in Figure 6.10. While the office building is in use, the average indoor air temperature is 22.5°C. Figure 6.11 presents the mean hourly CO<sub>2</sub>-concentration in the room. In the room the average CO<sub>2</sub>-concentration is 499 ppm. This is quite low since the outdoor CO<sub>2</sub>-concentration in the Netherlands is about 400 ppm. The mean hourly RH is shown in Figure 6.12. During the whole year average RH is 49%. Based on the requirements, the HVAC system provides most of the time a pleasant indoor climate.

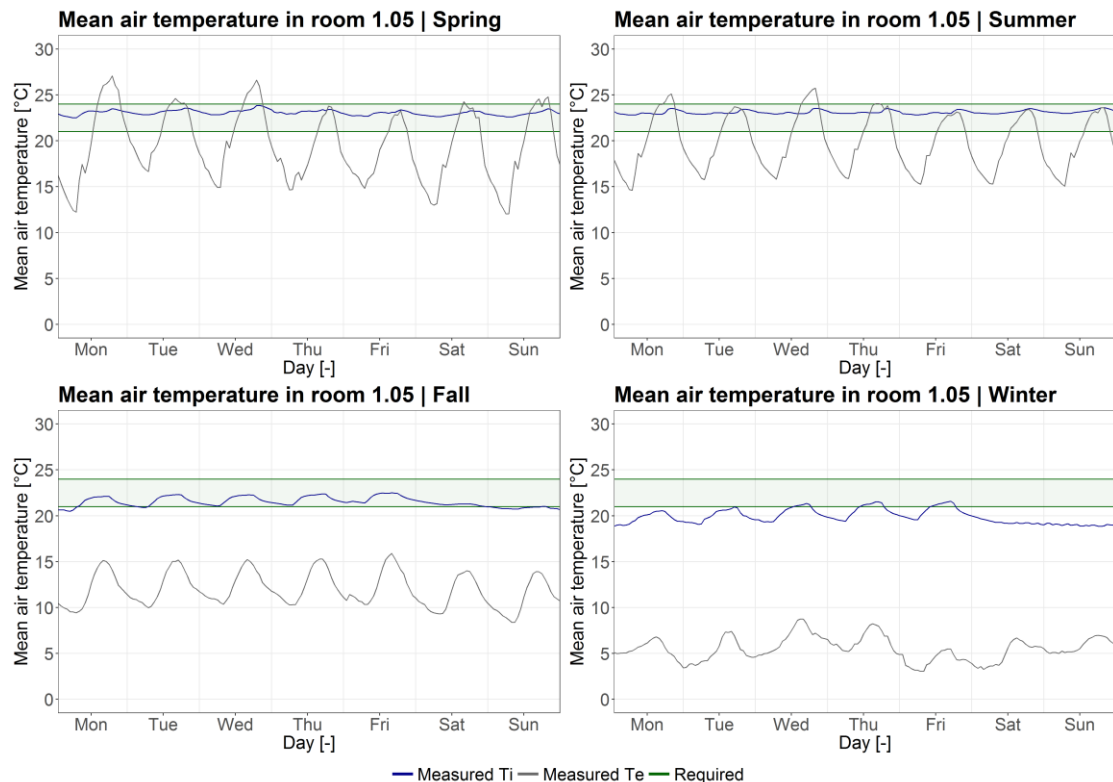


Figure 6.10. Mean hourly air temperature in room 1.05 during the seasons

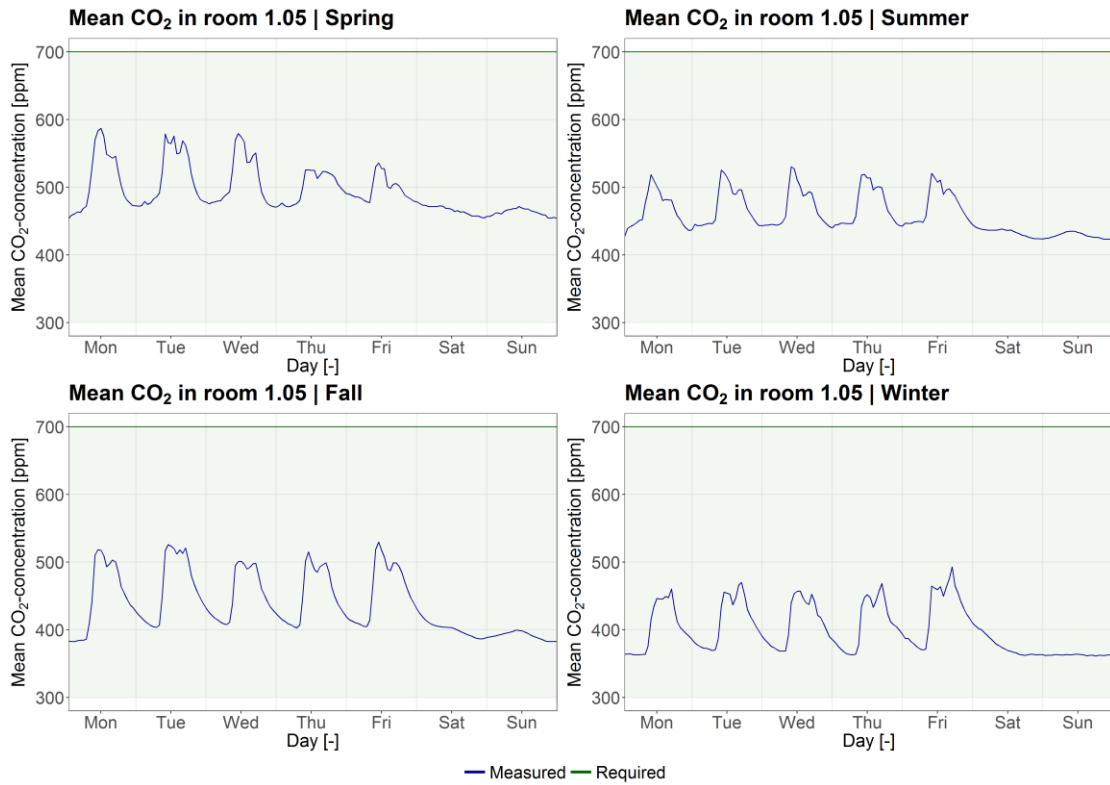


Figure 6.11. Mean hourly CO<sub>2</sub>-concentration in room 1.05 during the seasons

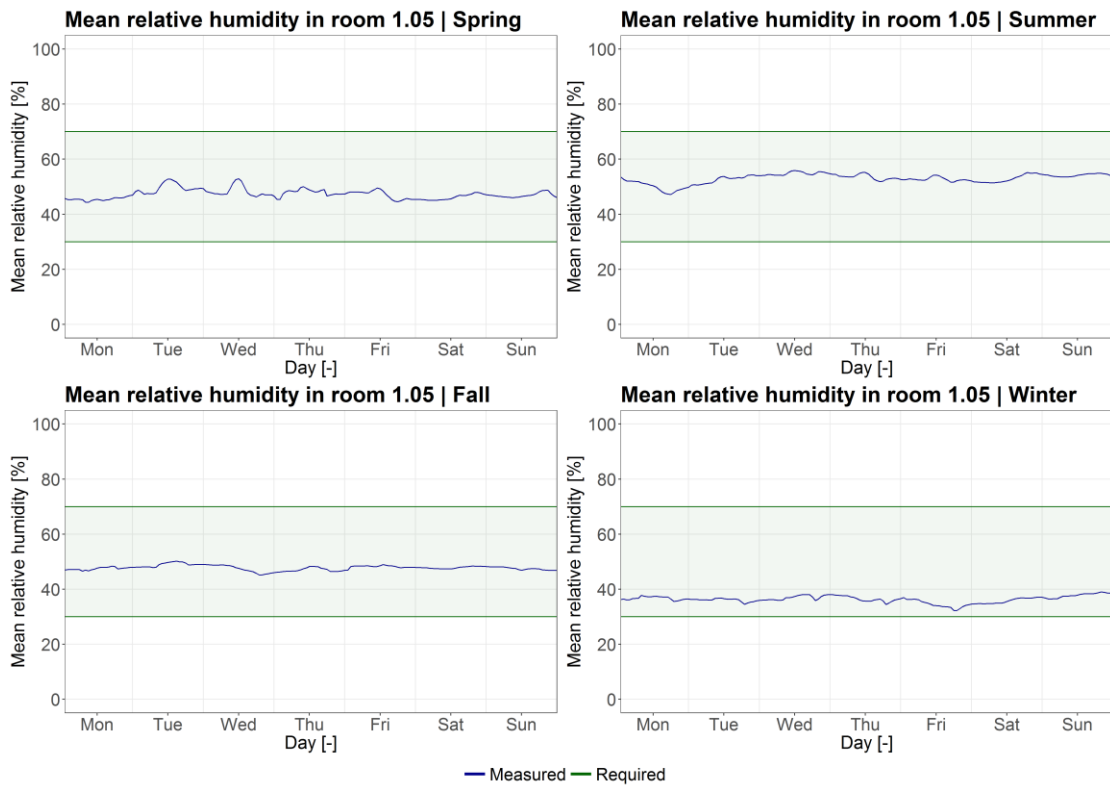


Figure 6.12. Mean hourly relative humidity in room 1.05 during the seasons

### 6.3.3 Energy conversion

#### Boiler and cooling machine

The heating and cooling consumption during the year and related to the outdoor temperature is shown in Figure 6.13. It clearly shows that the heating process starts at temperatures lower than about 21°C and the cooling process starts at temperatures higher than about 17°C. The large bandwidth of especially the heating consumption is generally caused during unoccupied hours, when the system starts heating the building.

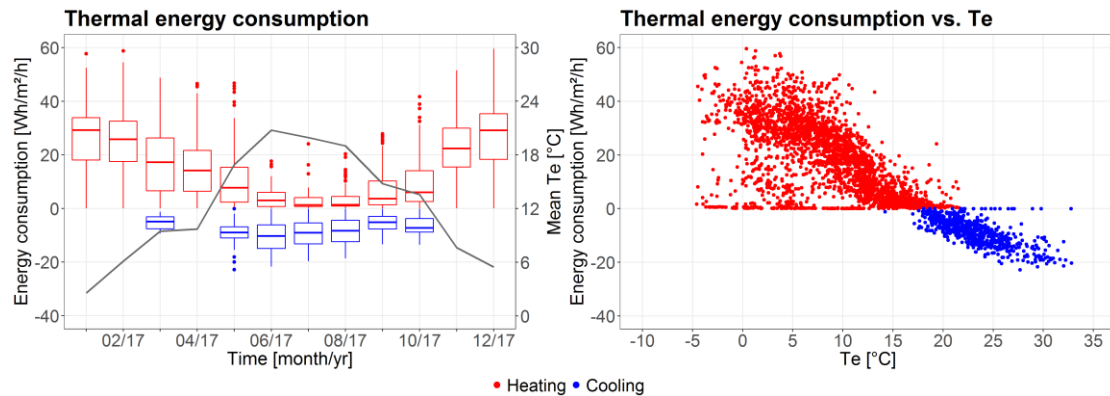


Figure 6.13: Hourly heating and cooling consumption during the year (left) and in relation to the outdoor temperature (right)

Therefore, the thermal energy consumption is divided into two periods, presented in Figure 6.14. The first period relates to the hours when the building is occupied, namely on weekdays between 09:00-17:00h. The second period is related to the hours that the building is not occupied. This results in a linear correlation between the thermal energy consumption and the outdoor temperature during occupied hours. Outside these hours, the consumption is very fluctuating. Since this could be energy waste, this is analyzed by means of the heat supply.

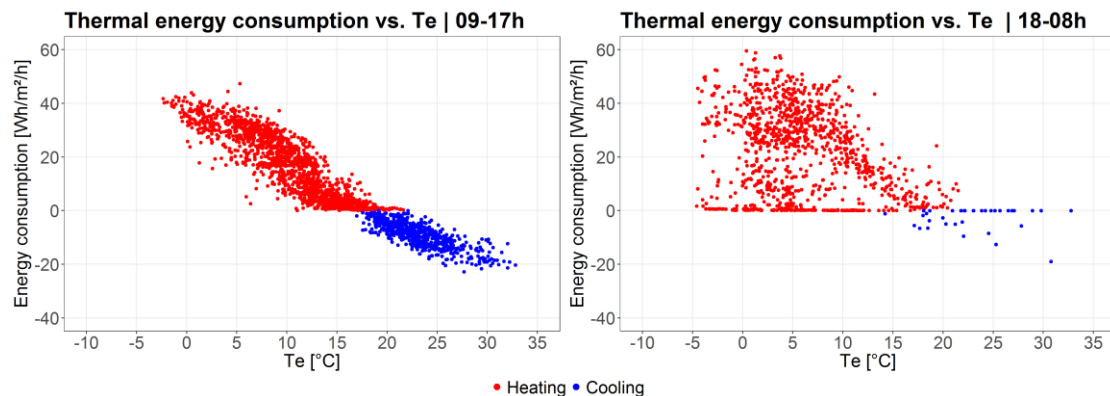


Figure 6.14: Hourly heating and cooling consumption in relation to the outdoor temperature between 09:00-17:00h (left) and 18:00-08:00h (right)

The mean hourly heating and cooling consumption during the seasons is presented in Figure 6.15. During the Spring, Fall and Winter, every workday starts with a heating peak, followed by a decrease until the end of the day. During the Summer, there is a cooling peak on every workday in the late afternoon. During the night and in the weekend the consumption is low.

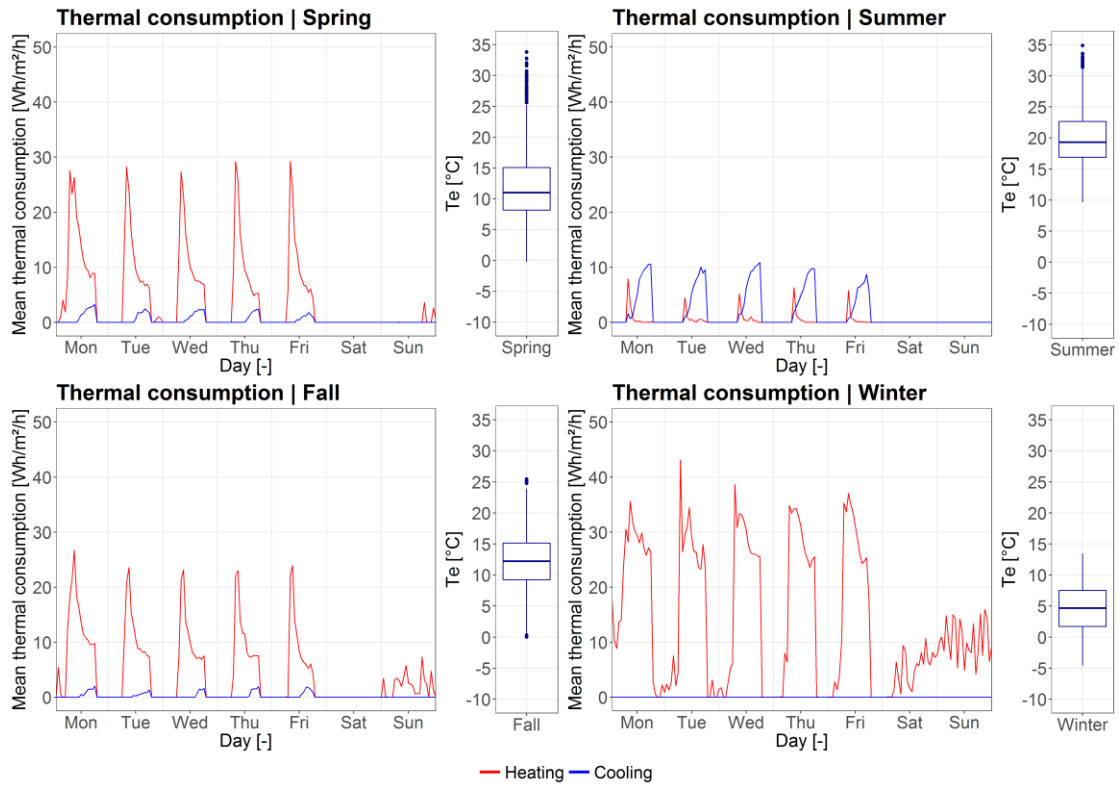


Figure 6.15: Mean hourly heating and cooling consumption during the seasons

### 6.3.4 Supply

#### Air handling unit

Figures 6.16 to 6.18 show the measured supply temperature of the AHU in three building parts during the year and related to the outdoor temperature, where the density of the measured points is indicated. It can be seen that the supply temperature in all parts is most of the time higher than the heating curve. Therefore, the performance of the AHU has to be analyzed in more detail.

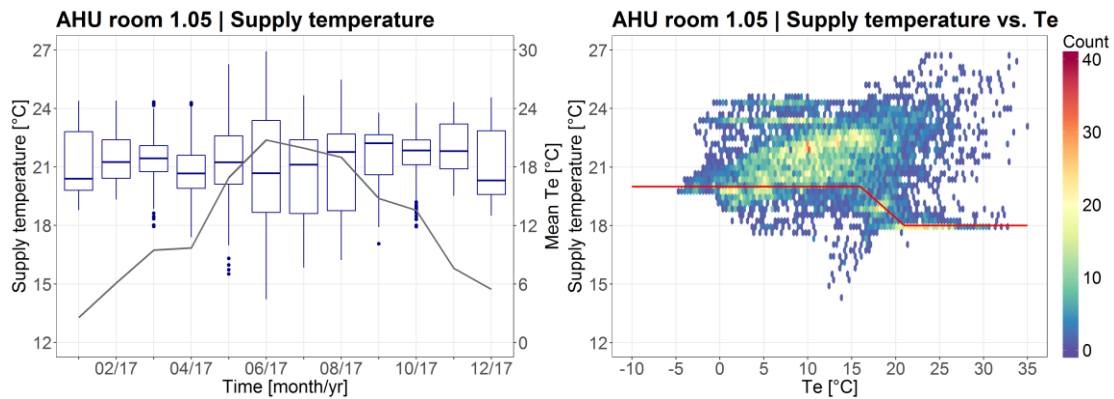


Figure 6.16: Supply temperature in room 1.05 during the year (left) and in relation to the outdoor temperature including the density of the measured points (right)

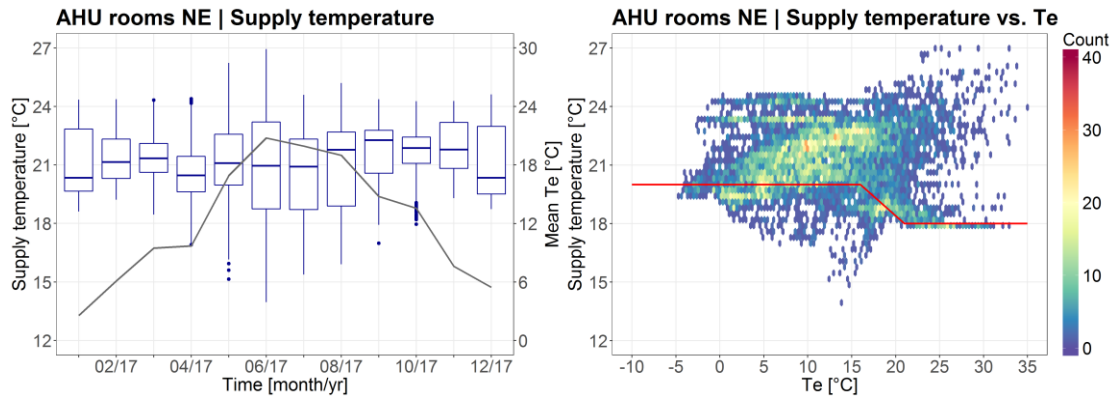


Figure 6.17: Supply temperature in the NE rooms during the year (left) and in relation to the outdoor temperature including the density of the measured points (right)

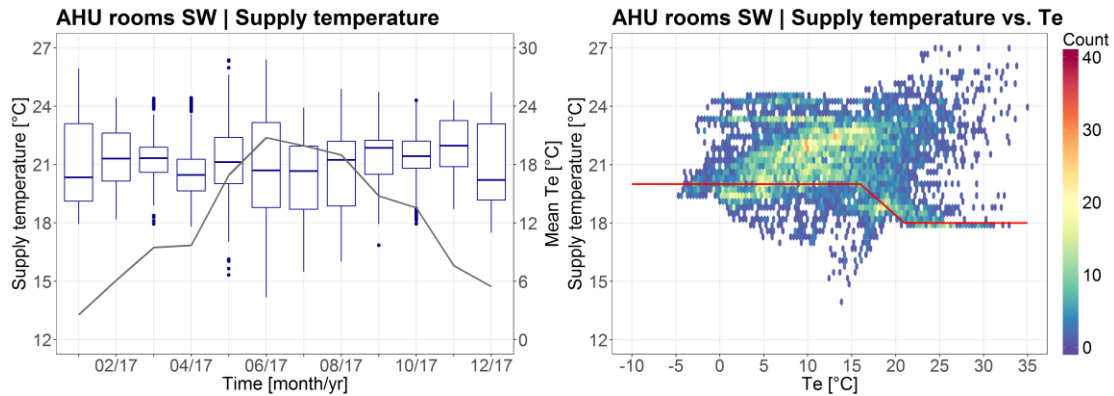


Figure 6.18: Supply temperature in the SW rooms during the year (left) and in relation to the outdoor temperature including the density of the measured points (right)

The supply and indoor temperature in room 1.05 during one typical week is presented in Figure 6.19. The temperature changes sometimes due to settings in regulation. However, the indoor temperature remains within the required range of 21-24°C during occupancy. Besides, the supply and indoor temperature are relatively high during the night and weekend. This explained the heating consumption of the boiler during unoccupied hours. Therefore, the regulation of the system can be adjusted while taking into account the indoor climate and the larger energy peaks that arise at the beginning of workday.

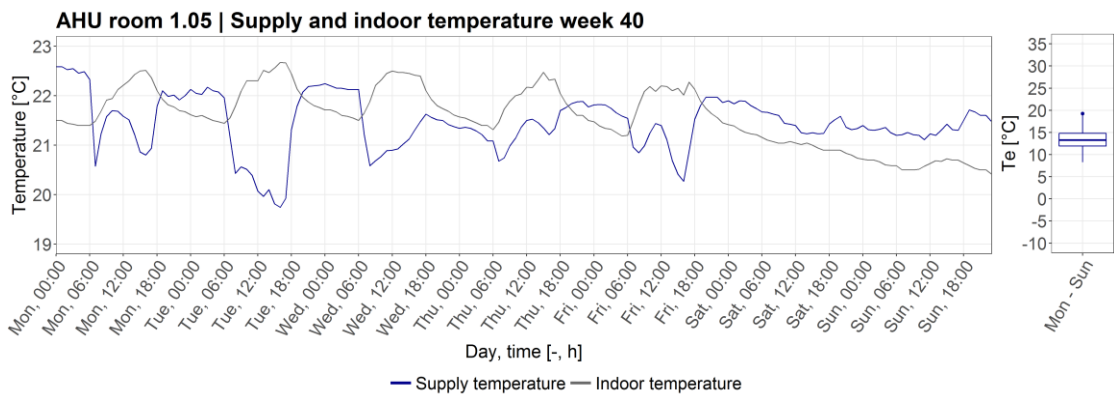


Figure 6.19: Supply and indoor temperature of the AHU at room 1.05 (left) and the mean outdoor temperature (right) from 2<sup>nd</sup> of October 2017 up to and including 8<sup>th</sup> of October 2017 (week 40)

### 6.3.5 Discussion

Overall, the analysis has shown that this case study building also performs fairly according to the design. Only the supply temperature of the AHU is higher than predicted during occupied and unoccupied hours. When this temperature is lower, the electricity and heating consumption will decrease. However, the measured indoor temperature meets the requirements. Therefore, a lower supply temperature of the AHU leads a higher energy consumption of the radiators in order to maintain a pleasant indoor climate.

## 6.4 LEAN energy analysis

The energy saving potential of the HVAC system is investigated based on the LEAN energy analysis. The performance modeling is conducted by comparing thermal energy benchmark models with historical data. These models can also be used to control the operational energy performance.

### 6.4.1 Benchmark model

As mentioned before, the main function of the thermal energy consumption is to bridge the difference between the outdoor temperature and the required indoor temperature and to provide hot water for hygiene purposes. The relation between the thermal energy consumption and the outdoor temperature is determined using linear regression. The results are evaluated by means of the  $R^2$  which indicates to which extent the dependent variable (thermal energy consumption) is predictable. The closer the value is to 1, the better the correlation of the parameters.

The heating and cooling consumption differs during the day due to time-dependent parameters, such as internal heat (occupants, equipment and lighting), solar irradiance, day and night set-points and stored energy in the thermal mass. Therefore, the regression is based on data of weekdays between 09:00-17:00h in order only to involve data with occupants. Besides, the daily mean consumption during these hours is used in order to better include the dynamic behavior of the HVAC system. The results of the regression are shown in Figure 6.20. The heating consumption correlates strongly with the outdoor temperature, since the  $R^2$  is 0.863. For the cooling consumption this relationship is reasonably acceptable, namely 0.662. Therefore, these models can be used as benchmark models.

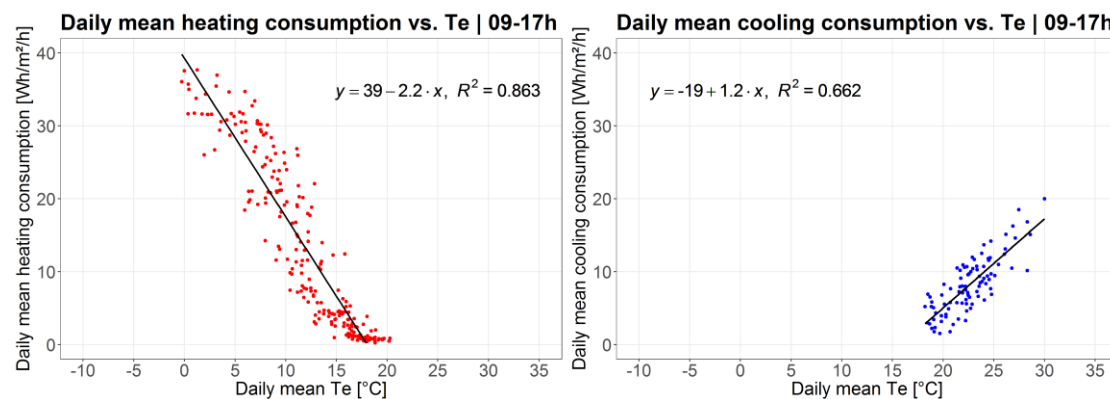


Figure 6.20: Regression for the daily mean heating (left) and cooling (right) consumption during weekdays between 09:00-17:00h as function of the outdoor temperature

The benchmark models are tested to determine the deviation of the residuals (predicted minus measured heat extraction). This is done by using 75% of the data set for training the model. To validate the model, the other 25% of the data set is used for testing. The R-script of both benchmark models can be found in Appendix B.5.

The results related to the heating consumption are presented in Figure 6.21. The deviation of the residuals is almost normally distributed (positive and negative). Figure 6.22 shows the results of the cooling consumption. In this case, the deviation of the residuals is also almost normally distributed.

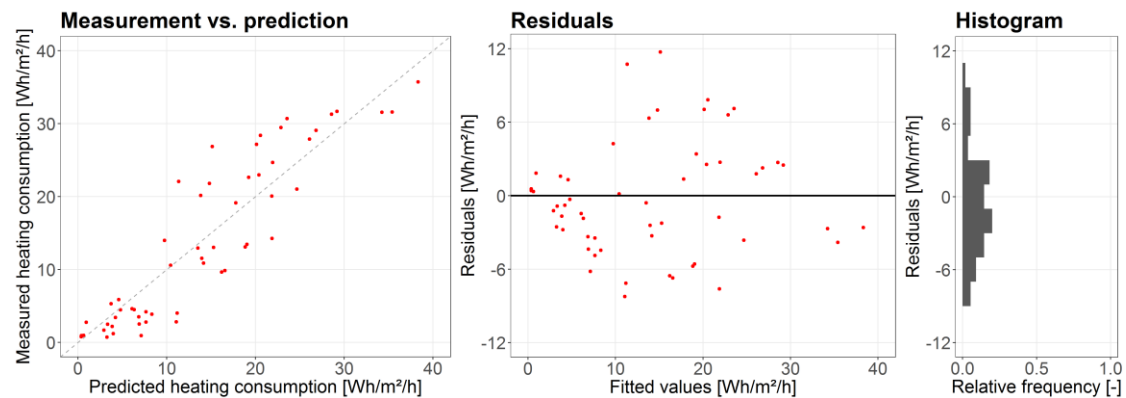


Figure 6.21: Deviation between the predicted and measured heating consumption (left), the deviation of the residuals (middle) and distribution of the residuals (right)

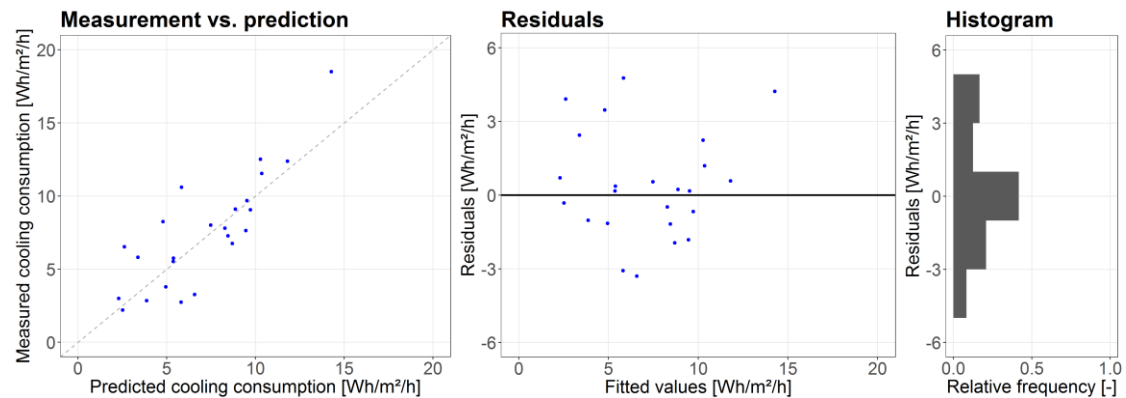


Figure 6.22: Deviation between the predicted and measured cooling consumption (left), the deviation of the residuals (middle) and distribution of the residuals (right)

## 6.4.2 Energy saving potential

The predicted energy extraction by benchmark models based on historical data and actual measured energy extraction are compared in order to provide an indication of energy saving potential. These models can also be used to assess the energy performance trends. The difference between the predicted and measured heating consumption from October 2017 up to and including December 2017 is shown in Figure 6.23. Figure 6.24 presents the difference between the predicted and measured cooling consumption from May 2017 up to and including July 2017.

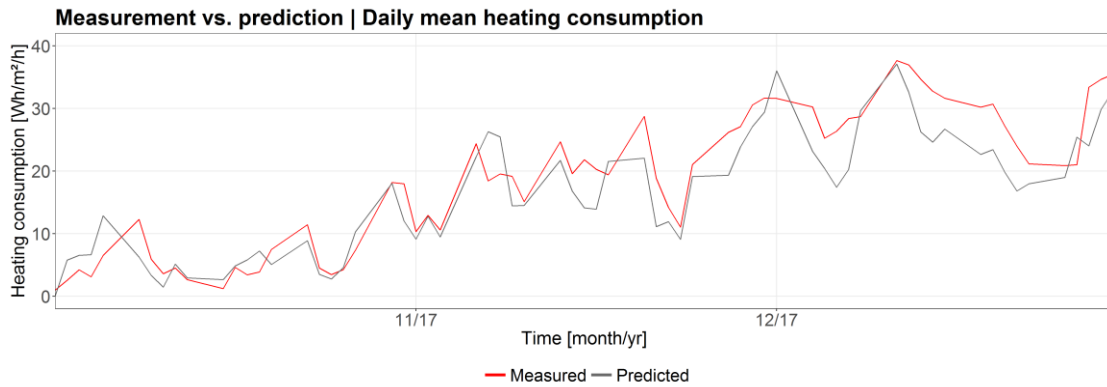


Figure 6.23: Difference between the predicted and measured heating consumption including an acceptable deviation from October 2017 up to and including December 2017

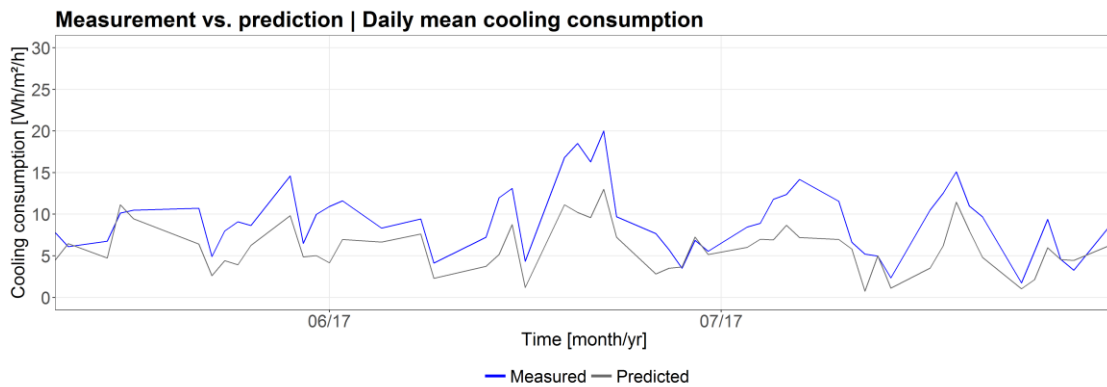


Figure 6.24: Difference between the predicted and measured cooling consumption including an acceptable deviation from May 2017 up to and including July 2017

The indication of the energy saving potential is calculated by using equation 5.4. The results of this calculation are shown in Table 6.5. The yearly energy saving potential of the heating consumption is 13%, while the energy saving potential of the cooling consumption is 41%. This is particularly caused by fluctuating supply temperature of the AHU.

Table 6.5: Indication of the yearly energy saving potential during occupancy (weekdays between 09:00-17:00h)

	Measured [kWh/m <sup>2</sup> ]	Energy saving potential [kWh/m <sup>2</sup> ]	Energy saving [%]
Heat consumption	24.9	3.3	13
Cold consumption	6.2	2.6	41

### 6.4.3 Discussion

As discussed before, benchmark models using regression are useful to investigate the energy saving potential. However, the results are dependent on the accuracy of the models. Nevertheless, the models can ensure that the energy consumption does not increase unexpectedly. In this case study, the benchmark models are also created by the historical operational data of the HVAC system.



## 7 Discussion

The study of this report has the following limitations with regard to the results.

### **Pareto analysis**

According to the Pareto analysis, 20% of the main parameters with highest impact on the energy consumption account for roughly 80% of the energy performance gap. However, in this study not all cases meet this condition. The main reason for this is that the building-related parameters have been left out of consideration in order to remain in line with the scope of the study. Besides, when more parameters are selected for the sensitivity analysis, more parameters belong to the 20%. Although both case study buildings have the same performance indicators in this study, more buildings need to be investigated in order to conclude under which conditions the applied indicators in this study are generally applicable. Nevertheless, the Pareto analysis contributes to stay focused on the most important parameters of buildings.

### **Performance analysis**

This study is performed by only using existing sensors of the BMS of both case study buildings including electricity and gas sensors, so that the method is directly applicable in other similar non-residential buildings. As expected, these sensors are sufficient for drawing conclusions about the overall measured HVAC performance. However, in order to draw more detailed conclusions about parts of the system, the number of sensors needs to be extended. Sometimes, the limited number of sensors can be compensated by calculations. An example of this, is the calculation of the amount of thermal energy extraction by the ATES system of Larisa. But real measurements are preferred for accuracy.

For the preprocessing and cleaning of the target data, it is necessary to obtain information about the time of use of the building and maintenance of the HVAC system, for example adjustment in settings. This is necessary to properly assess deviations in historical building data. Besides, the data has to be considered as realistic, since it has found that the sensors of the BMS can be inaccurate or unreliable. An example of this is the quite low measured pressure drop across the filter of an AHU of Larisa. Despite the fact that the data has been critically analyzed, some inaccuracies are not visible because calibration and maintenance of sensors and BMS are not considered in this study.

### **LEAN energy analysis**

In this study, the energy saving potential is investigated based on the LEAN energy analysis. According to the LEAN energy analysis, benchmark models are created using data of other buildings with similar type, use, and other characteristics if available. Another possibility is to compare data before and after a large retrofit. However, collecting this data was not an objective of this study. So in line with the LEAN approach, the benchmark models are created by using historical data in both case studies. The performance modeling is conducted by comparing these benchmark models with empirical data. This shows deviations from the regression line which gives an indication of the energy saving potential. However, the results are dependent on the accuracy of the created models.

The benchmark models are developed using regression in order to avoid a complex and time-consuming process. However, regression reduces the added value of large data sets because only a small amount of variables is used to develop the model. This leads to a limitation of the discovered knowledge for practical application. Therefore, in future research other techniques such as clustering and association can be used to discover more insights.

## 8 Conclusion

This study was performed to provide recommendations in order to optimize the energy performance of operational buildings by a systematic assessment. In this chapter the results of the research are evaluated by answering the formulated research questions.

### 8.1 Sub-questions

First the sub-questions are answered.

- I. *“What are the performance indicators of the case study buildings regarding the HVAC system and the occupant behavior?”*

Based on the Pareto analysis, the set-points for heating and cooling and the related supply temperatures are the most important parameters for the heating, cooling and electricity consumption. Both case study buildings have the same performance indicators which makes it more applicable to other non-residential buildings. However, the 20% major parameters are not always responsible for 80% of the performance gap in order to fully comply with the Pareto analysis. This is due to the fact that the building-related parameters have been left out of consideration in this study. Nevertheless, the analysis is very suitable to remain focused on the most important performance indicators when analyzing the performance of the building. This is necessary to obtain financially attractive business cases.

- II. *“Which parts of the HVAC system of the case study buildings are underperforming based on the performance indicators?”*

In general, especially the HVAC system of care center Larisa is underperforming compared to the design and settings. The ATES system of Larisa is in unbalance and the AHUs of both buildings supply higher temperatures than predicted. However, this is also needed to provide the required indoor climate. The unbalanced situation of the ATES system is caused by the higher heating than cooling demand, leading to a cold surplus of 38%. This has to be solved in order to prevent the depletion of the wells in the future and to comply with the Dutch law. Therefore, the amount of the heat injection has to be increased. In order to determine the exact cause of the high supply temperature of the AHUs, additional measurements on component level are needed. However, this is not possible with the current sensors of the BMS. Nevertheless, it can be concluded that this is caused by the system regulations.

- III. *“To which extent can data mining contribute to improving the overall energy performance of the case study buildings?”*

Building operational data is in fact the reflection of the actual building performance. This study shows that DM techniques are valuable for knowledge discovery in this data, since the BMS can only perform simple data analysis and visualizations based on a short period of historical data. Regression provides an indication of the energy saving potential of both case study buildings. The energy saving potential of Larisa is 7% on the heat extraction and 70% on the cold extraction by the ATES system. In addition, the energy saving potential of Kropman Breda is 13% on the heating consumption and 41% on the cooling consumption. However, these predictions are dependent on the accuracy of the created models.

For the interpretation of the discovered knowledge, solid domain knowledge is still needed. This results to insights that can lead to high energy savings with a short payback time due to low investment costs. Therefore, DM is very suitable in order to control and optimize the energy performance of operational buildings.

## 8.2 Main research question

After answering the sub-questions, the main research question is answered.

*“Which effective strategies can be used to improve underperforming HVAC systems of buildings using data mining techniques?”*

The process of building performance optimization starts after the order of the building owner. Therefore, it is very important that building owners become more aware of how energy efficient their buildings can operate by controlling and improving controllable parameters. In order to increase the interest of building owners, a short pay-back time is important. That is the reason why the considered strategies contribute to reduce the energy costs combined with low investment costs. The investment costs are twofold, namely related to the performance analysis process and to the actual improvement of the system by the building service company.

Nowadays, the HVAC performance is generally periodically controlled based on simple data analysis and visualizations of the BMS (mostly with a history of two weeks) and is heavily depending on the knowledge and experience of the particular investigator. Therefore, three main steps are necessary in order to systematically improve the underperforming HVAC systems.

The first step to improve the complex underperforming HVAC systems is the identification of the major performance indicators. Since the BMS in buildings contains massive data sets which can be unlimited stored in a database, the performance indicators ensure to remain focused on the most important parameters of the underperforming installations. This leads to an effective building performance analysis. In this study these indicators are obtained by the Pareto analysis which has proved to be an efficient approach.

The second step is the analysis of operational data regarding these indicators. It is advisable to make a plan about sensors which are needed. If the sensors of the BMS do not measure the data related to the indicators, additional measurements are needed. In addition, if the history of the logged data is too short, the dataset is not suitable to see trends and obtain knowledge about the operational building performance. Therefore, it is necessary to log the data for at least a few months, preferably over years. By means of the logged data, the operational energy performance can be analyzed. It is recommended to analyze the building system by means of a top-down approach. This leads to an efficient process to execute. Only when there is a specific complaint from the building users, a bottom-up approach can be more appropriate. To interpret the data analysis, the data measured by the sensors has to be assessed for accuracy and reliability. Due to sensor quality and false measurements the results can deviate considerably from the real operational conditions. This requires domain knowledge of the data analyst.

The third step is to investigate the energy saving potential. For this, DM techniques have shown to be very valuable. In this study regression is used to create the benchmark models. Regression is used in order to avoid a complex and time-consuming process by developing data models based on more advanced algorithms e.g. decision tree, artificial neural network and support vector machine. These models can be made in different ways. The models created in this study are based on historical data of the relevant building. Comparing the benchmark models with empirical data leads to an indication of the potential reduction of the energy performance gap. In addition, these models can be used to control the energy consumption.

## 9 Recommendations

In order to optimize the energy performance of future buildings, the next activities in the design and operational phase are recommended:

- First, it is recommended to make a plan about sensors which are needed. Nowadays, the sensors which are already part of the BMS can be used for the performance analysis. However, it seems that they are not always sufficient. For example, in order to determine inefficiencies of the specific installations, more sub energy meters are needed. In addition, the main function of a building is to provide a pleasant and healthy indoor climate. Therefore, a number of related sensors are advisable which can be used as a starting point for the analysis.
- When selecting sensors, attention must be paid to the specifications. The accuracy and reliability of the BMS sensors are essential for the success of control and optimization strategies of the HVAC system. In addition, the rounding of the measurements by the sensors must be taken into account. This is because all actions and decisions are made based on the measurements. Therefore, the consequences of faulty sensor signals could be erroneous. Building professionals can check the operational data. However, small differences between real and measured values cannot be traced. In case of doubt about the measured values, calibration is necessary.
- In order to analyze multiply buildings in a more efficient way, it is advisable to use generic names for the sensors. This enables that the created scripts can easily be applied to other buildings. Project Haystack aims to streamline working with data by pragmatic use of naming conventions and taxonomies. This open source initiative can be used as a guide for defining the sensor names.
- Besides, it is advisable to fill in a logbook about maintenance of the building system for the correct assessment and cleaning of the building operational data. This is very useful to clarify outliers in historical trends and to avoid inaccurate conclusions.
- State of art software tools such as RStudio and Matlab can be connected to database environments to perform analysis in a more automated and cost effective way. The created scripts that are used for these analyzes can easily be applied to other buildings.
- More data is needed to create benchmark models using data of buildings with similar type, use, and other characteristics. This means at least the energy consumption of the building in combination with the indoor and outdoor temperature and the time of use. In addition, the conditioned floor area is needed to normalize the energy consumption.
- The underperforming building installations can be improved by the building service company. When this is finished, a CCx process of the HVAC performance is advised. The use of a dashboard with the actual construction performance is very suitable for this process. This ensures that system inefficiencies are continuously detected and can be improved by the maintainer. In addition, this process results in a pleasant indoor climate combined with limited running costs.
- Finally, the building owners could be made more aware of the power they have to control their HVAC systems by a data driven approach. In fact, according to the General Data Protection Regulation (GDPR) they are the owner of the data and can request independent parties to check the performance by data analysis.

## References

- [1] Intergovernmental Panel on Climate Change (IPCC), "Climate Change 2014," 2014.
- [2] European Commission, "Europa 2020: A strategy for smart, sustainable and inclusive growth," 2010.
- [3] General Secretariat of the Council, "European Council (23 and 24 October 2014) - Conclusions," 2014.
- [4] European Commission, "A Roadmap for moving to a competitive low carbon economy in 2050," 2011.
- [5] J. Grözinger, T. Boermans, A. John, F. Wehringer and J. Seehusen, "Overview of Member States information on NZEBs," 2014.
- [6] C. Fan and F. Xiao, "Assessment of building operational performance using data mining techniques: a case study," 2017a.
- [7] European Commission, "Buildings," 1 August 2018. [Online]. Available: <https://ec.europa.eu/energy/en/topics/energy-efficiency/buildings>.
- [8] European Commission, "Energy Efficiency and its contribution to energy security and the 2030 Framework for climate and energy policy," 2014.
- [9] Carbon Trust, "Closing the gap - Lessons learned on realising the potential of low carbon building design," 2011.
- [10] International Energy Agency, "Final Report Annex 53, Total Energy Use in Buildings - Analysis and Evaluation Methods," 2013.
- [11] A. Hashemi, M. Sunikka-Blank, E. Mohareb, T. Vakhitova, D. Dantsiou, H. Ben and T. Sharmin, "Performance Gap? Energy, Health and Comfort Needs in Buildings," 2016.
- [12] F. Xiao and C. Fan, "Data mining in building automation system for improving building operational performance," 2014.
- [13] CarbonBuzz, 2018. [Online]. Available: <https://www.carbonbuzz.org/>. [Accessed 1 March 2018].
- [14] C. v. Dronkelaar, M. Dowson, C. Spataru and D. Mumovic, "A Review of the Regulatory energy Performance Gap and its Underlying Causes in Non-domestic Buildings," 2016.
- [15] Agentschap NL, "Gebouwmonitoring met energieprofielen; Energieverspilling eenvoudig opsporen en verhelpen," 2011a.
- [16] CBS, "Aandeel hernieuwbare energie 5,9 procent in 2016," 2017. [Online]. Available: <https://www.cbs.nl/nl-nl/nieuws/2017/22/aandeel-hernieuwbare-energie-5-9-procent-in-2016>. [Accessed 1 December 2017].
- [17] N. Aste, M. Manfren and G. Marenzi, "Building Automation and Control Systems and performance optimization: A framework for analysis," 2017.
- [18] J. Verhelst, G. V. Ham, D. Saelens and L. Helsen, "Model selection for continuous commissioning of HVAC-systems in office buildings: A review," 2017.
- [19] ASHRAE, "Commissioning Process for Buildings and Systems," 2012.
- [20] E. Mills and P. A. Mathew, "Monitoring-based Commissioning: Benchmarking Analysis of 24 University Buildings in California," 2012.
- [21] E. Maslesa, P. A. Jensen and M. Birkved, "Indicators for quantifying environmental building performance: A systematic literature review," 2018.

- [22] A. Kylili, P. A. Fokaides and P. A. L. Jimenez, "Key Performance Indicators (KPIs) approach in buildings renovation for the sustainability of the built environment: A review," 2016.
- [23] W. W. Piegorsch, "Statistical Data Analytics," 2015.
- [24] S. D'Oca and T. Hong, "Occupancy schedules learning process through a data mining framework," 2014.
- [25] U. Fayyad, G. Piatetsky-Shapiro and P. Smyth, "From Data Mining to Knowledge Discovery in Databases," 1996.
- [26] U. Shafique and H. Qaiser, "A Comparative Study of Data Mining Process Models (KDD, CRISP-DM and SEMMA)," 2014.
- [27] J. A. Lara, D. Lizcano, M. A. Martínez and J. Pazos, "Data preparation for KDD through automatic reasoning based on description logic," 2014.
- [28] S. Vadapalli, "Hands-on DevOps," 2017.
- [29] A. J. Huls, "Systematic energy performance assessment in operating office buildings," 2016.
- [30] B. M. Bartlett, "Powerful Strategic Planning Rules That Could Revolutionize Your Business And Life," [Online]. Available: <https://benmbartlett.com/powerful-strategic-planning-rules-that-could-revolutionize-your-business-and-life/>. [Accessed 1 11 2017].
- [31] J. K. Kissock and J. Seryak, "Lean Energy Analysis: Identifying, Discovering and Tracking Energy Savings Potential," 2004.
- [32] M. Donnelly, J. Kummer and K. Drees, "LEAN Energy Analysis: Using Regression Analysis to Assess Building Energy Performance," 2013.
- [33] I. Schoenmakers, W. Zeiler and G. Boxem, "KPI's energy consumption of isolation rooms in hospitals," 2016.
- [34] A. J. Huls, B. Lops and W. Zeiler, "Time series Analysis for Re-Commissioning of Building Service installations," 2018.
- [35] E. Borgstein, R. Lamberts and J. Hensen, "Evaluating energy performance in non-domestic buildings: A review," 2016.
- [36] C. Fan and F. Xiao, "Mining Gradual Patterns in Big Building Operational Data for Building Energy Efficiency Enhancement," 2017b.
- [37] D. J. Hand, H. Mannila and P. Smyth, "Principles of Data Mining," 2001.
- [38] C. Fan, F. Xiao, Z. Li and J. Wang, "Unsupervised data analytics in mining big building operational data for energy efficiency enhancement: A review," 2017b.
- [39] J. Han, M. Kamber and J. Pei, "Data Mining: Concepts and Techniques," 2012.
- [40] C. Fan and F. Xiao, "Mining big building operational data for improving building energy efficiency: A case study," 2017c.
- [41] C. Fan, F. Xiao and C. Yan, "A framework for knowledge discovery in massive building automation data and its application in building diagnostics," 2014.
- [42] EnergyPlus, "EnergyPlus," 2018. [Online]. Available: <https://energyplus.net/>. [Accessed 1 August 2018].
- [43] RStudio, "Why RStudio?," 2018. [Online]. Available: <https://www.rstudio.com/about/>. [Accessed 1 August 2018].
- [44] Architecten aan de Maas, "Larisa verpleegklinik," 2017. [Online]. Available: <https://www.architectenaandemaas.com/nl/projecten/2017/06/01/larisa-verpleegklinik/>. [Accessed 1 October 2017].

- [45] Rijksdienst voor Ondernemend Nederland (RVO), "Hulpmiddel omrekening naar primaire energie," [Online]. Available: <https://www.rvo.nl/file/hulpmiddel-omrekening-naar-primaire-energie>. [Accessed 1 April 2018].
- [46] ECN, "Nieuwe benchmark energieverbruik utiliteitsgebouwen en industriële sectoren," 2016.
- [47] Agentschap NL, "Energiezuinig koelen met warmte- en koudeopslag," 2011b.
- [48] DWA installatie- en energieadvies, "Onderzoek criteria energiebalans WKO," 2012.
- [49] IF Technology, "Rapportage bodemenergiesystemen in Nederland: Analyse van 125 projecten," 2016.
- [50] H. Velvis and R. J. Buunk, "District Aquifer Thermal Energy Storage (DATES)," 2017.
- [51] B. Bozkaya, R. Li, T. Labeodan, R. Kramer and W. Zeiler, "Development and evaluation of a building integrated aquifer thermal storage model," 2017.
- [52] D. Vanhoudt, J. Desmedt, J. V. Bael, N. Robeynb and H. Hoes, "An aquifer thermal storage system in a Belgian hospital: Long-term experimental evaluation of energy and cost savings," 2011.
- [53] N. Nassif, "The impact of air filter pressure drop on the performance of typical air-conditioning systems," 2012.
- [54] Z. Li, "A hybrid technique to improve measurement accuracy and reliability in AC systems," 2014.

# Appendix

Appendix A: **Case study 1: Larisa**

Appendix A.1: Building design

Appendix A.2: Pareto analysis

Appendix A.3: Designed performance analysis

Appendix A.4: Measured performance analysis

Appendix A.5: LEAN performance analysis

Appendix B: **Case study 2: Kropman Breda**

Appendix B.1: Building design

Appendix B.2: Pareto analysis

Appendix B.3: Designed performance analysis

Appendix B.4: Measured performance analysis

Appendix B.5: LEAN performance analysis



## A Case study 1: Larisa

### A.1 Building design

The floor plans of care center Larisa are presented in Figures A.1 to A.5.

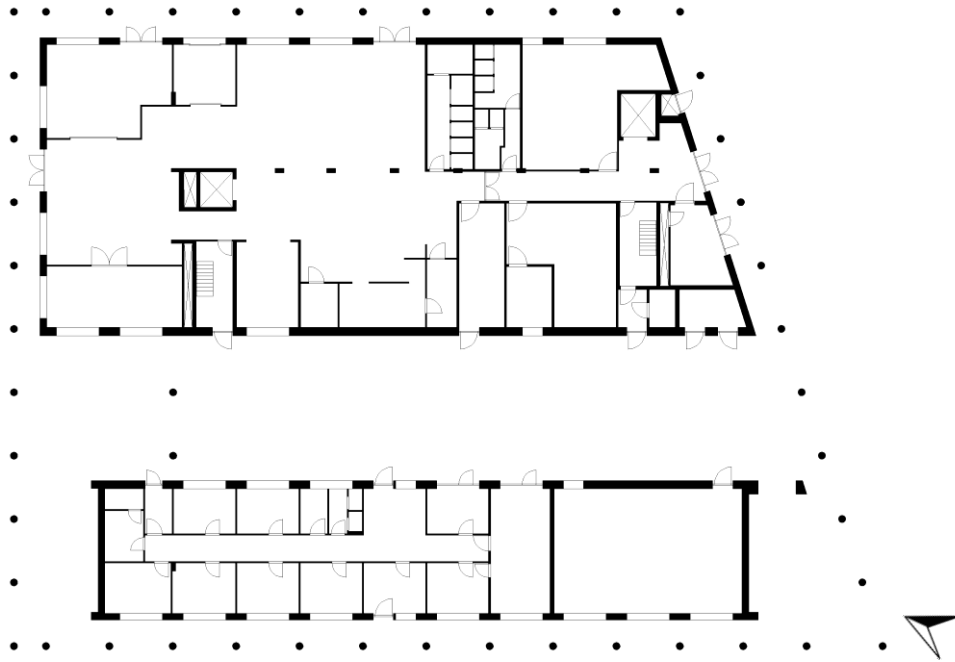


Figure A.1: Ground floor of Larisa (1:500)

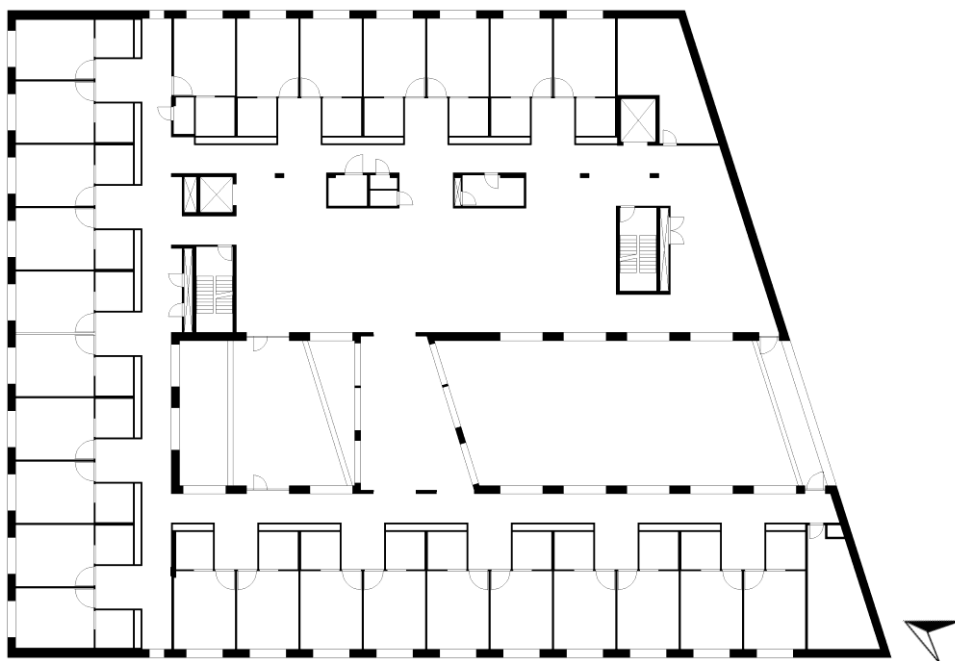


Figure A.2: First floor of Larisa (1:500)

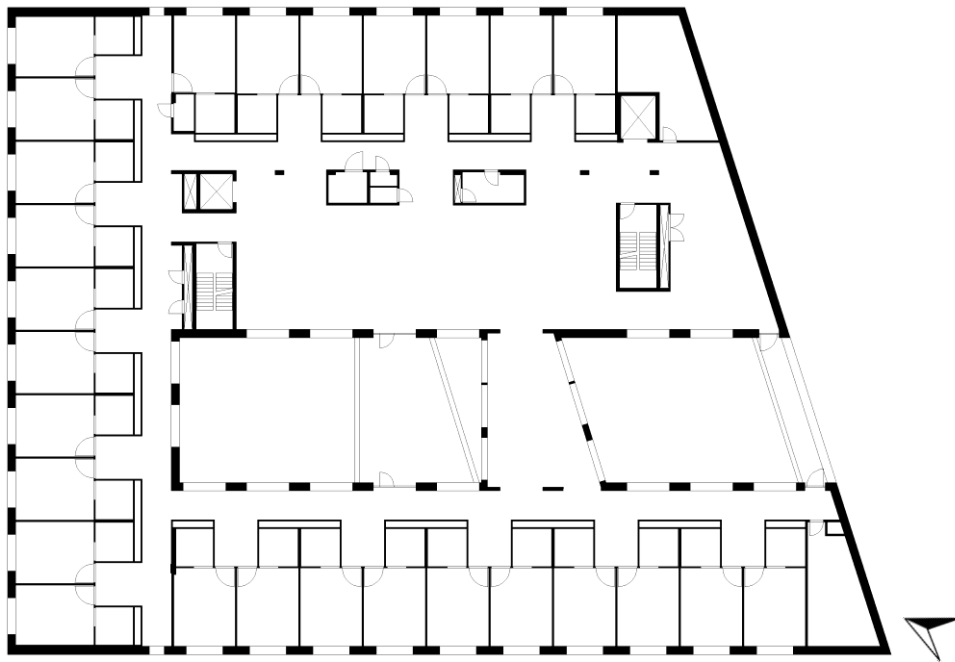


Figure A.3: Second floor of Larisa (1:500)

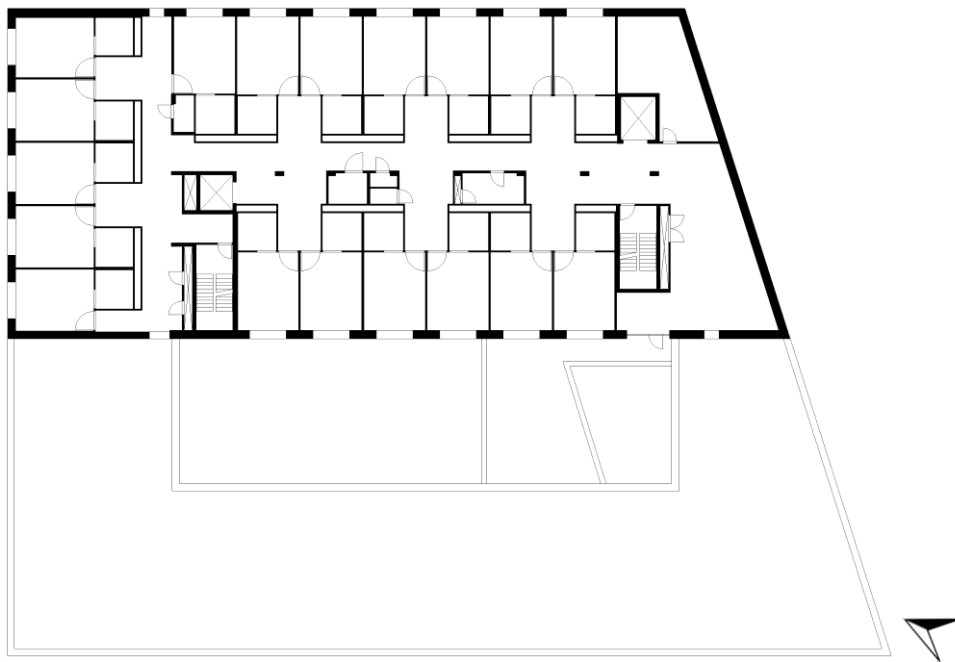


Figure A.4: Third floor of Larisa (1:500)

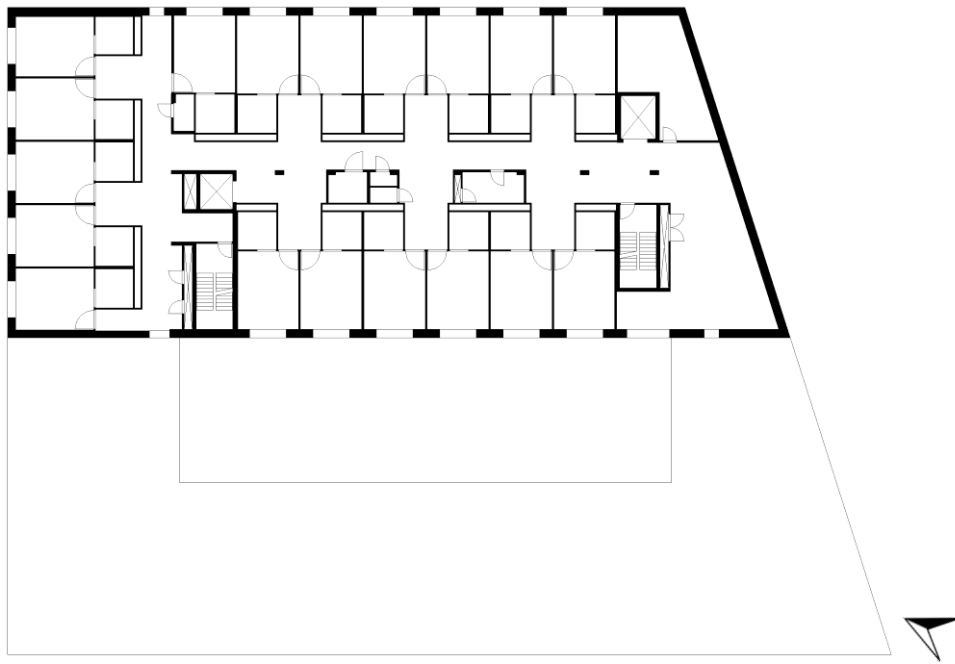
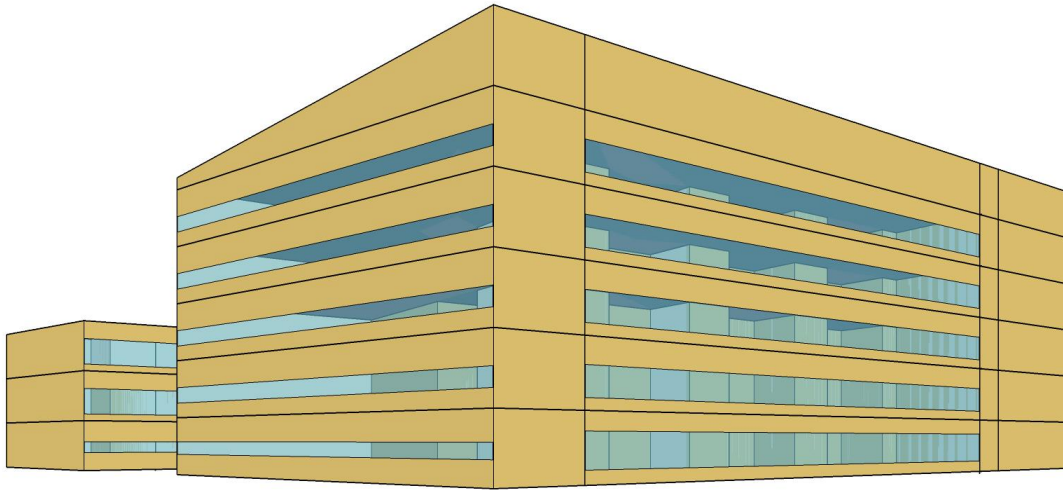


Figure A.5: Fourth floor of Larisa (1:500)

## A.2 Pareto analysis

The 3D model of Larisa is shown in Figure A.6. This model is used for the sensitivity analysis with EnergyPlus.



*Figure A.6: Created 3D model of Larisa in SketchUp*

### A.3 Designed performance analysis

#### ATES system with heat pump

The installation principle of the ATES system including the heat pump is presented in Figure A.7.

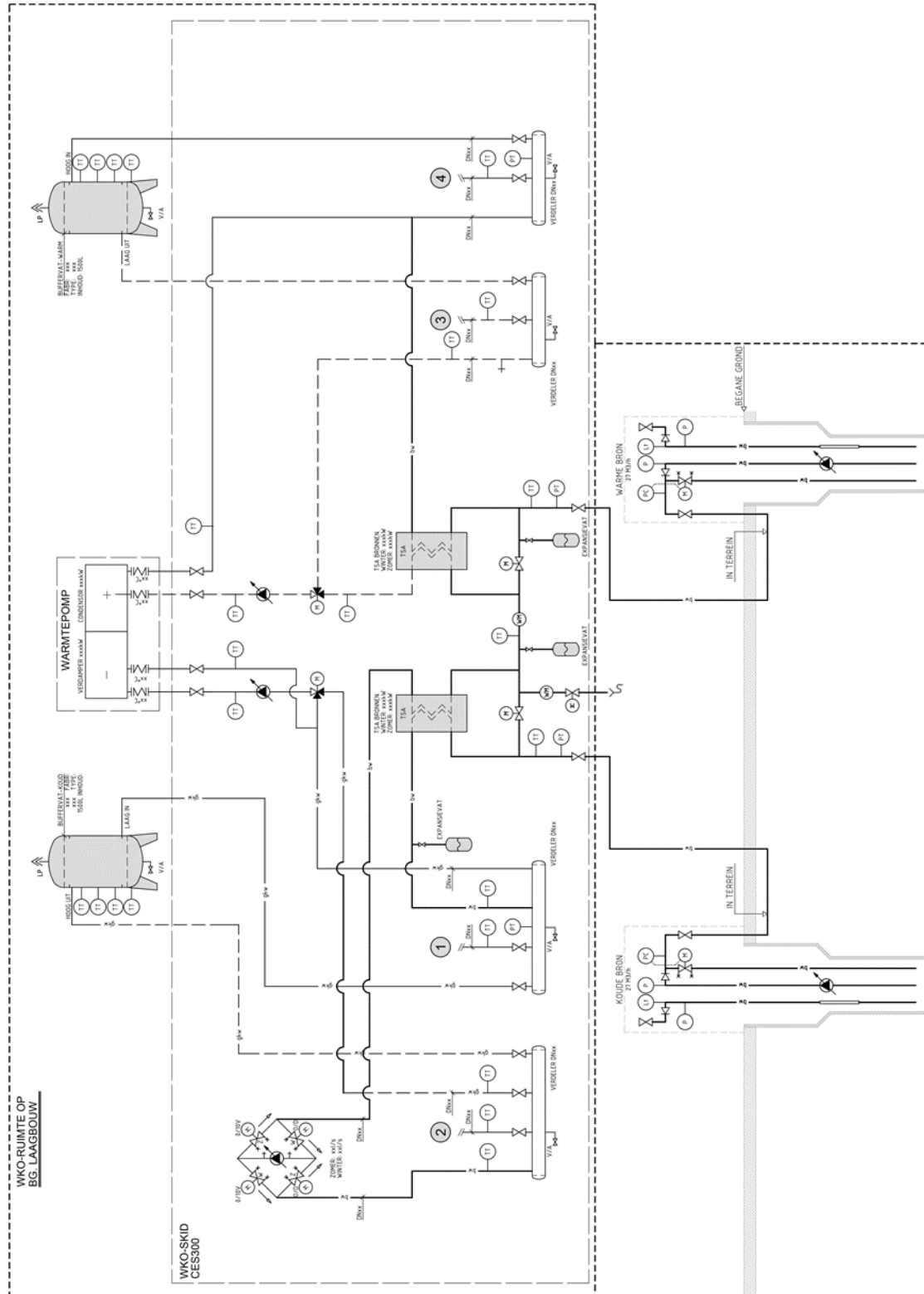



Figure A.7: Installation principle of the ATES system with heat pump

The technical specifications of the heat pump is shown in Figure A.8.



### 3 Technische specificatie

#### 3.1 CIAT warmtepomp / watergekoelde koelmachine, gegevens per machine

**DynaCIAT Power** **LG(P) 700V**

Aantal koudemiddelcircuits	stuks	2
Capaciteitsregeling	%	100-78-71-50-28-21-0
Koudemiddel / Vulling	type / kg	R410A / 12,5 + 12,5
EER bij deze bedrijfscondities		4,27

Deellast prestaties bij EUROVENT condities				
EER 100%	EER 75%	EER 50%	EER 25%	ESEER
4,50	5,14	5,75	5,83	5,53

**Compressor, gegevens zijn voor de totale machine**

Bouwwijze		scroll
Aantal	stuks	4
Opgenomen vermogen	kW	47,9

**Verdamper**

Koelvermogen	kW	204,4
Vloeistofsoort		water
Vloeistoftraject	°C	11,5 – 5,5
Vloeistofhoeveelheid	m <sup>3</sup> /h	30,0
Waterzijdige weerstand	kPa	28,5
Waterzijdige weerstand filter	kPa	7
Vervuilingfactor	m <sup>2</sup> .K/kW	0,044

**Condensor**

Thermisch vermogen	kW	253,8
COP bij vollast		5,25
Vloeistofsoort		water
Vloeistoftraject	°C	28,7 - 36
Vloeistofhoeveelheid	m <sup>3</sup> /h	30
Waterzijdige weerstand	kPa	34,0
Waterzijdige weerstand filter	kPa	10
Vervuilingfactor	m <sup>2</sup> .K/kW	0,044

**Geluidrukniveau, gemeten op 5 meter in het vrije veld**

Xtra low noise uitvoering	dB(A)	52
---------------------------	-------	----

**Elektrische gegevens**

Aansluitspanning	V / ph / Hz	400 / 3 / 50 + Aarde
Maximale nominaalstroom*)	A	140
Maximale aanloopstroom met softstarters	A	230

**Algemeen**

Afmeting (l x b x h)	mm	2.099 x 996 x 1.869
Bedrijfgewicht	kg	1.088
Hijsgewicht	kg	1.044

\*) Dit is de waarde welke benodigd is bij de berekening van de elektrische voeding.

---

20150112 pagina 5 van 8

Figure A.8: Technical specifications of the heat pump

## A.4 Measured performance analysis

### Sensors

The sensors of the BMS are presented in Table A.1. These sensors are installed for monitoring and controlling the operational performance.

Table A.1. Sensors of the BMS

ID	Description	Unit	ID	Description	Unit
1	Condensator temperatuur uit	°C	54	Aanvoertemperatuur	°C
2	Temperatuur TSA uit	°C	55	Ruimtetemperatuur verdieping 4	°C
3	Condensator temperatuur in	°C	56	Ruimtetemperatuur LB 2e Noord (defect)	°C
4	Verdamper temperatuur in	°C	57	Ruimtetemperatuur LB 2e Zuid (defect)	°C
5	Capaciteit	%	58	Ruimtetemperatuur verdieping 3	°C
6	Verdamper temperatuur in	°C	59	Relatief buitenvocht	%
7	Verdamper regelklep terugmelding	%	60	Buitentemperatuur meting (defect)	°C
8	Temperatuur voor GWK verdeler TSA1 uit	°C	61	Condensatietemperatuur	°C
9	Temperatuur tussen TSA's	°C	62	Filter afzuigkanaal	Pa
10	Temperatuur voor GWK verdeler TSA1 in	°C	63	Retourluchttemperatuur	°C
11	Flowmeter bronsysteem	m³/h	64	Inblaas temperatuur	°C
12	Temperatuur warme bron	°C	65	SP aanvoertemperatuur CV (defect)	°C
13	Temperatuur naar condensator	°C	66	SP aanvoertemperatuur GWK (defect)	°C
14	CV druk	bar	67	Aanvoertemperatuur	°C
15	CV aanvoer afnemer	°C	68	Retourtemperatuur	°C
16	Gew. centrale aanvoertemperatuur	°C	69	Vloertemperatuur	°C
17	Temperatuur warmte buffer hoog	°C	70	Retourtemperatuur verwarming	°C
18	Temperatuur warmte buffer midden 1	°C	71	Niveau koude bron	mH2O
19	Temperatuur warmte buffer midden 2	°C	72	Niveau warme bron	mH2O
20	Temperatuur warmte buffer laag	°C	73	Gewenste aanvoertemperatuur	°C
21	Druksensor koude bron	bar	74	Centrale aanvoertemperatuur	°C
22	Temperatuur koude bron	°C	75	Buitentemperatuur (daggemiddelde 3 dagen)	°C
23	Druksensor warme bron	bar	76	Bedrijfsituatie	1, 2, 3
24	GWK druk	bar	77	Gew. aanvoertemperatuur	°C
25	Temperatuur koude bron hoog	°C	78	Filter aanzuigkanaal	Pa
26	Temperatuur koude buffer midden 1	°C	79	Omloopklep toev. Plaatw.	%
27	Temperatuur koude buffer midden 2	°C	80	Druk toevoerkanaal	Pa
28	Temperatuur koude buffer laag	°C	81	Druk afzuigkanaal	Pa
29	GWK retour afnemer	°C	82	Ber. Aanvoertemperatuur ketelregeling	°C
30	Temperatuur naar verdamper	°C	83	Centrale toev. temperatuur	°C
31	Filter afzuigkanaal	Pa	84	Gewenste aanvoertemperatuur	°C
32	Condensatietemperatuur	°C	85	Centrale retourtemperatuur	°C
33	Buitentemperatuur	°C	86	Aanvoertemperatuur transportgr.	°C
34	Filter aanzuigkanaal	Pa	87	Retourtemperatuur transportgr.	°C
35	Retourtemperatuur verdamper	°C	88	Retourtemperatuur tapwater boiler 1	°C
36	Druk afzuigkanaal	Pa	89	Centrale retourtemperatuur tapwater	°C
37	Retourluchttemperatuur	°C	90	Centrale aanvoertemperatuur tapwater	°C
38	Omloopklep toev. plaatw.	%	91	Aanvoertemperatuur tapwater boiler 1	°C
39	Aanvoertemperatuur transp. BKA	°C	92	Retourtemperatuur tapwater boiler 2	°C
40	Retourtemperatuur transp. BKA	°C	93	Boiler 1	status
41	Aanvoertemperatuur transp. LBK	°C	94	Aanvoertemperatuur tapwater boiler 2	°C
42	Retourtemperatuur transp. LBK	°C	95	Retourtemperatuur verwarmers	°C
43	Retourtemperatuur	°C	96	Vloertemperatuur	°C
44	Aanvoertemperatuur	°C	97	Condensatietemperatuur	°C
45	SP aanvoertemperatuur GWK	°C	98	Omloopklep toev. plaatw.	%
46	SP aanvoertemperatuur CV	°C	99	Filter aanzuigkanaal	Pa
47	Inblaas temperatuur	°C	100	Druk toevoerkanaal	°C
48	Druk toevoerkanaal	Pa	101	Inblaas temperatuur	°C
49	Vloertemperatuur	°C	102	Retourluchttemperatuur	°C
50	Ruimtetemperatuur	°C	103	Druk afzuigkanaal	Pa
51	Gew. aanvoertemperatuur	°C	104	Filter afzuigkanaal	Pa
52	Buitentemperatuur	°C	105	Aanvoertemperatuur convectoren	°C
53	Retourtemperatuur	°C	106	Retourluchttemperatuur convectoren	°C

**Energy consumption**

The heat maps of the measured outdoor temperature and the energy consumption are shown in Figures A.9 to A.11.

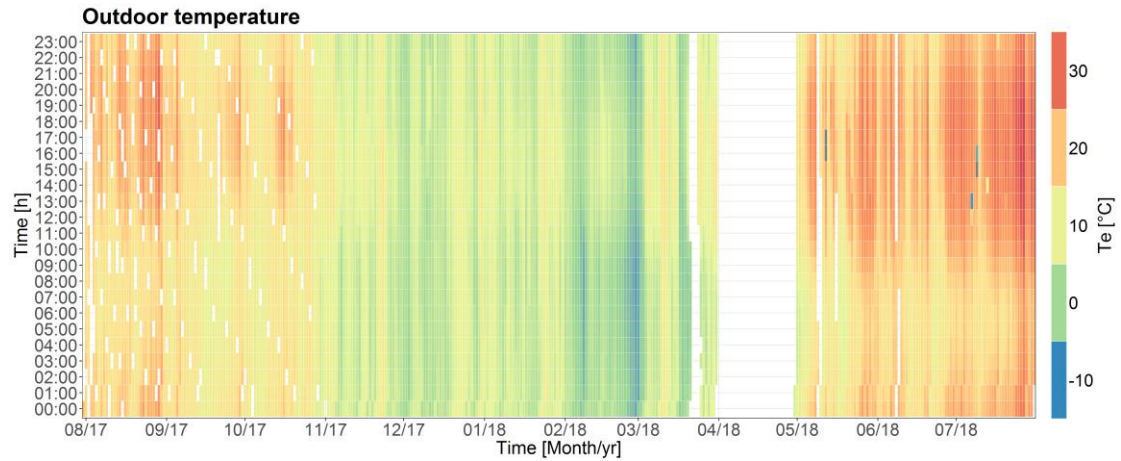


Figure A.9: Heat map of the measured outdoor temperature

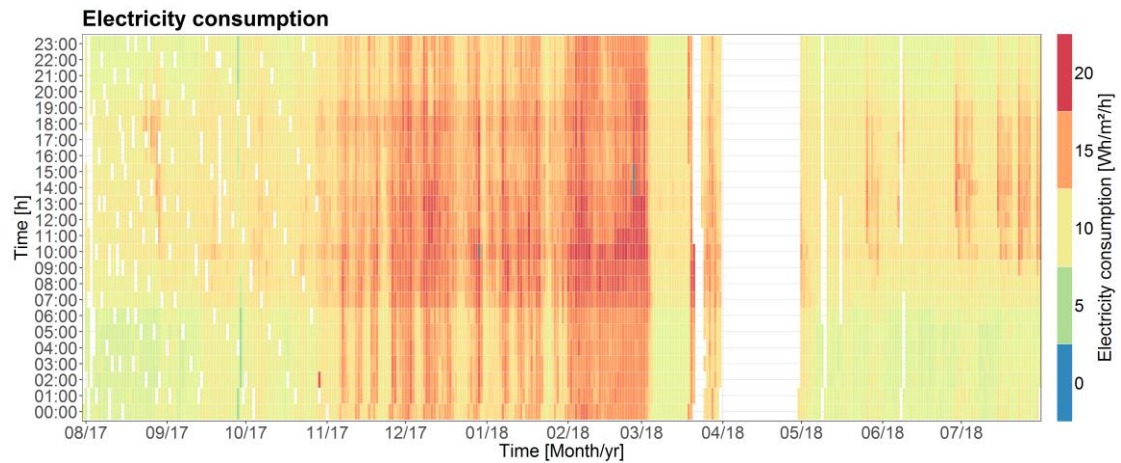


Figure A.10: Heat map of the measured electricity consumption

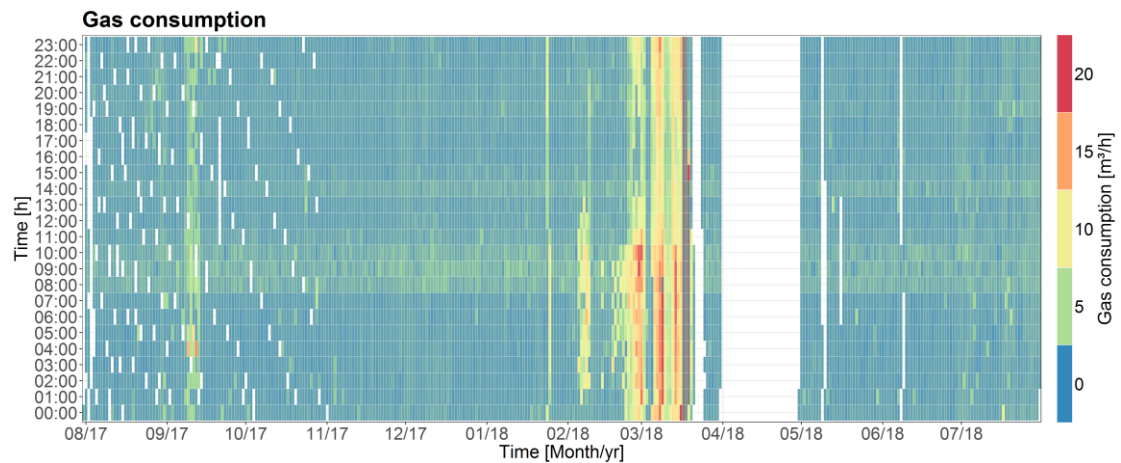


Figure A.11: Heat map of the measured gas consumption



**ATES system with heat pump**

The extracted heat and cold by the ATES system is calculated by multiplying the used power (equation 5.1) with time. Due to the direction of the flow is not measured, the determination of the thermal extraction is assumed, following the decision tree shown in Figure A.12. When a flow is measured, heat or cold is extracted from the wells (Figure A.13). For heating, the heat pump should always have a capacity (Figure A.14). For cooling, the heat pump is only running when the directly extracted cold is not sufficient. Therefore, the forward and return temperatures of the condenser and evaporator of the heat pump are analyzed (Figure A.15). The maximum forward temperature of the evaporator during only heating months is 12.4°C. Based on this fact, the cooling mode of the heat pump is determined; when the forward temperature of the evaporator is above this value, the heat pump is in cooling mode.

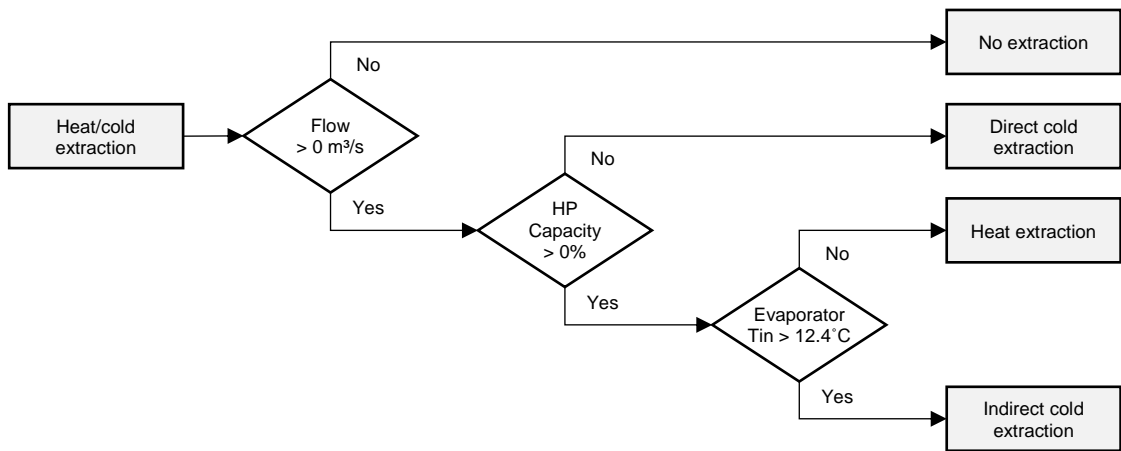


Figure A.12: Decision tree for the determination whether the extracted energy is related to heating or cooling

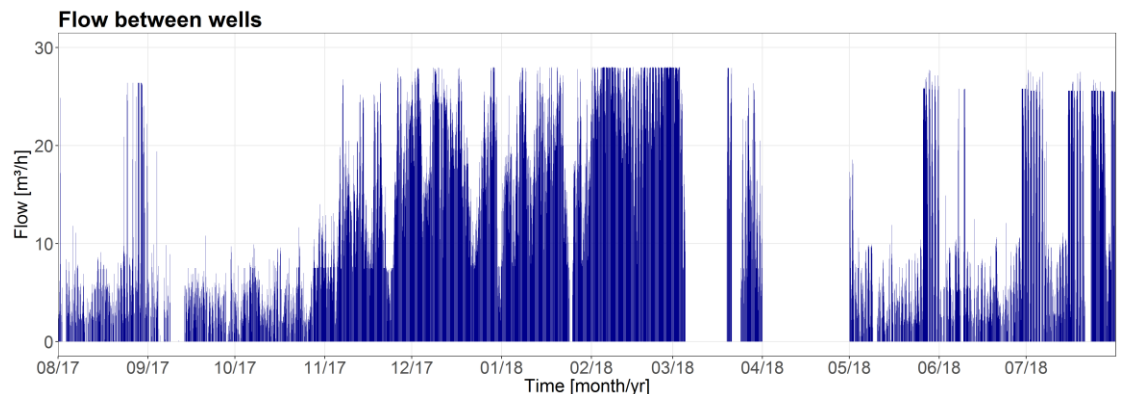


Figure A.13: Flow between the wells of the ATES system

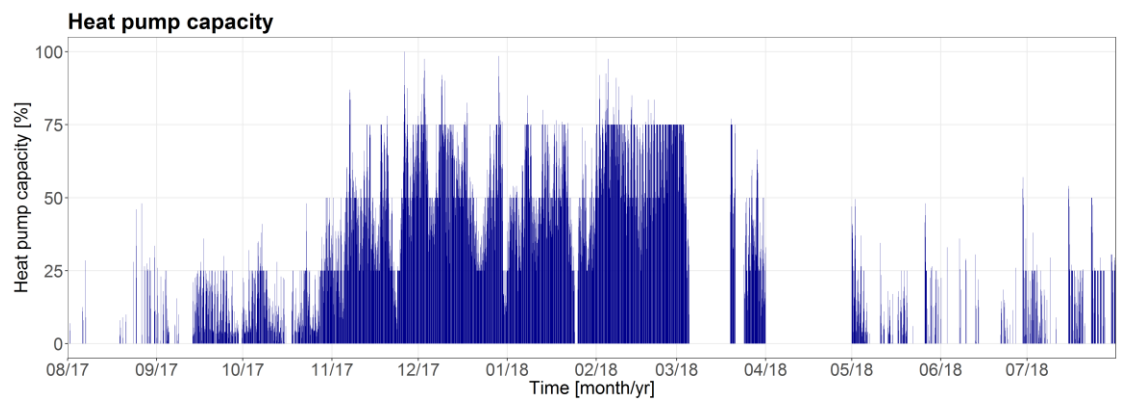


Figure A.14: Capacity of the heat pump

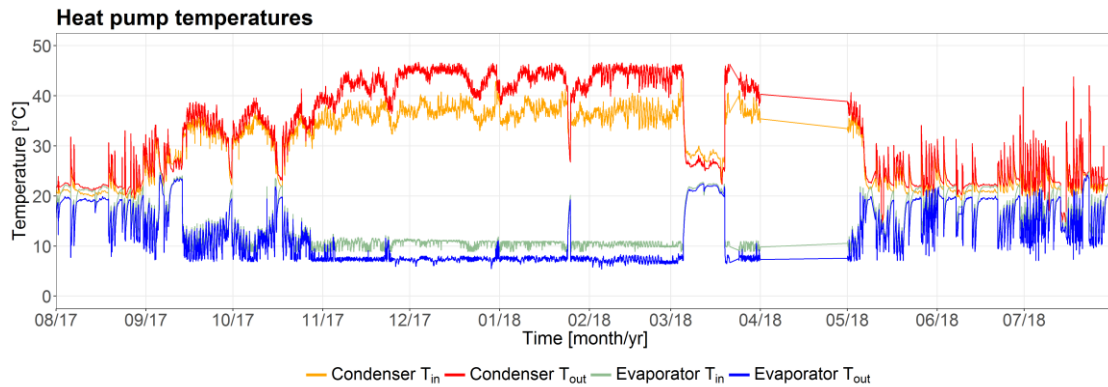


Figure A.15: Temperatures of the condenser and the evaporator of the heat pump

The results are validated with real measured data obtained by an energy service company (Table A.2). There can be concluded that the deviation is acceptable.

Table A.2: Difference between the measured and calculated thermal energy extraction

	Measured energy extraction		Calculated energy extraction		Deviation energy extraction	
	Heat [MWh]	Cold [MWh]	Heat [MWh]	Cold [MWh]	Heat [%]	Cold [%]
August	0	25	1	22	-	-12
September	8	1	7	2	-12	100
October	17	2	14	2	-18	0
November	54	0	54	0	0	0
December	67	0	68	0	1	0
Total	146	28	144	26	-1	-7

The thermal balance can be calculated with equation 5.2. The results per month are shown in Table A.3. During the whole measurement period, the thermal balance is negative which leads to a cold surplus of 38%. Hereby the note that the system was not in operation during two weeks of March and the data of April was not logged. Since there is a higher heating than cooling demand during these months, the thermal unbalance is in fact still larger. In order to comply with Dutch law, this unbalance must be solved.

Table A.3: Heat and cold extraction of the ATES

Month/year	Heat extraction [MWh]	Cold extraction [MWh]	Thermal unbalance [%]
08/2017	1	22	94
09/2017	7	2	-53
10/2017	14	2	-72
11/2017	54	0	-100
12/2017	68	0	-100
01/2018	60	0	-100
02/2018	75	0	-100
03/2018 <sup>[1]</sup>	25	0	-100
04/2018 <sup>[2]</sup>	-	-	-
05/2018	6	24	61
06/2018	1	22	90
07/2018	4	68	88

[1]: System two weeks not in operation

[2]: Data not logged

The heat maps of the measured outdoor temperature and thermal extraction by the ATES are presented in Figures A.16 to A.18.

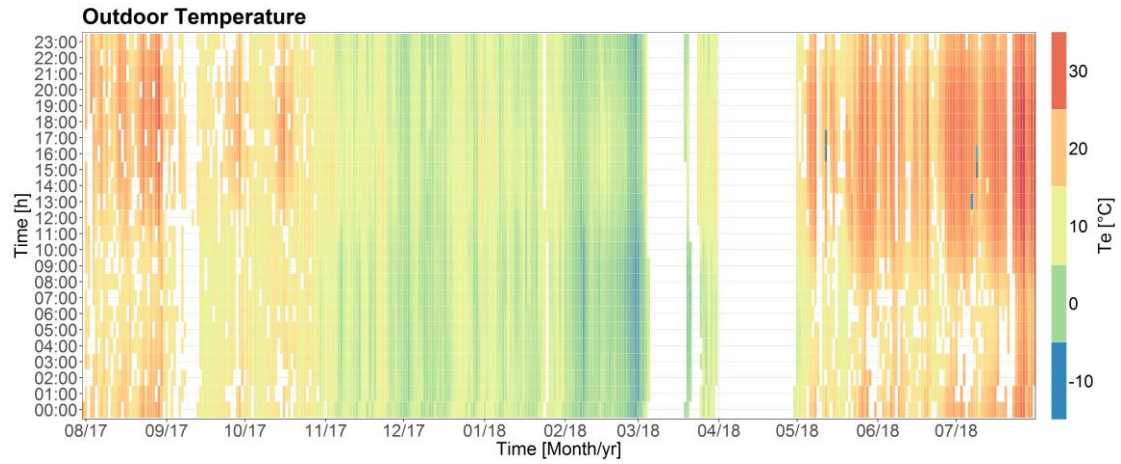


Figure A.16: Heat map of the measured outdoor temperature

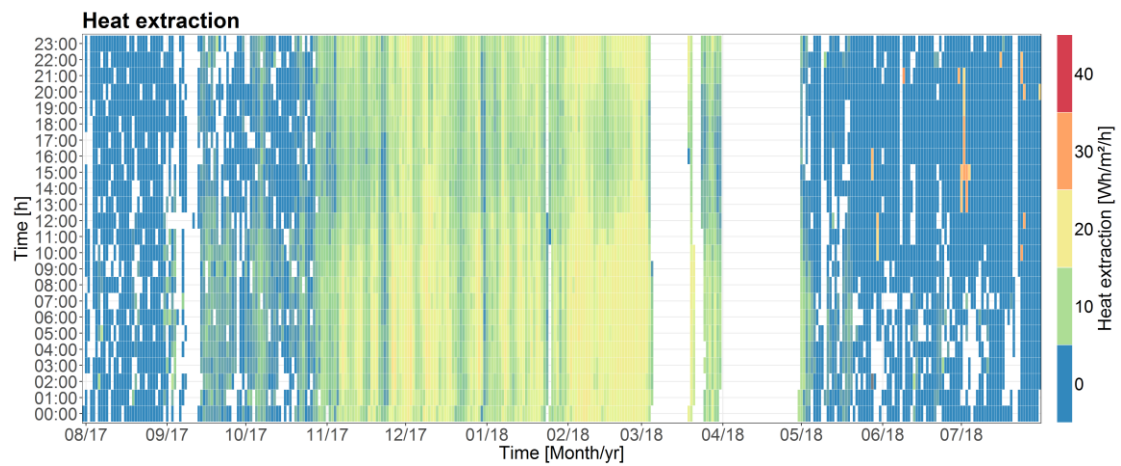


Figure A.17: Heat map of the heat extraction

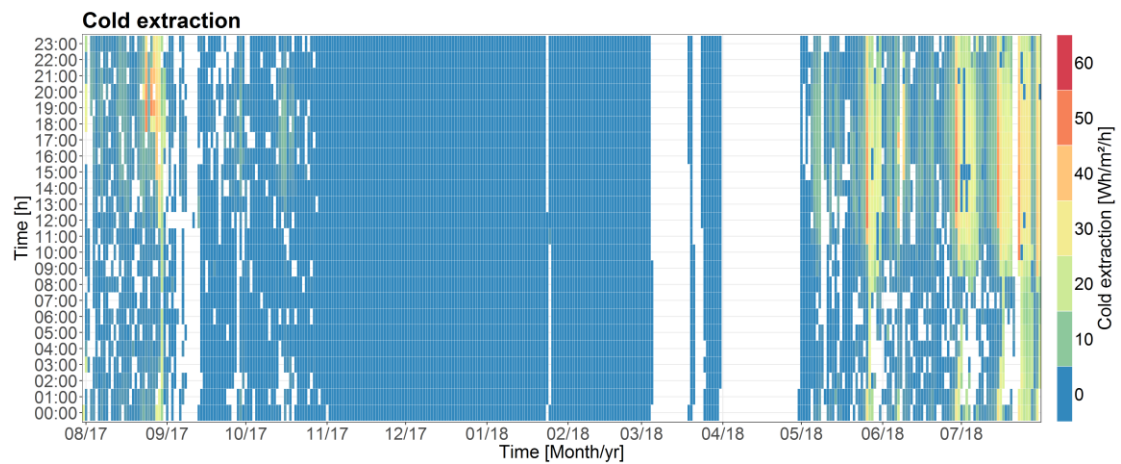


Figure A.18: Heat map of the cold extraction

**R-script**

```

# Constants
rho    <- 999
cp     <- 4.18

# Extracted thermal energy ATES
ATES_HP <- filter(Server, Flow > 0 & Capacity > 0)

ATES_HP$Extracted_Heating <- ATES_HP$Flow / 3600 * rho * cp * (ATES_HP$warm_well -
ATES_HP$cold_well)

ATES_HP$Extracted_Heating <- ifelse(ATES_HP$HP_Evaporator_Tin > 13, 0,
ATES_HP$Extracted_Heating)

ATES_HP$Extracted_Cooling <- ATES_HP$Flow / 3600 * rho * cp * (ATES_HP$cold_well -
ATES_HP$warm_well) * -1

ATES_HP$Extracted_Cooling <- ifelse(ATES_HP$HP_Evaporator_Tin > 13,
ATES_HP$Extracted_Cooling, 0)

ATES_Direct <- filter(Server, Flow > 0 & Capacity == 0)

ATES_Direct$Extracted_Heating <- 0

ATES_Direct$Extracted_Cooling <- ATES_Direct$Flow / 3600 * rho * cp *
(ATES_Direct$cold_well - ATES_Direct$warm_well) * -1

ATES <- rbind(ATES_HP, ATES_Direct)

# Extracted temperatures ATES
ATES$warm_well_Tin <- ifelse(ATES$Extracted_Cooling > 0, ATES$warm_well, 0)

ATES$warm_well_Tout <- ifelse(ATES$Extracted_Heating > 0, ATES$warm_well, 0)

ATES$cold_well_Tin <- ifelse(ATES$Extracted_Heating > 0, ATES$cold_well, 0)

ATES$cold_well_Tout <- ifelse(ATES$Extracted_Cooling > 0, ATES$cold_well, 0)

# COP heat pump
HP <- ATES

HP$Heating <- HP$Flow / 3600 * rho * cp * (HP$HP_Condenser_T.out -
HP$HP_Condenser_T.in)

HP$Cooling <- HP$Flow / 3600 * rho * cp * (HP$HP_Evaporator_T.in -
HP$HP_Evaporator_T.out)

```

```
HP$COP_Heating      <- ifelse(HP$Extracted_Heating > 0, (HP$HP_Heating /  
  (HP$HP_Heating - HP$HP_Cooling)), 0)  
  
HP$COP_Cooling      <- ifelse(HP$Extracted_Cooling > 0, (HP$HP_Cooling /  
  (HP$HP_Heating - HP$HP_Cooling)), 0)
```

## A.5 LEAN performance analysis

### R-script

```

# Sampling of train and test dataset
smp_size          <- floor(0.75 * nrow(ATES))

set.seed(123)
train_data        <- sample(seq_len(nrow(ATES)), size = smp_size)

# Heating
Heating_train     <- ATES[train_data, ]
Heating_test      <- ATES[-train_data, ]

## Linear model
Heating_fit       <- lm(Extracted_Heating ~ Outdoor_Temperature, data =
Heating_train)

## Prediction
Heating_test$prediction <- predict(Heating_fit, Heating_test)
Heating_test        <- filter(Heating_test, prediction >= 0)

## Calculation RMSE
Heating_test$residuals <- Heating_test$Extracted_Heating -
Heating_test$prediction
Heating_test$prediction <- predict(Heating_fit, Heating_test)

# Cooling
Cooling_train     <- ATES[train_data, ]
Cooling_test      <- ATES[-train_data, ]

## Linear model
Cooling_fit       <- lm(Extracted_Cooling ~ Outdoor_Temperature, data =
Cooling_train)

## Prediction
Cooling_test$prediction <- predict(Cooling_fit, Cooling_test)
Cooling_test        <- filter(Cooling_test, prediction >= 0)

## Calculation RMSE
Cooling_test$residuals <- Cooling_test$Extracted_Cooling -
Cooling_test$prediction
Cooling_test$prediction <- predict(Cooling_fit, Cooling_test)

```

## B Case study 2: Kropman Breda

### B.1 Building design

#### Floor plans

The floor plans of office building Kropman Breda are shown in Figures B.1 to B.3.

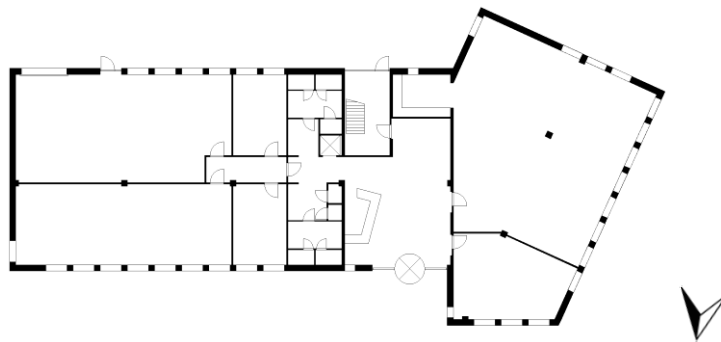


Figure B.1: Ground floor of Kropman Breda (1:500)

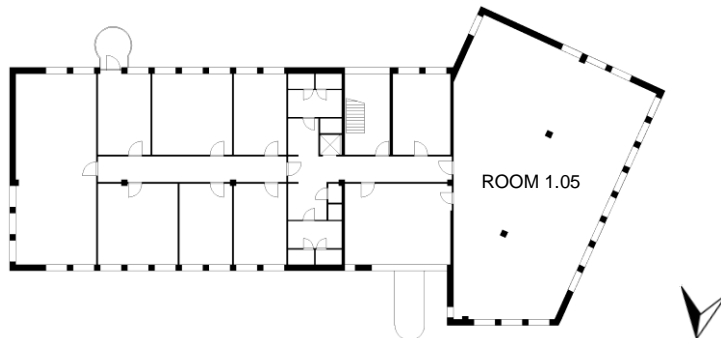


Figure B.2: First floor of Kropman Breda(1:500)

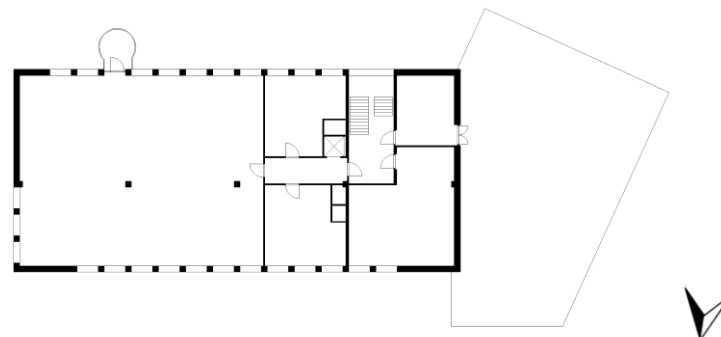
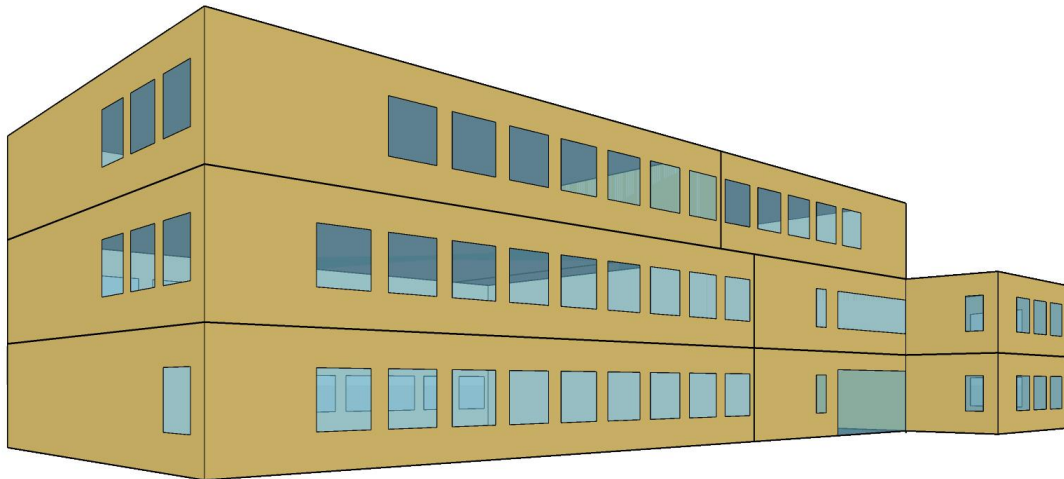


Figure B.3: Second floor of Kropman Breda (1:500)

## B.2 Pareto analysis

The 3D model of Kropman Breda is presented in Figure B.4. This model is used for the sensitivity analysis with EnergyPlus.



*Figure B.4: Created 3D model of Kropman Breda in SketchUp*



### B.3 Designed performance analysis

#### Heating system

The installation principle of the heating system is shown in Figure B.5.

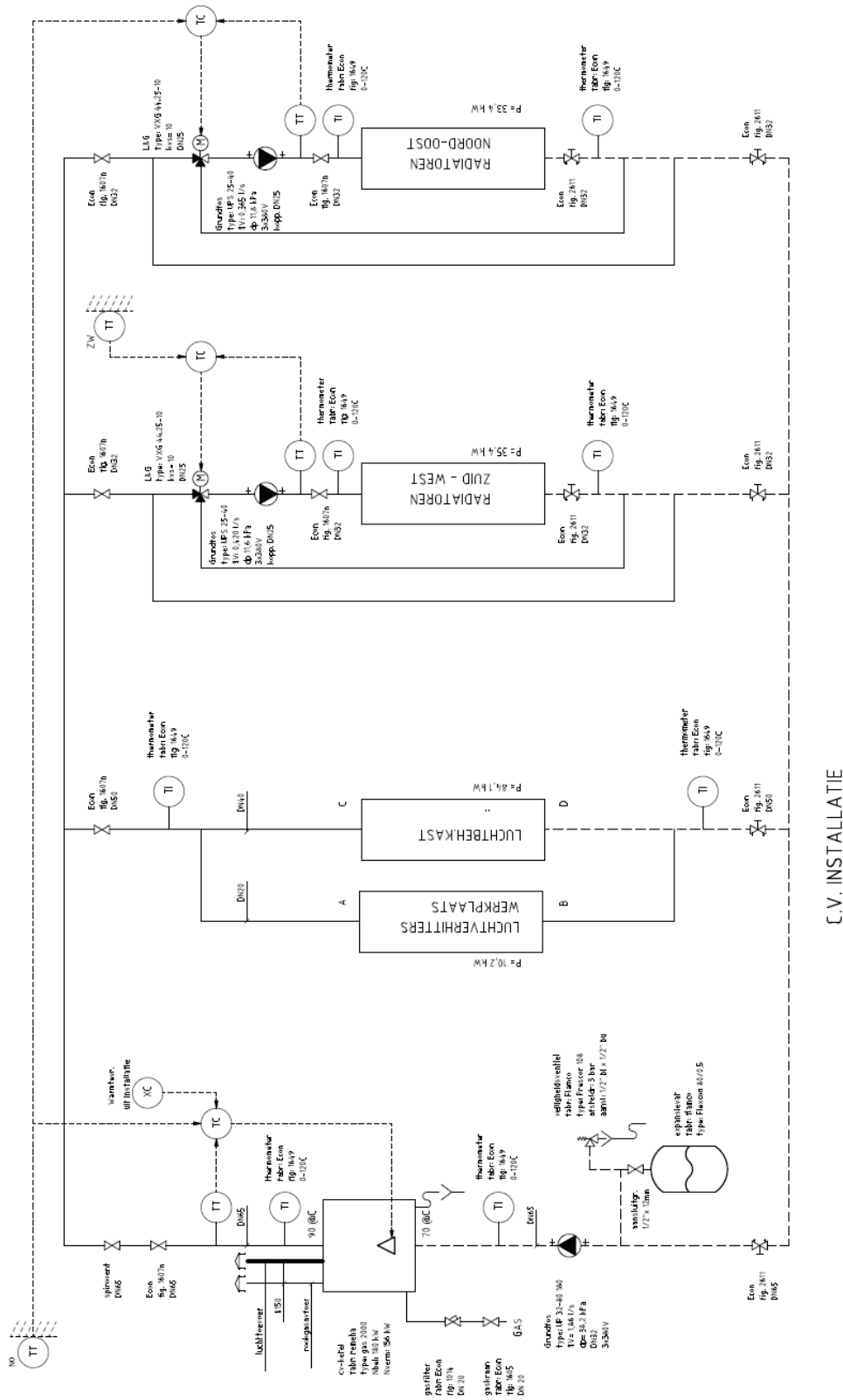
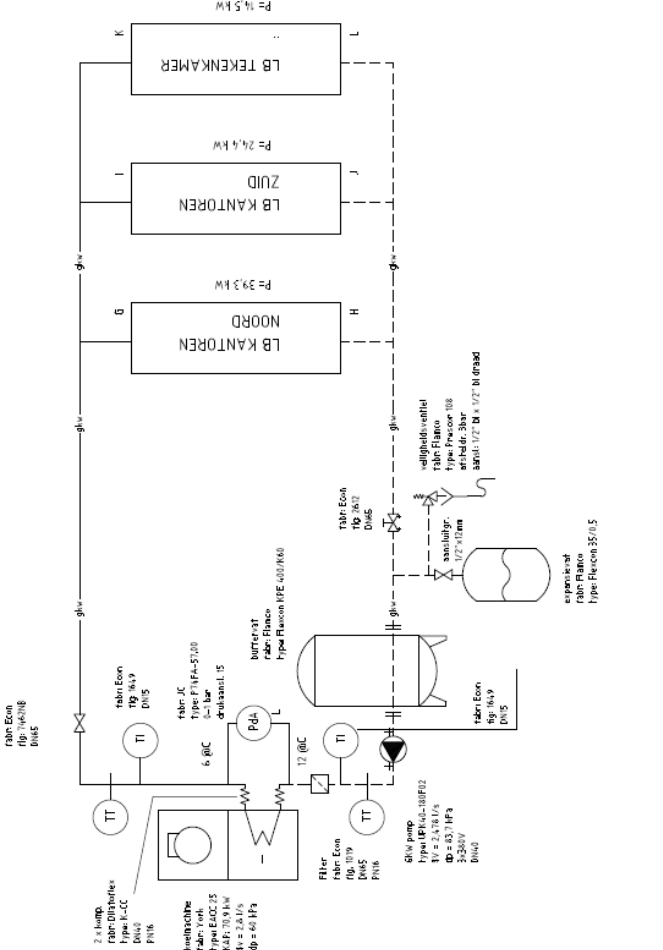


Figure B.5: Installation principle of the heating system

### Cooling system

The installation principle of the cooling system is shown in Figure B.6.



G.K.W. INSTALLATIE

Figure B.6: Installation principle of the cooling system

## B.4 Measured performance analysis

### Sensors

The sensors of the BMS are presented in Table B.1. These sensors are installed for monitoring and controlling the operational performance.

Table B.1. sensors of the BMS

ID	Description	Unit	ID	Description	Unit
1	Buitentemperatuur NO [Weerstation]	°C	102	Verl. 5a Ruimte G	W
2	Buitentemperatuur ZW [Weerstation]	°C	103	Verl. 6b Ruimte G	W
3	Aanvoertemperatuur [C.V. ketel]	°C	104	Netw. 4	W
4	Retourtemperatuur [C.V. ketel]	°C	105	Netw. 3	W
5	Ber. aanvoertemperatuur Ketel [C.V. ketel]	°C	106	WCD Ruimte E	W
6	Aanvoertemperatuur Radiatoren NO [C.V. verdeler]	°C	107	Verl. 6b Ruimte A	W
7	Ber. aanvoertemperatuur Radiatoren NO [C.V. verdeler]	°C	108	Verl. 5a Ruimte A	W
8	Retourtemperatuur Radiatoren NO [C.V. verdeler]	%	109	Bedrijfsuren per dag \ maand [Warmtewiel vervolg]	Uur
9	Regelafsluiter Radiatoren NO [C.V. verdeler]	%	110	Geleverd vermogen ketel per uur	kWh
10	Aanvoertemperatuur Radiatoren ZW [C.V. verdeler]	°C	111	Geleverd vermogen koelmachine per uur	kWh
11	Ber. Aanvoertemperatuur Radiatoren ZW [C.V. verdeler]	°C	112	Mom. Koelvermogen [Koudeopwekking - Koelmachine]	KW
12	Retourtemperatuur Radiatoren ZW [C.V. verdeler]	%	113	Mom. Cv Vermogen [Warmteopwekking - C.V. installatie]	KW
13	Regelafsluiter Radiatoren ZW [C.V. verdeler]	%	114	Koelmachine kWh meting per dag [Energie meters]	kWh
14	Uitredetemperatuur [Koelmachine]	°C	115	Hoofdverdeler Licht kWh meting per uur [Energie meters]	kWh
15	Intredetemperatuur [Koelmachine]	°C	116	Hoofdverdeler Kracht kWh meting per uur [Energie meters]	kWh
16	Regelafsluiter Nakoeleer ZW [Koelmachine]	%	117	HV Kracht Lijnstroom L2 [Energie Meters]	A
17	Regelafsluiter Nakoeleer NO [Koelmachine]	%	118	HV Licht Lijnstroom L2 [Energie Meters]	A
18	Gew. Uitrede temperatuur [Koelmachine]	°C	119	HV Licht Lijnstroom L3 [Energie Meters]	A
19	Regelafsluiter Nakoeleer E-afd. [Koelmachine]	%	120	HV Licht Lijnstroom L1 [Energie Meters]	A
20	Ber. Inblaastemperatuur NO [Overzicht lucht]	°C	121	HV Kracht Lijnstroom L3 [Energie Meters]	A
21	Ber. Inblaastemperatuur ZW [Overzicht lucht]	°C	122	HV Kracht Lijnstroom L1 [Energie Meters]	A
22	Ber. Inblaastemperatuur E-afdeling [Overzicht lucht]	°C	123	HV Kracht Lijnstroom L1 [Energie Meters]	V
23	Inblaastemperatuur E-afdeling [Overzicht lucht]	°C	124	HV Kracht Lijnstroom L1 [Energie Meters]	V
24	Ruimtetemperatuur E-afdeling [Overzicht lucht]	°C	125	HV Kracht Fasespanning L3-N [Energie Meters]	V
25	Ber. Afzuigtemperatuur NO [Overzicht lucht]	°C	126	HV Kracht Fasespanning L2-N [Energie Meters]	V
26	Ber. Afzuigtemperatuur ZW [Overzicht lucht]	°C	127	HV Licht Fasespanning L1-N [Energie Meters]	V
27	Inblaastemperatuur noord oost	°C	128	HV Kracht Fasespanning L1-N [Energie Meters]	V
28	Afzuigtemperatuur NO & kantine	°C	129	HV Licht Vermogen Schijnbaar [Energie Meters]	kVA
29	Afzuigtemperatuur ZW	°C	130	HV Licht Vermogen Werkelijk [Energie Meters]	KW
30	Inblaastemperatuur zuid west	°C	131	HV Kracht Vermogen Schijnbaar [Energie Meters]	kVA
31	Inblaastemperatuur LBK [Overzicht lucht]	°C	132	HV Kracht Vermogen Werkelijk [Energie Meters]	kW
32	Ber. Ruimtetemperatuur e. afd. [Overzicht lucht]	°C	133	HV Kracht Vermogen Blind [Energie Meters]	kVA
33	Regelafsluiter Radiatoren Kantine [Naregeling kantine]	%	134	HV Licht Vermogen Blind [Energie Meters]	kVA
34	Setpoint Ruimtetemperatuur [Naregeling kantine]	°C	135	Koelmachine Lijnstroom L1 [Energie Meters]	A
35	Toevoerluchtlep [Naregeling kantine]	%	136	Regelkast HVAC Lijnstroom L2 [Energie Meters]	A
36	Ruimtetemperatuur kantine	°C	137	Stoombevochtiger Lijnstroom L2 [Energie Meters]	A
37	Setpoint Ruimtetemperatuur [Naregeling spreekkamer]	°C	138	Stoombevochtiger Vermogen Blind [Energie Meters]	kVA
38	Regelafsluiter Radiatoren [Naregeling spreekkamer]	%	139	Regelkast HVAC Vermogen Schijnbaar [Energie Meters]	kVA
39	Ruimtetemperatuur spreekkamer	°C	140	Regelkast HVAC Vermogen Werkelijk [Energie Meters]	KW
40	Instelling Setpoint [Recirculatieventilatie magazijn]	°C	141	Koelmachine Vermogen Werkelijk [Energie Meters]	KW
41	Ruimtemp. Magazijn	°C	142	Koelmachine Vermogen Schijnbaar [Energie Meters]	kVA
42	Relatief Inblaasluuchtvocht [Luchtbehandelingskast]	%	143	Stoombevochtiger Vermogen Werkelijk [Energie Meters]	KW
43	Gem. Druk Toevoerkanaal [Luchtbehandelingskast]	Pa	144	Stoombevochtiger Vermogen Werkelijk [Energie Meters]	kVA
44	Druk over afvoerfilter [Luchtbehandelingskast]	Pa	145	Regelkast HVAC Vermogen Blind [Energie Meters]	kVA
45	Absoluut Inblaasvocht [Luchtbehandeling - LBK]	g/kg	146	Koelmachine Vermogen Blind [Energie Meters]	kVA
46	Ber. Aanvoerwatertemperatuur [Luchtbehandelingskast]	°C	147	Regelkast HVAC Fasespanning L1-N [Energie Meters]	V
47	Bevochtiger [Luchtbehandelingskast]	%	148	Koelmachine Fasespanning L1-N [Energie Meters]	V
48	Toevoerent. Toerental	O/min	149	Stoombevochtiger Fasespanning L1-N [Energie Meters]	V
49	Afzuigvent. Toerental	O/min	150	Regelkast HVAC Fasespanning L2-N [Energie Meters]	V
50	Aanvoertemp. verwamer	°C	151	Regelkast HVAC Lijnstroom L3 [Energie Meters]	A
51	Ber. inblaastemperatuur [Luchtbehandelingskast]	°C	152	Regelkast HVAC Lijnstroom L1 [Energie Meters]	A
52	Regelafsluiter verwamer [Luchtbehandelingskast]	%	153	Koelmachine Fasespanning L3-N [Energie Meters]	V
53	Ber. inblaastemperatuur [Luchtbehandelingskast]	°C	154	Koelmachine Lijnstroom L2 [Energie Meters]	A
54	Gewogen gemiddelde ruimtetemperatuur [Overzicht lucht]	°C	155	Stoombevochtiger Fasespanning L3-N [Energie Meters]	V
55	Koelmachine [Koelmachine]	%	156	Stoombevochtiger Fasespanning L2-N [Energie Meters]	V
56	ROR-sturing warmtewiel [LBK Kantoren]	%	157	Stoombevochtiger Lijnstroom L3 [Energie Meters]	A
57	Gemeten vermogen Ketel [Warmteopwekking - C.V. installatie]	KW	158	Stoombevochtiger Lijnstroom L1 [Energie Meters]	A
58	Aanvoertemperatuur ketel [Warmteopwekking - C.V. installatie]	°C	159	Regelkast HVAC Fasespanning L3-N [Energie Meters]	V
59	Retourtemperatuur ketel [Warmteopwekking - C.V. installatie]	°C	160	Koelmachine Fasespanning L2-N [Energie Meters]	V
60	kWh-verbr. puls - koelm. per uur [Energieregistratie]	kWh	161	Koelmachine Lijnstroom L3 [Energie Meters]	A
61	kWh-verbr. puls - stoombev. per uur [Energieregistratie]	kWh	162	Zonnehoek	°
62	kWh-verbr. puls - regelkast per uur [Energieregistratie]	kWh	163	Zonnehoogte	°
63	Gasverbruik puls - uur [Energieregistratie]	m <sup>3</sup>	164	Druk over toevoerfilter [Luchtbehandeling - LBK]	Pa
64	Verl. 5a Ruimte F [Plugwise]	W	165	Regelkast HVAC Wh meting per uur [Energie meters]	Wh
65	Verl. 6b Ruimte F [Plugwise]	W	166	Koelmachine Wh meting per uur [Energie meters]	Wh
66	Verl. Split Unit Ruimte G [Plugwise]	W	167	Stoombevochtiger Wh meting per uur [Energie meters]	
67	Verl. 5a en 6b Ruimte G [Plugwise]	W	168	Hoofdverdeler Licht Wh meting per uur [Energie meters]	
68	Netw. 4 Hal H [Plugwise]	W	169	Hoofdverdeler Kracht Wh meting per uur [Energie meters]	
69	Netw. 3 Hal K [Plugwise]	W	170	Reg. waarde panelen per uur	
70	Netw. 3 Hal K [Plugwise]	W	171	Temperatuur TT-2.8 [PV algemeen]	
71	Verl. 6b Ruimte C [Plugwise]	W	172	Temperatuur TT-2.19 [PV algemeen]	
72	Verl. 5a Ruimte D [Plugwise]	W	173	Temperatuur TT-2.21 [PV algemeen]	
73	Verl. 6b Ruimte D [Plugwise]	W	174	Temperatuur TT-2.30 [PV algemeen]	
74	Verl. 6a Ruimte E [Plugwise]	W	175	Temperatuur TT-1.5 [PV algemeen]	
75	Verl. 6b Ruimte E [Plugwise]	W	176	Temperatuur TT-1.21 [PV algemeen]	
76	Verl. 5c Ruimte E [Plugwise]	W	177	PV-panelen Lijnstroom L1 [Energie Meters]	
77	Verl. 5a Ruimte A [Plugwise]	W	178	PV-panelen Lijnstroom L2 [Energie Meters]	
78	Verl. 6b Ruimte A [Plugwise]	W	179	PV-panelen Lijnstroom L3 [Energie Meters]	
79	Verl. 5a Ruimte C [Plugwise]	W	180	PV-panelen Fasespanning L1-N [Energie Meters]	V
80	Verl. 6b Ruimte B [Plugwise]	W	181	PV-panelen Fasespanning L2-N [Energie Meters]	V
81	Verl. 5a Ruimte B [Plugwise]	W	182	PV-panelen Fasespanning L3-N [Energie Meters]	V
82	Verl. 6b Ruimte B [Plugwise]	W	183	PV-panelen Vermogen Werkelijk [Energie Meters]	KW
83	Verl. 5a Ruimte B [Plugwise]	W	184	PV-panelen Vermogen Blind [Energie Meters]	kVA
84	Ruimtetemperatuur No [Plattegrond 2e verdieping]	°C	185	PV-panelen Vermogen Schijnbaar [Energie Meters]	kVA
85	Stoombevochtiger kWh meting per uur [Energie meters]	kWh	186	Accusysteem Lijnstroom L1 [Energie Meters]	A
86	Koelmachine kWh meting per uur [Energie meters]	kWh	187	Accusysteem Lijnstroom L3 [Energie Meters]	A
87	Kwh meter modbus koelmach. per dag [Kwh Meters]	kWh	188	Accusysteem Fasespanning L1-N [Energie Meters]	V
88	Regelkast HVAC kWh meting per uur [Energie meters]	kWh	189	Accusysteem Fasespanning L2-N [Energie Meters]	V
89	Verl. 5a Ruimte B	W	190	Accusysteem Fasespanning L3-N [Energie Meters]	V
90	Verl. 6b Ruimte B	W	191	Accusysteem Vermogen Werkelijk [Energie Meters]	KW
91	Verl. 5a Ruimte B	W	192	Accusysteem Vermogen Blind [Energie Meters]	kVA
92	Verl. 6b Ruimte B	W	193	Accusysteem Vermogen Schijnbaar [Energie Meters]	kVA
93	Verl. 5a Ruimte C	W	194	Battery Pack Reg.waarde Per Uur [PV algemeen]	Wh
94	Verl. 6b Ruimte C	W	195	Battery Pack Reg.waarde Per Dag [PV algemeen]	Wh
95	Verl. 5a Ruimte D	W	196	Pyranometer [PV algemeen]	W/m <sup>2</sup>
96	Verl. 6b Ruimte D	W	197	Winddichting [PV algemeen]	°
97	Verl. 6a Ruimte E	W	198	Windsnelheid [PV algemeen]	m/s
98	Verl. 6b Ruimte E	W	199	Relatief vocht [PV algemeen]	%
99	Verl. 5c Ruimte E	W	200	Buitentemperatuur [PV algemeen]	°C
100	Verl. 5c Ruimte E	W	201	State_of_charge [Battery pack]	%
101	Verl. 6b Ruimte F	W	202	Actual Dc Current [Battery pack]	A

Table B.1. sensors of the building system (continued)

ID	Description	Unit	ID	Description	Unit
203	Actual Ac Current [Battery pack]	A	313	Intbatteryvoltage B4 [Overzicht Accu Strings]	V
204	Actual Dc Voltage [Battery pack]	V	314	Intbatteryvoltage A4 [Overzicht Accu Strings]	V
205	Actual Ac Voltage [Battery pack]	V	315	Intbatterycurrent A3 [Overzicht Accu Strings]	A
206	Apparent Ac Current [Battery pack]	A	316	Intbatterytempscaled E3 [Overzicht Accu Strings]	°C
207	Freq. Ac-side [Battery pack]	Hz	317	Intbatterytempscaled D3 [Overzicht Accu Strings]	°C
208	Actual Dc Power [Battery pack]	W	318	Intbatterytempscaled C3 [Overzicht Accu Strings]	°C
209	Max. Charge Current [Battery pack]	A	319	Intbatterytempscaled B3 [Overzicht Accu Strings]	°C
210	Max. Discharge Current [Battery pack]	A	320	Intbatterytempscaled A3 [Overzicht Accu Strings]	°C
211	Highest Temp. [Battery pack]	°C	321	Intbatterypressure E3 [Overzicht Accu Strings]	
212	Request Current [Battery pack]	A	322	Intbatterypressure D3 [Overzicht Accu Strings]	
213	Request Re Current [Battery pack]	A	323	Intbatterypressure C3 [Overzicht Accu Strings]	
214	Ruimte temperatuur technische ruimte [PV algemeen]	°C	324	Intbatterypressure B3 [Overzicht Accu Strings]	
215	Absoluut vocht [PV algemeen]	g/kg	325	Intbatterypressure A3 [Overzicht Accu Strings]	
216	Totaal werkelijk vermogen [Energie Meters]	KW	326	Intbatteryvoltage E3 [Overzicht Accu Strings]	
217	Intbatterycurrent A7 [Overzicht Accu Strings]	A	327	Intbatteryvoltage D3 [Overzicht Accu Strings]	V
218	Intbatterytempscaled E7 [Overzicht Accu Strings]	°C	328	Intbatteryvoltage C3 [Overzicht Accu Strings]	V
219	Intbatterytempscaled D7 [Overzicht Accu Strings]	°C	329	Intbatteryvoltage B3 [Overzicht Accu Strings]	V
220	Intbatterytempscaled C7 [Overzicht Accu Strings]	°C	330	Intbatteryvoltage A3 [Overzicht Accu Strings]	V
221	Intbatterytempscaled B7 [Overzicht Accu Strings]	°C	331	Intbatterycurrent A2 [Overzicht Accu Strings]	A
222	Intbatterytempscaled A7 [Overzicht Accu Strings]	°C	332	Intbatterytempscaled E2 [Overzicht Accu Strings]	°C
223	Intbatterypressure E7 [Overzicht Accu Strings]		333	Intbatterytempscaled D2 [Overzicht Accu Strings]	°C
224	Intbatterypressure D7 [Overzicht Accu Strings]		334	Intbatterytempscaled C2 [Overzicht Accu Strings]	°C
225	Intbatterypressure C7 [Overzicht Accu Strings]		335	Intbatterytempscaled B2 [Overzicht Accu Strings]	°C
226	Intbatterypressure B7 [Overzicht Accu Strings]		336	Intbatterytempscaled A2 [Overzicht Accu Strings]	°C
227	Intbatterypressure A7 [Overzicht Accu Strings]		337	Intbatterypressure E2 [Overzicht Accu Strings]	
228	Intbatteryvoltage E7 [Overzicht Accu Strings]	V	338	Intbatterypressure D2 [Overzicht Accu Strings]	
229	Intbatteryvoltage D7 [Overzicht Accu Strings]	V	339	Intbatterypressure C2 [Overzicht Accu Strings]	
230	Intbatteryvoltage C7 [Overzicht Accu Strings]	V	340	Intbatterypressure B2 [Overzicht Accu Strings]	
231	Intbatteryvoltage B7 [Overzicht Accu Strings]	V	341	Intbatterypressure A2 [Overzicht Accu Strings]	
232	Intbatteryvoltage A7 [Overzicht Accu Strings]	V	342	Intbatteryvoltage E2 [Overzicht Accu Strings]	V
233	Intbatterycurrent A6 [Overzicht Accu Strings]	A	343	Intbatteryvoltage D2 [Overzicht Accu Strings]	V
234	Intbatterytempscaled E6 [Overzicht Accu Strings]	°C	344	Intbatteryvoltage C2 [Overzicht Accu Strings]	V
235	Intbatterytempscaled D6 [Overzicht Accu Strings]	°C	345	Intbatteryvoltage B2 [Overzicht Accu Strings]	V
236	Intbatterytempscaled C6 [Overzicht Accu Strings]	°C	346	Intbatteryvoltage A2 [Overzicht Accu Strings]	V
237	Intbatterytempscaled B6 [Overzicht Accu Strings]	°C	347	Intbatterycurrent A1 [Overzicht Accu Strings]	A
238	Intbatterytempscaled A6 [Overzicht Accu Strings]	°C	348	Intbatterytempscaled E1 [Overzicht Accu Strings]	°C
239	Intbatterypressure E6 [Overzicht Accu Strings]		349	Intbatterytempscaled D1 [Overzicht Accu Strings]	°C
240	Intbatterypressure D6 [Overzicht Accu Strings]		350	Intbatterytempscaled C1 [Overzicht Accu Strings]	°C
241	Intbatterypressure C6 [Overzicht Accu Strings]		351	Intbatterytempscaled B1 [Overzicht Accu Strings]	°C
242	Intbatterypressure B6 [Overzicht Accu Strings]		352	Intbatterytempscaled A1 [Overzicht Accu Strings]	°C
243	Intbatterypressure A6 [Overzicht Accu Strings]		353	Intbatterypressure E1 [Overzicht Accu Strings]	
244	Intbatteryvoltage E6 [Overzicht Accu Strings]	V	354	Intbatterypressure D1 [Overzicht Accu Strings]	
245	Intbatteryvoltage D6 [Overzicht Accu Strings]	V	355	Intbatterypressure C1 [Overzicht Accu Strings]	
246	Intbatteryvoltage C6 [Overzicht Accu Strings]	V	356	Intbatterypressure B1 [Overzicht Accu Strings]	
247	Intbatteryvoltage B6 [Overzicht Accu Strings]	V	357	Intbatterypressure A1 [Overzicht Accu Strings]	
248	Intbatteryvoltage A6 [Overzicht Accu Strings]	V	358	Intbatteryvoltage E1 [Overzicht Accu Strings]	V
249	Intbatterycurrent A5 [Overzicht Accu Strings]	A	359	Intbatteryvoltage D1 [Overzicht Accu Strings]	V
250	Intbatterytempscaled E5 [Overzicht Accu Strings]	°C	360	Intbatteryvoltage C1 [Overzicht Accu Strings]	V
251	Intbatterytempscaled D5 [Overzicht Accu Strings]	°C	361	Intbatteryvoltage B1 [Overzicht Accu Strings]	V
252	Intbatterytempscaled C5 [Overzicht Accu Strings]	°C	362	Intbatteryvoltage A1 [Overzicht Accu Strings]	V
253	Intbatterytempscaled B5 [Overzicht Accu Strings]	°C	363	Lichtintensiteit West LS4	klux
254	Intbatterytempscaled A5 [Overzicht Accu Strings]	°C	364	Lichtintensiteit Zuid LS3 [Parkeerplaats Kropman]	klux
255	Intbatterypressure E5 [Overzicht Accu Strings]		365	Lichtintensiteit Oost LS2 [Begraafplaats zijde]	klux
256	Intbatterypressure D5 [Overzicht Accu Strings]		366	Lichtintensiteit Noord LS1 [Mercedes dealer zijde]	klux
257	Intbatterypressure C5 [Overzicht Accu Strings]		367	Temperatuur TT-1.21 [PV algemeen]	°C
258	Intbatterypressure B5 [Overzicht Accu Strings]		368	Temperatuur TT-2.21 [PV algemeen]	°C
259	Intbatterypressure A5 [Overzicht Accu Strings]		369	Temperatuur TT-1.5 [PV algemeen]	°C
260	Intbatteryvoltage E6 [Overzicht Accu Strings]	V	370	Temperatuur TT-2.30 [PV algemeen]	°C
261	Intbatteryvoltage D5 [Overzicht Accu Strings]	V	371	Temperatuur TT-2.8 [PV algemeen]	°C
262	Intbatteryvoltage C5 [Overzicht Accu Strings]	V	372	Temperatuur TT-2.19 [PV algemeen]	°C
263	Intbatteryvoltage B5 [Overzicht Accu Strings]	V	373	Lux 1 [lvNext Dali Lon Module]	
264	Intbatteryvoltage A5 [Overzicht Accu Strings]	V	374	Lux 2 [lvNext Dali Lon Module]	
265	Intbatterycurrent A4 [Overzicht Accu Strings]	A	375	Lux 3 [lvNext Dali Lon Module]	
266	Intbatterytempscaled E4 [Overzicht Accu Strings]	°C	376	Lux 4 [lvNext Dali Lon Module]	
267	Intbatterytempscaled D4 [Overzicht Accu Strings]	°C	377	Lux 5 [lvNext Dali Lon Module]	
268	Intbatterytempscaled C4 [Overzicht Accu Strings]	°C	378	Lux 6 [lvNext Dali Lon Module]	
269	Intbatterytempscaled B4 [Overzicht Accu Strings]	°C	379	Lux 7 [lvNext Dali Lon Module]	
270	Intbatterytempscaled A4 [Overzicht Accu Strings]	°C	380	Lux 8 [lvNext Dali Lon Module]	
271	Intbatterypressure E4 [Overzicht Accu Strings]		381	Lux 9 [lvNext Dali Lon Module]	
272	Intbatterypressure D4 [Overzicht Accu Strings]		382	Lux 10 [lvNext Dali Lon Module]	
273	Intbatterypressure C4 [Overzicht Accu Strings]		383	Lux 11 [lvNext Dali Lon Module]	
274	Intbatterypressure B4 [Overzicht Accu Strings]		384	Lux 12 [lvNext Dali Lon Module]	
275	Intbatterypressure A4 [Overzicht Accu Strings]		385	Lux 13 [lvNext Dali Lon Module]	
276	Intbatteryvoltage E4 [Overzicht Accu Strings]	V	386	Lux 14 [lvNext Dali Lon Module]	
277	Intbatteryvoltage D4 [Overzicht Accu Strings]	V	387	Accusysteem Lijnstroom L2 [Energie Meters]	A
278	Intbatteryvoltage C4 [Overzicht Accu Strings]	V	388	Frequentie [Algemeen]	Hz
279	Intbatteryvoltage B4 [Overzicht Accu Strings]	V	389	Aanwezigheid werkplek 1 [Verlichting E-afdeling]	
280	Intbatteryvoltage A4 [Overzicht Accu Strings]	V	390	Aanwezigheid werkplek 2 [Verlichting E-afdeling]	
281	Intbatterycurrent A3 [Overzicht Accu Strings]	A	391	Aanwezigheid werkplek 3 [Verlichting E-afdeling]	
282	Intbatterytempscaled E3 [Overzicht Accu Strings]	°C	392	Aanwezigheid werkplek 4 [Verlichting E-afdeling]	
283	Intbatterytempscaled D3 [Overzicht Accu Strings]	°C	393	Aanwezigheid werkplek 5 [Verlichting E-afdeling]	
284	Intbatterytempscaled C3 [Overzicht Accu Strings]	°C	394	Aanwezigheid werkplek 6 [Verlichting E-afdeling]	
285	Intbatterytempscaled B3 [Overzicht Accu Strings]	°C	395	Aanwezigheid werkplek 7 [Verlichting E-afdeling]	
286	Intbatterytempscaled A3 [Overzicht Accu Strings]	°C	396	Aanwezigheid werkplek 8 [Verlichting E-afdeling]	
287	Intbatterypressure E3 [Overzicht Accu Strings]		397	Aanwezigheid werkplek 9 [Verlichting E-afdeling]	
288	Intbatterypressure D3 [Overzicht Accu Strings]		398	Aanwezigheid werkplek 10 [Verlichting E-afdeling]	
289	Intbatterypressure C3 [Overzicht Accu Strings]		399	Aanwezigheid werkplek 11 [Verlichting E-afdeling]	
290	Intbatterypressure B3 [Overzicht Accu Strings]		400	Aanwezigheid werkplek 12 [Verlichting E-afdeling]	
291	Intbatterypressure A3 [Overzicht Accu Strings]		401	Aanwezigheid werkplek 13 [Verlichting E-afdeling]	
292	Intbatterypressure B5 [Overzicht Accu Strings]		402	Aanwezigheid werkplek 14 [Verlichting E-afdeling]	
293	Intbatterypressure A5 [Overzicht Accu Strings]		403	Lucht kwaliteit Retourkanaal [Naregelingen - Ruimte 1.05]	Ppm
294	Intbatteryvoltage E6 [Overzicht Accu Strings]	V	404	Verlichting ruimte 1.05 – per uur [Energie registratie]	kWh
295	Intbatteryvoltage D5 [Overzicht Accu Strings]	V	405	kWh-verbr. - Split-unit - per uur [Energie registratie]	kWh
296	Intbatteryvoltage C5 [Overzicht Accu Strings]	V	406	Voc Retourkanaal 1.05 [Naregelingen - Ruimte 1.05]	%
297	Intbatteryvoltage B5 [Overzicht Accu Strings]	V	407	Kp [Pid]	
298	Intbatteryvoltage A5 [Overzicht Accu Strings]	V	408	Ki [Pid]	
299	Intbatterycurrent A4 [Overzicht Accu Strings]	A	409	Kd [Pid]	
300	Intbatterytempscaled E4 [Overzicht Accu Strings]	°C	410	Relatieve ruimtevocht 1.05 [Overzicht lucht]	%
301	Intbatterytempscaled D4 [Overzicht Accu Strings]	°C	411	Tijdprogramma [Naregelingen - Ruimte 1.05]	
302	Intbatterytempscaled C4 [Overzicht Accu Strings]	°C	412	Toerenreg. Toevoent. Regelaar Percent [LBK Kantoren]	%
303	Intbatterytempscaled B4 [Overzicht Accu Strings]	°C	413	Toerenreg. Afzuigvent. Regelaar Percenta [LBK Kantoren]	%
304	Intbatterytempscaled A4 [Overzicht Accu Strings]	°C	414	Occupancy	
305	Intbatterypressure E4 [Overzicht Accu Strings]		415	Occupancy 8	
306	Intbatterypressure D4 [Overzicht Accu Strings]		416	Occupancy 12	
307	Intbatterypressure C4 [Overzicht Accu Strings]		417	Overwerk kantine [Tijdprogramma's]	
308	Intbatterypressure B4 [Overzicht Accu Strings]		418	Overwerk algemeen [Tijdprogramma's]	
309	Intbatterypressure A4 [Overzicht Accu Strings]		419	Sturing VAV-regelaar [Naregelingen - Ruimte 1.05]	%
310	Intbatteryvoltage E4 [Overzicht Accu Strings]	V	420	PID-sturing nuttig verwarmert warmtewiel [LBK Kantoren]	%
311	Intbatteryvoltage D4 [Overzicht Accu Strings]	V	421	PID-sturing nuttig koeler warmtewiel [LBK Kantoren]	%
312	Intbatteryvoltage C4 [Overzicht Accu Strings]	V	422	Tijdprogramma Comfortlevering	

**Energy consumption**

The heat maps of the measured outdoor temperature and the energy consumption are shown in Figures B.7 to B.11.

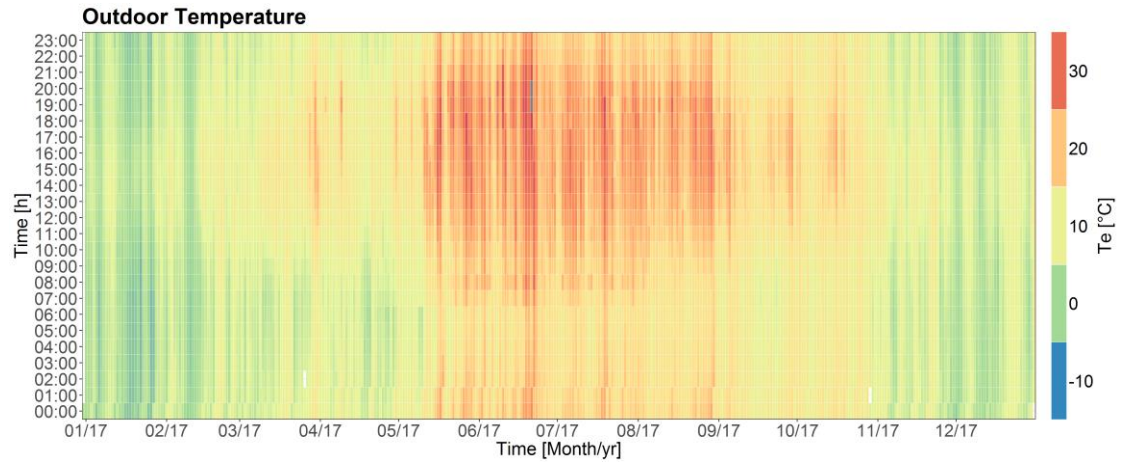


Figure B.7: Heat map of the measured outdoor temperature

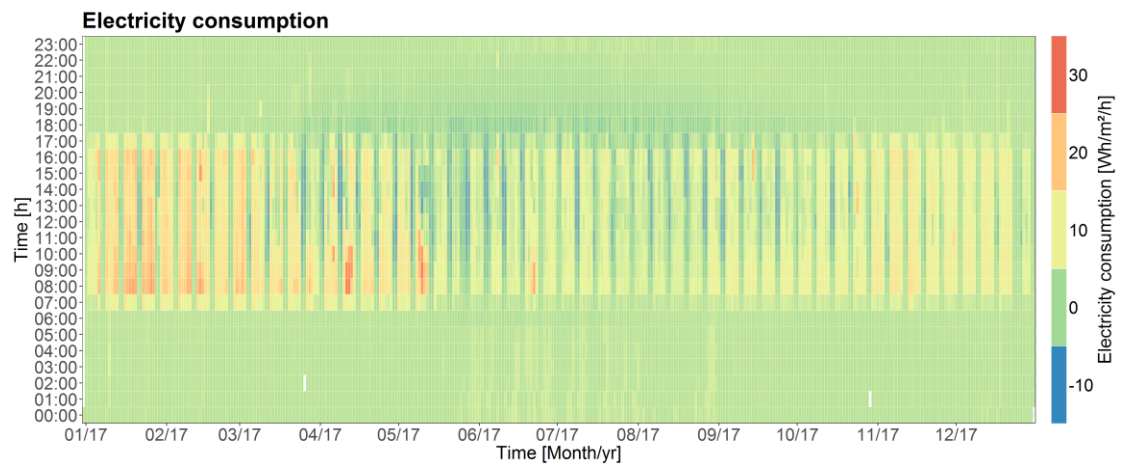


Figure B.8: Heat map of the measured electricity consumption

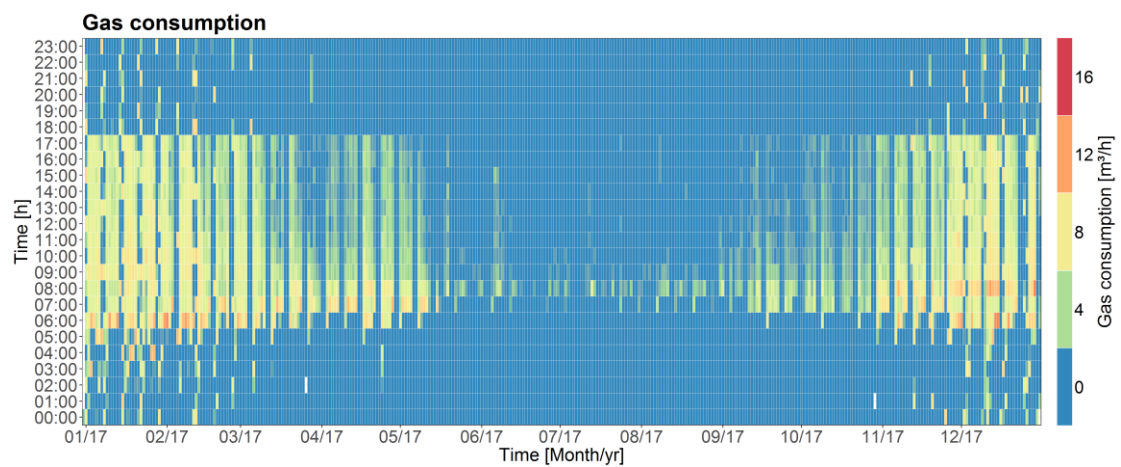


Figure B.9: Heat map of the measured gas consumption

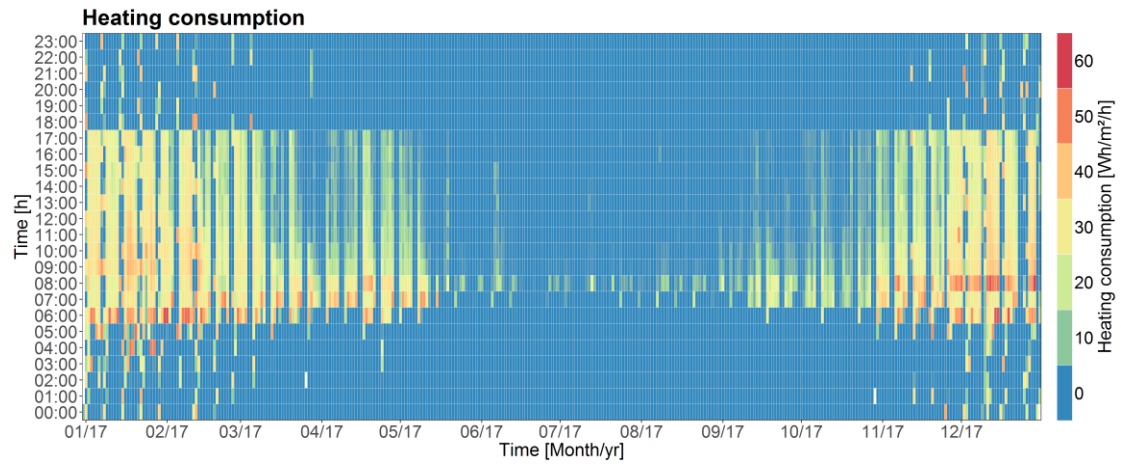


Figure B.10: Heat map of the measured heating consumption

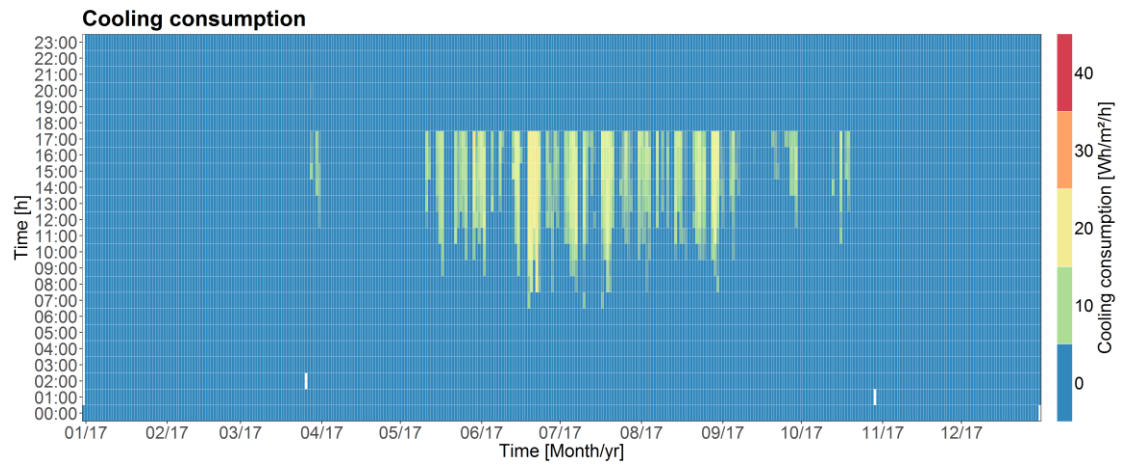


Figure B.11: Heat map of the measured cooling consumption

## B.5 LEAN performance analysis

### R-script

```

# Sampling of train and test dataset
smp_size          <- floor(0.75 * nrow(Thermal_Consumption))

set.seed(123)
train_data        <- sample(seq_len(nrow(Thermal_Consumption)), size =
                           smp_size)

# Heating
Heating_train     <- Thermal_Consumption[train_data, ]
Heating_test      <- Thermal_Consumption[-train_data, ]

## Linear model
Heating_fit       <- lm(Heating_Consumption ~ Outdoor_Temperature, data =
                           Heating_train)

## Prediction
Heating_test$Prediction <- predict(Heating_fit, Heating_test)
Heating_test        <- filter(Heating_test, prediction >= 0)

## Calculation RMSE
Heating_test$Residuals <- Heating_test$Heating_Consumption -
                           Heating_test$prediction
Heating_test$Prediction <- predict(Heating_fit, Heating_test)

# Cooling
Cooling_train     <- Thermal_Consumption[train_data, ]
Cooling_test      <- Thermal_Consumption[-train_data, ]

## Linear model
Cooling_fit       <- lm(Cooling_Consumption ~ Outdoor_Temperature, data =
                           Cooling_train)

## Prediction
Cooling_test$Prediction <- predict(Cooling_fit, Cooling_test)
Cooling_test        <- filter(Cooling_test, prediction >= 0)

## Calculation RMSE
Cooling_test$Residuals <- Cooling_test$Cooling_Consumption -
                           Cooling_test$prediction
Cooling_test$Prediction <- predict(Cooling_fit, Cooling_test)

```